1-1-2004

Semi-Biosynthesis of DNA Nanostructures

Aoune Barhoumi
barhoumi1@marshall.edu

Semi-Biosynthesis of DNA Nanostructures

Thesis submitted to
The Graduate College of
Marshall University

In Partial Fulfillment of the
Requirements for the Degree of
Master of Science

by

Aoune Barhoumi

Marshall University

May 2004

List of Tables

List of Figures

ABSTRACT

Nanotechnology refers to all technologies aiming to build objects, make measurements, and carry out processes on the nanometer length scale. In particular molecular nanotechnology exemplifies the so-called "bottom up" approach, which is briefly defined as the ability to build useful nanostructures with molecular precision, such as molecular machinery. Such capability for controlling matter at the molecular scale has always been the dream of scientists.

All living things are nanofoundries. Billions of years ago, nature perfectly provided all living things with the most accurate biological nanotechnology systems. Cellular internal dynamics, communicative resonance in protein conformational states, viruses as microreplicators, nanoscale life mechanisms, (e.g. repairing and replication) and nanoscale energy exchanges are examples of these systems. It is clear that learning and using some biological techniques (DNA replication), or even using some of the molecular tools provided by nature (enzymes) will be most relevant to nanotechnology development.

In this project we demonstrate how we can derive benefit from employing biological techniques, such as Rolling Circle Amplification, Polymerase Chain Reaction, and cloning to address the challenge of emplacing DNA nanoarrays at pre-determined locations on a surface.

In vitro, rolling Circle amplification (RCA) driven by DNA polymerization was first reported by Eric T. Kool and coworkers in 1995. DNA products resulting from RCA are repeating head-to-tail multimeric copies of the DNA template. We report the design and synthesis of both single stranded circular DNA (used as a template) and a multimeric product. Using the RCA technique, long tandem repeats, consisting of multiple copies of a 95 base pair sequence have been produced. We incorporated two specific, unique sequences at each end of these synthesized DNA strands, which can be used as recognition sites for surface hybridization. For the first time, heterogeneity has been introduced into a repetitive system to yield a modular nanostructured macromolecule. This product was further cloned into bacterial host cells. The DNA fragments were extracted and sequenced. The results not only confirm success in these particular experiments, but they also verify the general validity of this technique for generating nano-constructs semi- biosynthetically.

In order to demonstrate applicability of the RCA product to nanotechnology, we used these strands as scaffolds for gold nanoparticle patterning.

1) INTRODUCTION

For the last few decades the electronics industry has mainly been based on a top down, solid state approach to fabricating devices. Many techniques have been developed to keep up with the market needs. Miniaturization is the biggest challenge that has been facing microelectronics fabrication facilities all over the world. In 1965 Gordon Moore, co-founder of Intel Corporation, made his famous observation, just four years after the first planar integrated circuit was discovered. What is now known as Moore's law claims that the number of transistors will double per square inch on integrated circuits in a given chip every 18 months, an exponential growth pattern that has allowed computers to get both cheaper and more powerful at the same time. Since then Intel has been successfully minimizing the size of the transistor and packing more and more in a single chip.

In the last few years many problems, such as heat dissipation, leakage from device to device, and the high cost of photolithography techniques have become more and more substantial. Shrinking the size of transistor is leading to a weird world that has not been really investigated by the semiconductor makers, it is the quantum mechanics world where things behave like nothing known in our every day world. When the length of the gate (the thinnest part of a transistor) gets below 5 nanometers, tunneling will begin to occur. Electrons will simply pass through the channel on their own, because the source and the drain will be extremely close. Many scientists and engineers think that it is a fundamental limit, at least with the approach that has been used so far. Some approaches have been developed to solve the problem. Changing the whole shape of the transistor

and moving from a one to a two dimensional architecture, in order to increase the control over the current flow through the gate is one approach. The other was suggested by the Nobel Prize Laureate Richard Feynman at 1959, summarized in his famous saying “there is plenty of room at the bottom” (1).

He introduced a new field of science now called molecular electronics.

The field of molecular electronics seeks to use individual molecules to perform functions in electronic circuitry now performed by semiconductor devices. Individual molecules are hundreds of times smaller than the smallest features conceivably attainable by semiconductor technology. Electronic devices constructed from molecules will be hundreds of times smaller than their semiconductor-based counterparts. Moreover, individual molecules are easily fabricated defect-free in enormous numbers and with much lower cost. Considering the difficulty of manipulating single molecules, the option which is considered more viable uses the self-assembly and self-recognition properties of molecules to achieve placement of molecules on surfaces with nanometer resolution. Such an approach offers many potential advantages versus the bulk or top down material approach used so far.

In order to make use of these electronically active molecules we need to address them to a very determined specific surface location. This process must place these molecules one next to the other so they can form a complete electronic system, such as a microchip. Researchers were able to target different molecules with different functionalities (thiol group, biotin, etc), but they have not had much success positioning them in different localities on the same surface. Consequently, a few researchers have begun developing

the biological analog of the integrated circuit, the so called DNA nanoarray. The idea is based on making DNA blocks formed of a given number of single stranded DNA oligomers, and then self assembled to produce a bigger crystal. Using the self recognition properties of nucleic acid polymers these arrays can be of potential interest. To the best of my knowledge these arrays have been annealed in liquid solution then monitored on mica substrate for further processing (2).

Growing the arrays in liquid is a fascinating achievement; however it has two problems that need to be overcome. First of all, there is no control over the size of the arrays, and even controlling the concentrations of strands forming the blocks does not obviously determine the size of the crystals. Second, for almost any electronic application arrays should be fixed on a surface, which means that we will run back to the same problem of manipulating single molecules.

We pioneer here a new approach of synthesizing controlled solid state DNA nanoarrays on a silicon wafer. The first step is creating a one dimensional nanoarray single stranded DNA (termed a director strand) 1-2 microns in length with repeat unit of ca 30 nm. Ideally a 2-D DNA crystal consisting of A and B blocks (as will be described later) will be sequentially assembled on this director strand. By having the Director strand localized at a defined location on the surface, we can build a substrate for use as a scaffold appropriate for assembly of a variety of single molecules. The single molecules will be differently labeled then directed to their precise locations on the substrate using the specific bonding between DNA base pairs. We believe that our substrate will have a potential use in DNA microchip, molecular electronics, optics etc.

DNA nanoarrays

First reported by Nadrian C. Seeman (2), the DNA nanoarray is a two-dimensional crystalline form of DNA that self assembles from synthetic DNA double-crossover molecules. By means of Watson-Crick complementarity, designed "sticky ends" of two structural units (blocks) were programmed to form a specific periodic pattern on the nanometer scale. I will emphasize here the simplest non-trivial set of blocks: block A and B (Fig. 1.1a), which self-assemble in solution into two-dimensional crystals with a well defined subunit structure. Each block (2x4x16 nm in size) is formed of 5 single stranded DNA molecules fit together to form single-domain crystals as large as 2x8 μm with a uniform thickness of 2 nm. The design involves two small nicked circular strands in addition to four infinite strands, two of which extend horizontally and two of which extend vertically (Fig. 1.1b). To make the crystal observable by the AFM, two hairpins are incorporated into the block B structure, giving stripes above the surface at intervals of 32 nm.

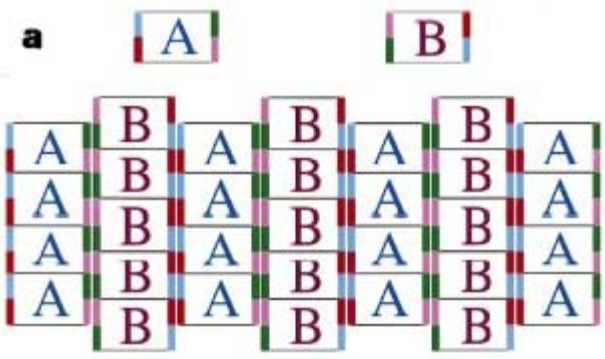

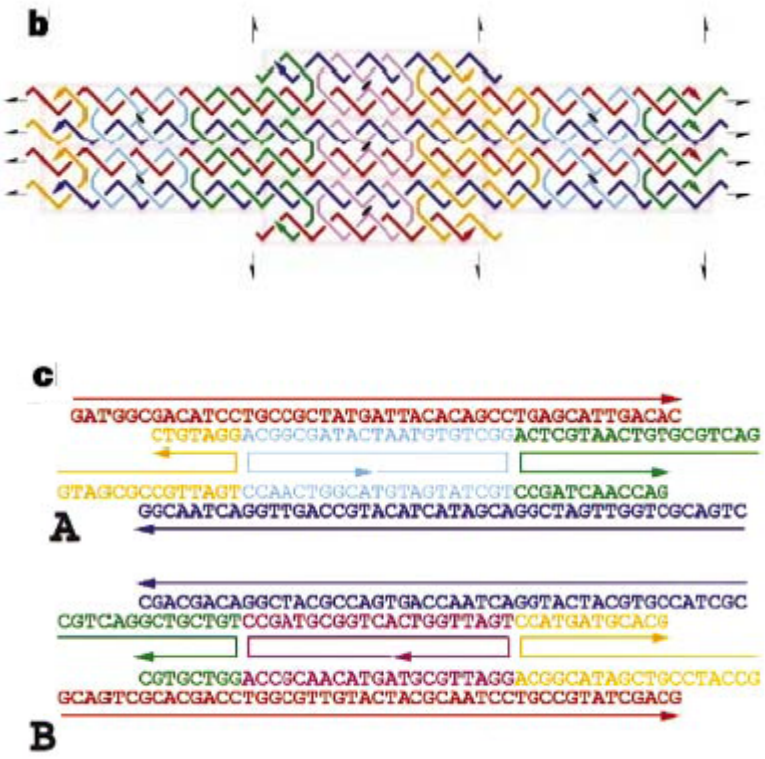

Figure 1.1 Design of nanoarray structure and arrangement into 2-D lattice **a**, A and B blocks have four colored edge regions each of which match exactly one colored region of the adjacent type B blocks. **b**, the lattice topology produced by the 10 strand system. A unique color is chosen for each strand. **c**, the actual sequences used in the experiment.
Adopted from (E. Winfree, F. Liu, L. A. Wenzler and N. C. Seeman *Nature* **394**, 539-44 (1998))

In this project we will make use of the fact that there are infinite strands in the lattice structure, and we will employ one of these two strands (blue strand). This strand will be used as a nucleation site for the crystals to grow on. Upon attaching this strand to specific locations on a given surface, we will be able to grow the nanoarray sequentially with more control. As is shown in Fig. 1.2 the blue strand consists of multiple copies of a 95 base sequence which runs throughout the two blocks (A and B), extending horizontally through the lattice (as also depicted in Fig. 1.3).

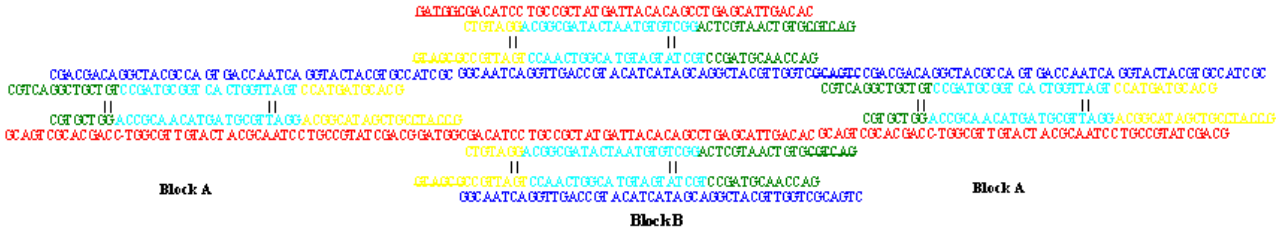

Figure 1.2 Diagram shows the formation of the long blue strand as a result of the assembly of different units of the array. Diagram shows just 4 blocks

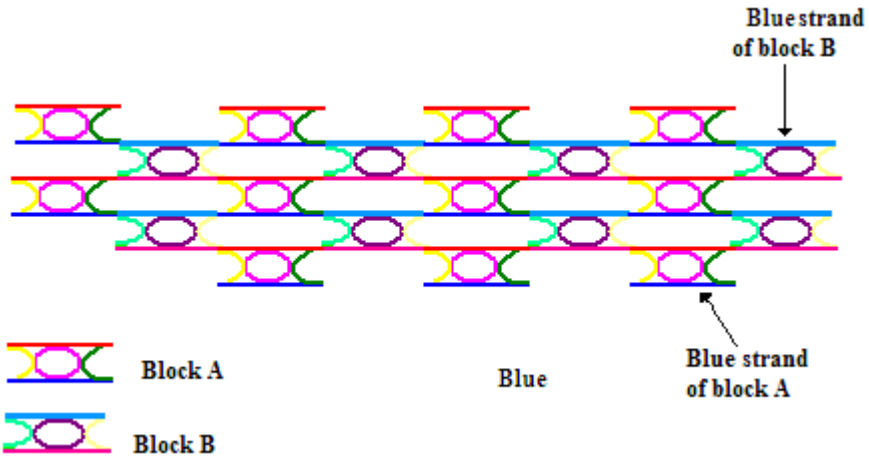

Figure 1.3 Diagram of the 2-D lattice showing the blue strand formed by combining the blue strand of block A and the blue strand of block B.

In an example system, proposed to DEPSCOR in Sep 2003, a glass or silicon substrate will be patterned with gold and platinum dots at 2 μm spacing, and then selectively two different capture strands (30 bases each) will be attached to the surface. The two strands are chemically modified to assure selectivity of binding. One strand is isocyanide labeled to enhance attachment to the platinum dots, the other is thiol modified to drive attachment to the gold spots.

This step should lead to an ordered array of two different DNA recognition sites (Fig. 1.4). After forming the two recognition sites the substrate will be exposed to a solution of the blue strands (multiple copies of the 95 bases formed by the two blue strands of block A and B), which ideally will have two specific ends complementary to the capture strands. We believe that by doing so we will form an ordered array of multiple similar nucleation sites attached to the surface.

The second step will be to expose the substrate sequentially to the optimum volume of solution containing block A and/or B. It is worth noting that modified blocks or totally different blocks that can bind to the assembly can be incorporated into the array as well. The flow of the different solutions (block A, block B, buffer, etc) will be monitored electronically using a controlled microfluidic device. All the experiments will take place in solution, but the arrays will be formed at well defined locations on the surface.

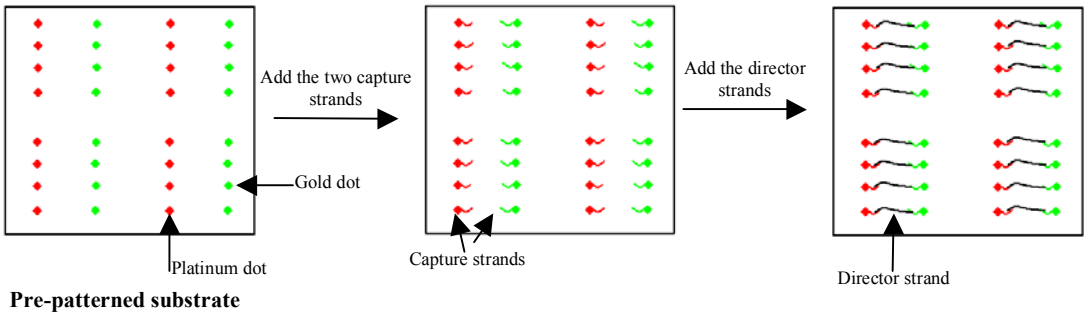

Figure 1.4 Diagrams showing the different steps for making an array of director strands. After patterning the surface with arranged gold and platinum spots, self directed capture strands are exposed to the surface. The two strands selectively bind to the gold or platinum dots via respectively thiol or isocyanide modification. Then the long director strand, with two specific ends, is added. The director strand will stretch out between the two capture strands, where the sequential growth of the nanoassembly will take place.

Now that we have introduced the problem, herein we describe our approach to overcome this problem. We will first use a viral amplification technique called Rolling Circle Amplification. Briefly, RCA is non-thermal amplification procedure, driven by DNA polymerase in the presence of a single stranded DNA circle and primer, which will produce multiple complementary copies of the template (ss-DNA circle). A complement strand of the long blue (95 bases formed by the two blue strands of block A and B) must be chemically synthesized. Then this 95 base strand is circularized and used as the template for a RCA reaction. The multiple copies of synthesized DNA will be further modified to incorporate two specific sequences into the two ends of the DNA strand. These two ends are purposely designed to have two different restriction sites. Finally, the new double stranded DNA will be inserted in bacteria plasmids (cloned) to give the desired single stranded DNA. In addition, the multimeric DNA strand will be evaluated as a substrate for possible use in the generation of one-dimensional nanoarrays. Having a spacing of ca 30 nm (95 bases) in the DNA strand has a big advantage for one and even two dimensional patterning. We present efforts directed toward decorating this DNA with gold nanocrystals.

2) DESIGN AND SYNTHESIS OF ROLLING CIRCLE AMPLIFICATION PRODUCT

INTRODUCTION

Many plasmids and bacteriophage (pC221, lambda phage and M13) and certain pathogenic RNAs, such as viroids replicate their genetic material (DNA or RNA) by the mechanism called “rolling circle”

Bacteriophage λ:

λ phage is a typical example of bacteriophage with a 49 Kb linear double stranded DNA genome (3). This linear molecule consists of two complementary strands of DNA with two free 12 base sequences cached at the ends. The two sticky ends are complementary and can base pair to form completely circular double stranded DNA. The λ cohesive ends are called the cos sites and they play two distinct roles. First they allow the phage genome to be circularized inside the cell host, which allows the phage genome to be replicated with the rolling circle replication mechanism. Circularization also protects the genome from degradation by bacterial exonucleases. Second these cos sites will play the role of recognition sequences for the endonuclease that cleaves the long DNA repeat producing individual copies of the λ genome. Circularization is also an essential step if bacteriophage lambda chooses a lysogenic mode of growth.

Bacteriophage lambda replicates in two stages, early replication also called **theta** phase then after 15 to 20 minutes bacteriophage λ switches to replication by a rolling circle mechanism. It is not known what causes the switch from one mechanism to the other.

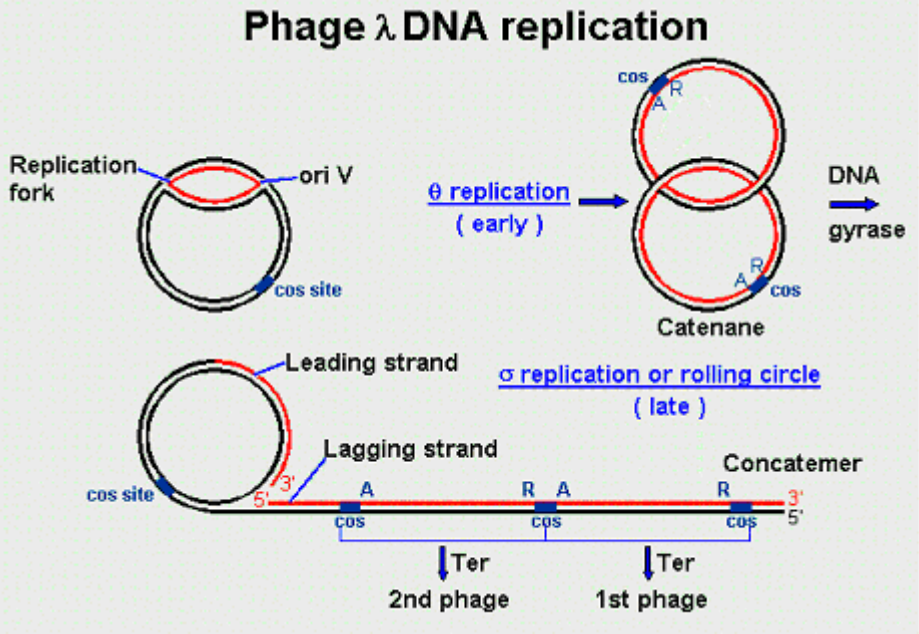

Figure 2.1: Schemes of replication machinery of lambda phage (http://www.brunel.ac.uk/depts/bl/project/molgen/virus/lysogen/dnarbac.htm)

Bacteriophage M13

Bacteriophage M13 is an example of a filamentous phage. The M13 DNA molecule is much smaller than the λ genome, being only 6407 bases in length (4). It is circular and interestingly enough that it consists entirely of single stranded DNA. When the phage attaches to an *E. coli* cell, this DNA molecule is injected into the cell where most of it is coated with single-strand binding protein (SSB). Since bacteriophage M13 does not code for its own DNA polymerase, it must use the host cell machinery in order to replicate.

Its single stranded DNA genome is a perfect template for DNA synthesis by the rolling circle replication machinery. However, although most of the genome is single-stranded, one part of it forms a double-stranded hairpin. This region somehow can serve as a promoter for the host cell RNA polymerase, which transcribes a short RNA primer. Transcription also disrupts the hairpin. DNA Pol III can then take over and synthesizes a double stranded DNA molecule. This double stranded DNA molecule is known as RFI-replicative form I. Further replication of RFI proceeds by means of rolling circle replication. The gp2 endonuclease, which is encoded by the phage gene 2, nicks the RFI DNA at a specific site. Rolling circle replication now occurs with displacement of a single strand.

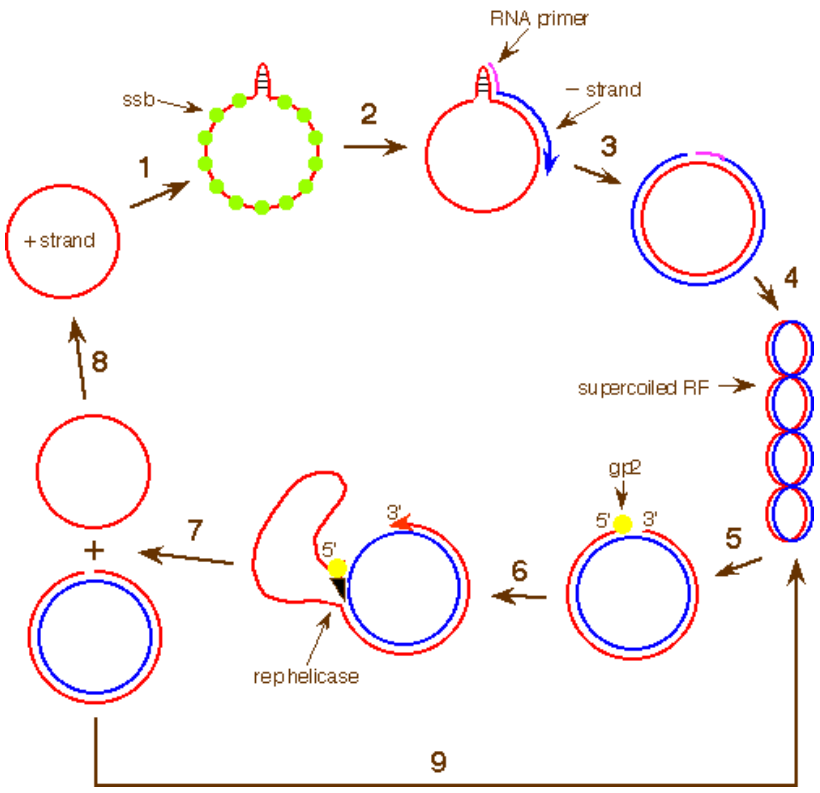

Figure 2.2: Replication schemes of simple single strand DNA phages, like M13 (http://www.bio.jhu.edu/~020.330/m13dna.htm)

The synthesis of long repeat DNA by rolling circle replication is possible *in vitro* using a single stranded DNA circle, highly specialized polymerase enzyme and a primer which provides a free OH group and initiates the polymerization.

We describe here the enzymatic ligation of a 95 base linear oligonucleotide followed by its use as a substrates for DNA polymerases. We find that the 95 mer circles can serve as efficient templates, and that tandem repeat strands as long as 10,000 bases are produced. Our studies further demonstrate the repetitive nature of the product by enzymatic cleavage yielding unit-length oligonucleotides. This rolling circle amplification technique represents a potential useful method that might be used in several ways such as in DNA diagnostic techniques, gene therapy, and as components in DNA nanostructure.

MATERIALS AND METHODS

Gel Electrophoresis

Gel electrophoresis is a method that separates macromolecules, either nucleic acids or proteins, on the basis of size, electric charge, and other physical properties. A gel is a colloid in a solid form. The term electrophoresis describes the migration of a charged particle under the influence of an electric field. In this study we used TBE-Urea precast

gels from ***(BIO-RAD)***, and made agarose gels (SeaPlaque GTG agarose from ***(CAMBREX)***. The caption for each gel image includes a description of the gel. 1X TBE buffer was used as the running buffer, SYBR Green I ***(Molecular Probes)*** 1:10000 in 1X TBE buffer was used for all gel staining.

Atomic Force Microscopy

The atomic force microscope is one of about two dozens types of scanned-proximity probe microscopes. All of these microscopes work by measuring a local property such as height, optical absorption, or magnetism with a probe or "tip" placed very close to the sample. The small probe-sample separation (on the order of the instrument's resolution) makes it possible to take measurements over a small area.

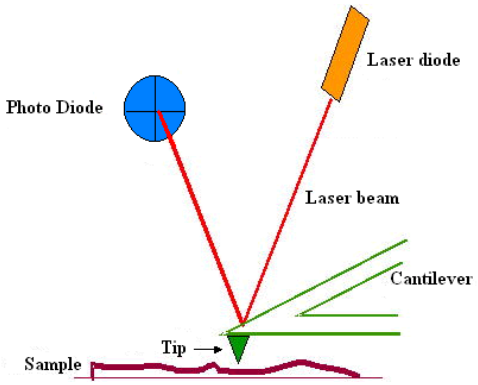

Figure 2.3: Concept of AFM and the optical lever

Preparation of ssDNA Circles

-95 base linear, 5'-Phosphorylated oligonucleotide:

5'/5Phos/GCTGCTGTCCGATGCGGTCACTGGTTAGTCCATGATGCACGGTAGCG

CCGTTAGTCCAACTGGCATGTAGTATCGTCCGATGCAACCAGCGTCAG-3'

-24 linear oligonucleotide (Splint): 5'-TCGGACAGCAGCCTGACGCTGGTT-3'

The synthetic strategy is elucidated in Fig. 2.4. A mixture of 28 pmol of the 95 base oligomer, 50 pmol of splint, 4 μmol of 100 mM DTT, 40μL 10X ligase buffer and 307 μL water was maintained at 65 ^{o}C for 10 min, then the solution was allowed to cool down to room temperature. The reaction mixture was further cooled to 16 ^{o}C, and 7.5 μL of T4 DNA ligase 20 U/μL **(*Promega*)**, was added. After incubation over night at 16^{o}C, the reaction mixture was extracted by phenol/chloroform/isoamylalcohol (25:24:1), ethanol precipitated (see protocol in Appendix A) then dissolved in either water or TE buffer. The remaining linear precursor and the splint were subsequently removed by treatment of the sample with exonucleaseVII ***(USB)***, an exonuclease that digests DNA from either the 5' or 3' end. The sample was then desalted by gel filtration on MicroSpin G-50 columns ***(Amersham Pharmacia Biotech).*** In order to denature and digest the splint that may remain bound to the circles after ligation the sample was heated to 80 ^{o}C for 3 min then chilled in ice before treatment with the exonuclease. The extraction and precipitation procedure was then repeated to completely remove exonucleases and single nucleotides. The analysis of the resulting sample on a denaturing polyacrylamide gel showed that pure ssDNA circles were synthesized (Fig. 2.5). The concentration of the circular DNA was determined by OD measurement.

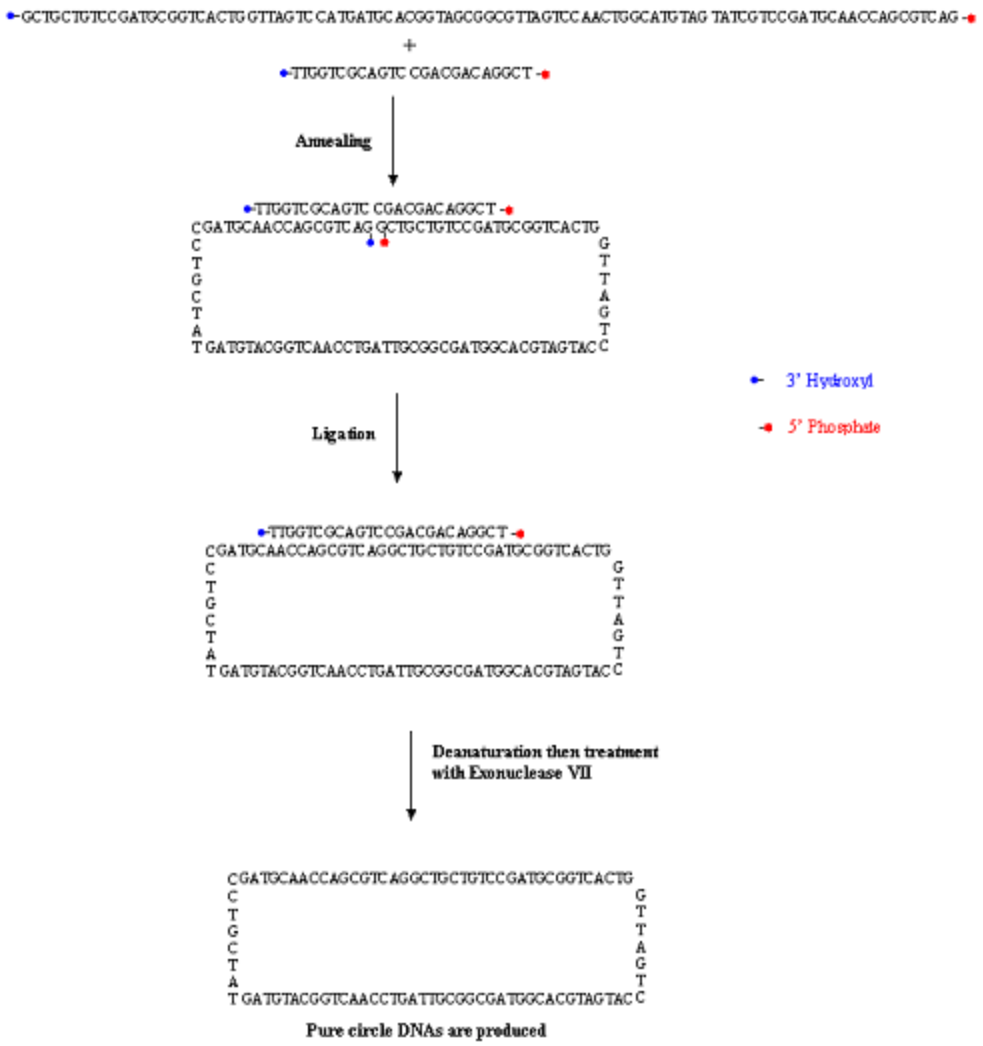

Figure 2.4: Scheme of ssDNA circularization using splint oligonucleotides followed by degradation of non-circularized DNA and splint by exonuclease VII

RCA Reactions

In the RCA reaction the splint is used as a primer, we used Sequenase Version 2.0 from ***(USB)*** as polymerase. A mixture of 1 pmol of pure circles, 10 pmol of primer, 20 μL of 5X reaction buffer (supplied with the polymerase), and 76 μL water was heated to 80 ^{o}C

for 3 min then allowed to cool to room temperature. Then 10 μL of 100 mM DTT, 4 μL of a mixture containing all four dNTPs (25 mM each), 2.5 μL of SSB protein, and 4 μL of Sequenase 2.0 (13U/μL) were added and the reaction mixture was incubated over night at 37 ^{o}C. Finally the reaction mixture was extracted by phenol/chloroform/isoamylalcohol (25:24:1), ethanol precipitated then dissolved in either water or TE buffer. Fig. 2.6 shows that the non-circularized ssDNA and the splint are totally digested.

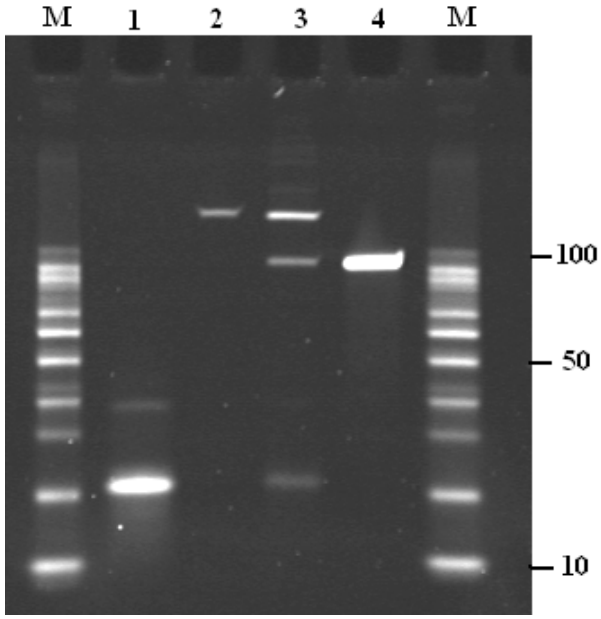

Figure 2.5: Analysis of the 95 base ssDNA circle by10 % precast TBE-Urea gel Electrophoresis. Lane M, 10 bp ladder; lane 1and 4 splint and linear single stranded 95 mer DNA strands, respectively; lane 3 reaction mixture containing circles after enzymatic ligation and remaining ssDNA and splint; lane 2 purified circles after degradation of non-circularized oligonucliotides by exonuclease VII.

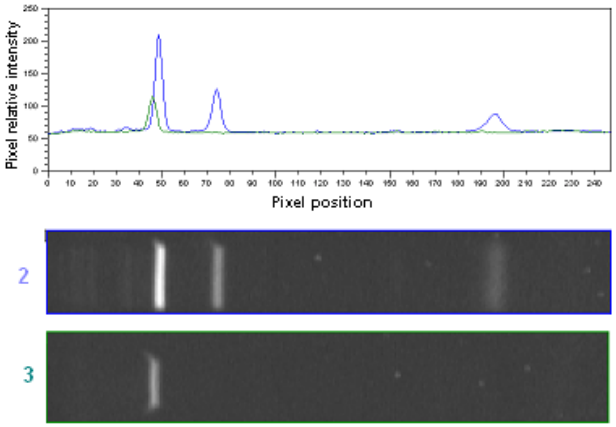

Figure 2.6: Plot of pixel intensity versus distance (pixel number position) as sampled along lanes 2 and 3 from gel in Fig. 2.5. Left is top of lane, areas under curves are quantitative approximation of DNA mass in each band.

Cleavage of RCA Products into Unit-Length Oligonucleotides

For some applications it might be desirable to cleave the long repetitive RCA product into unit lengths since oligonucleotides have many uses. Moreover partial and complete cleavages provide further evidence that the long DNA strands being synthesized are true repeating copies of the circle.

To test this we ran PCR (Polymerase Chain Reaction) on a sample of the RCA products. The double stranded DNA produced was checked for restriction enzymes sites. We found that the *Cfo I* (restriction enzyme with double stranded cleavage activity) has only one recognition site in every single repeat of the multimeric product.

1- PCR Reaction

A sample reaction composed of 38 μL of master mixture (312 μL water, 60 μL 10 X *Taq* polymerase reaction buffers, 72 μL of 25mM $MgCl_2$, 12 μL of a mixture containing all four dNTPs 3 μL each, and 1μL of *Taq* polymerase ***(New England Biolabs)*** 5U/μL), 2 μL of primers (1 μL each), and 10 μL templates. The settings of PCR are as follows:

- Initial melting 85 degrees C for 5 min
- Cycles 1-32 95 degrees C 10 sec, 45 degrees C for 45 sec, 72 degrees C for 3 min

Another proof of the repetitive nature of the RCA product is demonstrated using single primer PCR. In contrast to normal PCR we proved that DNA replication of the multimeric products is possible using only one primer (24 bases complementary to the template) and the template itself acts as a second primer. Gel analysis of PCR products show a relative increase in length arises from using the template as a second primer (Fig. 2.12)

2- Partial Digestion

The partial digestion was performed, and the progress of the reaction, at 0^0 C, was monitored as a function of time. Aliquots were taken every 5 min, stopped with 2 μL 0.5 mM EDTA and analyzed using 1% non-denaturing agarose gel electrophoresis. The reaction mixture was composed of 2.5 μg double stranded DNA (PCR of RCA product described previously), 5.7 μL B reaction buffer, 0.57 μL BSA and 1 μL *Cfo I* (***Promega).*** Fig. 2.13 presents the banding pattern obtained.

3- Complete Digestion

The same reaction mixture used for partial digestion was incubated for 1 hour at 37^0 C then analyzed by 10% precast TBE-Urea gel Electrophoresis. Fig. 2.14 shows that the long multimeric product is cleaved to unit-length oligonucleotides having the same size as the initial templates. The reproduction of the starting material demonstrates that the rolling circle amplification combined with an efficient digestion might be useful method for preparing specific DNA sequences at a large scale.

RESULTS AND DISCUSSION

The scheme for ssDNA circularization using a splint is displayed in Fig. 2.4. The reaction was performed at a very low concentration of both 95-mer ssDNA and splint (see materials and methods) favoring intra-ligation versus inter-ligation. Analysis of the reaction mixture after circularization using gel electrophoresis demonstrates one type of inter-ligation product; long DNA strands produced by end-to-end ligation. Treating the RCA templates with exonuclease, which digests ssDNA from either the 5' or 3' end, reduces the possibility of RCA product contamination with multimerization products. Fig. 2.5 and Fig. 2.6 demonstrate the purity of the free ssDNA circles synthesized.

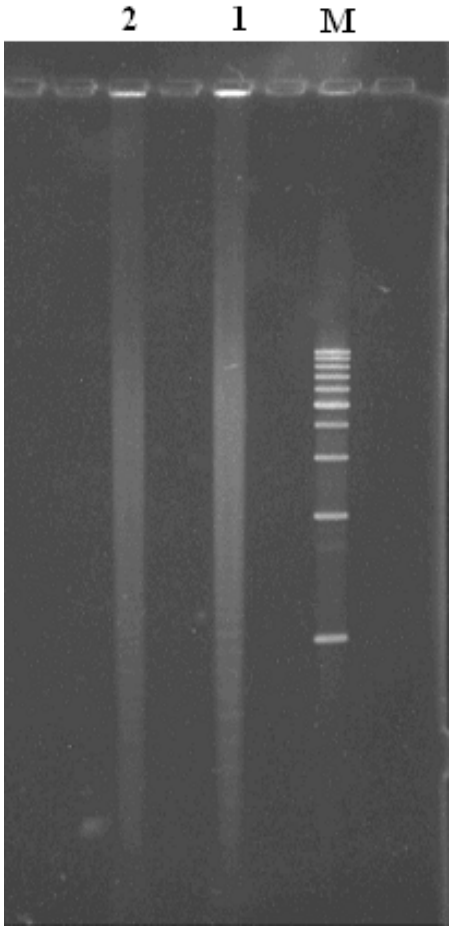

Figure 2.7: Analysis of RCA products by 1% non-denaturing agarose gel electrophoresis. Reaction was performed as described in the experimental section. Lane M, 1 Kb marker; lane1 and 2 RCA products using normal and biotinylated primers, respectively.

Fig. 2.7 shows the continuous size distribution of the RCA product, which ranges between 0.5 to 15 Kb, indicating that the templates are amplified approximately 5 to 150 times. The reaction continues as long as the enzyme, circle and product are complexed. When the complex disassembles the reaction ceases. The smear-type of RCA product shown is explained by the non-specified ending of the amplification mechanism; all product lengths are equally likely. The specific reasons for complex disassembly are currently ill-defined. We believe that the size of the circle is a critical factor determining

the binding strength between the enzyme and the template, and implicitly the size of the multimeric product. In this study the size and sequence of the template was defined for use in further research, other researchers have shown the size-dependence of RCA product as related to the size of template circles (5), but the phenomena is not fully understood.

Another aspect of the Rolling Circle Amplification mechanism is the banding pattern shown in the bottom part of the gel image (difficult to discern in Fig. 2.7); similar results were reported by other researchers (6). One explanation could be the existence of one or more "weak sites" in the template where the enzyme/product complex is most likely to fall off, ending the amplification process. Another possibility is that the primer excess interrupts replication. It has also been reported (6) that this banding pattern might be explained by the formation of double stranded DNA product by an undetermined miss-priming process. Thus we see in the gel results a series of bands, each approximately one monomer unit larger than the last, reflecting the increased likelihood that products will be of defined length $l = n \times 95$, where l is length in bases, n is an integer representing the number of cycles the circle has undergone.

It is worth noting that by introducing a second primer complementary to the RCA product a so-called geometric hyperbranched RCA (HRCA) product will be generated. The signal amplification in an HRCA is much faster with very high yield (10^5 times higher than linear RCA, (6)). In addition, for reasons different than those discussed above, distinct ladder-type bands characterize HRCA product, also the product is double stranded. Other experiments using our RCA product as probe for short DNA sequences were successfully performed, excluding the possibility of our product being double stranded.

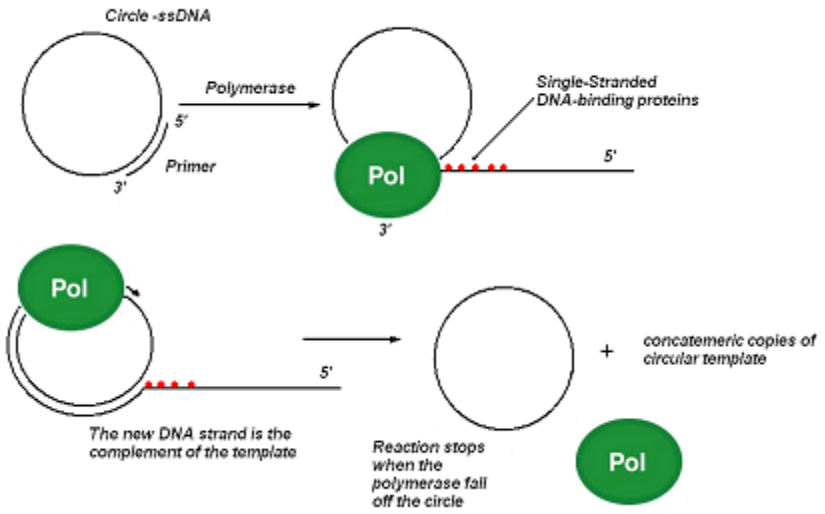

Figure 2.8. Schematic of DNA synthesis by rolling circle amplification, in which ssDNA circles act as templates for DNA polymerases. Multimeric repeats of the template is generated.

One purpose of this study is the microscopic investigation of our RCA product. Atomic Force Microscopy (AFM) as an imaging technique will be of central interest in determining the structural topography of DNA strands at the nano-level. Fig. 2.9 and Fig. 2.10 are AFM representations of the RCA product on mica. One limitation of the AFM technique is the discrepancy in x/y dimension as compared to z measurement. The AFM tip shape defines the resolution in the x-y plane (Fig. 2.3), whereas the z resolution is defined by a different AFM component (z piezo-electric crystal). A broadened tip tends to widen features in the x-y plane but has little effect on height plane data, for this reason our DNA appears broader (5 to 10 nm) than it is high (1 to 3 nm). Note also that Fig. 2.10 shows nearly complete coverage of the mica when we applied a relatively concentrated DNA sample to the surface.

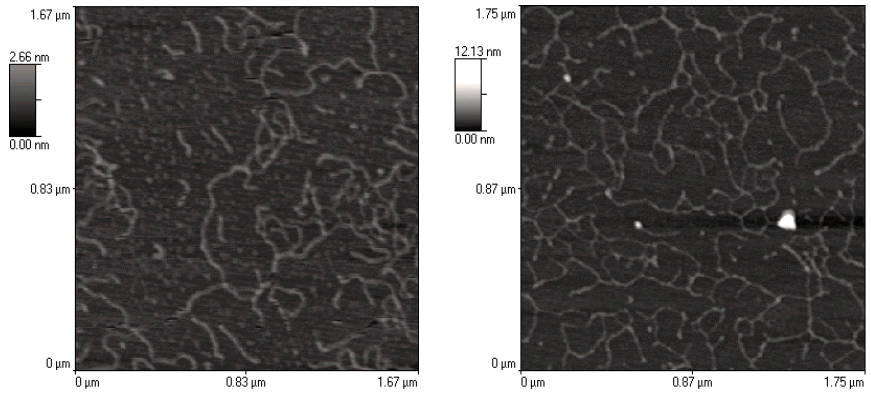

Figure 2.9: AFM image of RCA product, average length approx 2µm

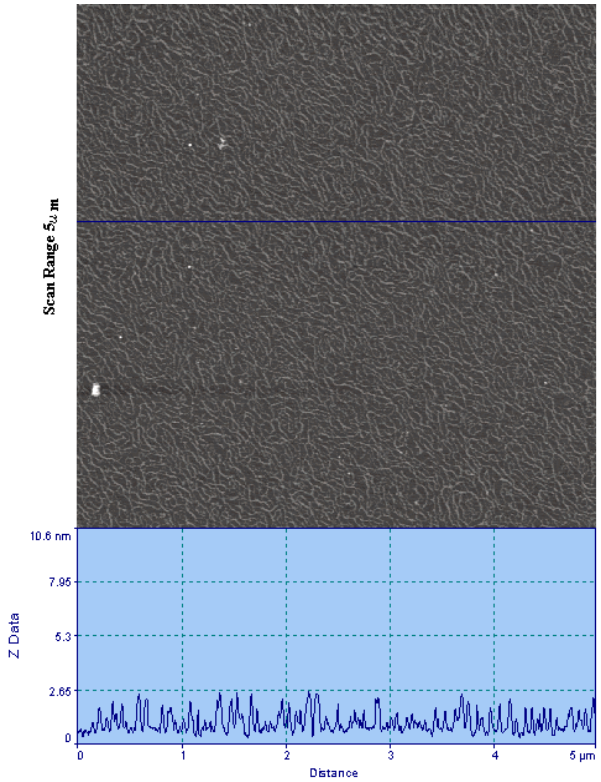

Figure 2.10: A low magnification AFM image showing plentiful RCA product on mica Note consistent z axis (height) measurement of 1.5 nm for each DNA strand as sampled along the blue line in the image.

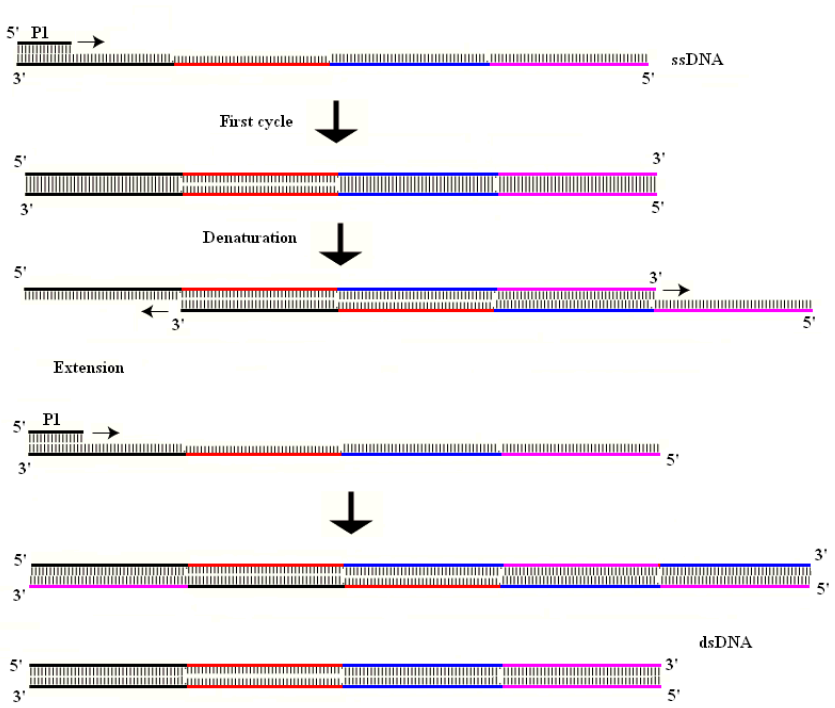

Figure 2.11: Schematic of PCR reaction using one primer. The scheme shows how the multimeric product it self can act as a second primer giving longer dsDNA product

Fig. 2.11 shows schematically how a PCR reaction might work using just one primer. The repetitive nature of the RCA product makes it possible that the two strands synthesized during the first cycle can be shifted and rebind without full complementarily after denaturition. That will leave free single stranded regions at both ends to be filled in by the polymerase. Augmentation in PCR product size is clearly seen in Fig.2.12 where 2 primer PCR was run as control. Increasing the size of product in this unusual PCR reaction is directly related to the way the two strands rebind. If small oligomers with short complementary regions could bind to high molecular weight molecules one might expect a large increase in size distribution with single primer PCR. However, ssDNA

molecules are unlikely to bind without significant complementary overlap. Thus most product-product annealing leaves relatively short single stranded regions so the length increase is subtle.

By looking at the previous scheme one may expect a ladder-type product due to the difference in size being multiples of 95. Our gel results reflect a predominantly smear-type ill defined product distribution. In explanation, the scheme shows the RCA product as n-copies of 95 bases, this model is an over simplification of the real process. The equation $l = (n \times 95) + m$ is a more accurate prediction of RCA product length (where m is that undefined fraction of the final cycle before termination). Thus as our PCR uses our RCA product as both template and primer the same ill-defined sequence of bases (m) will appear in all PCR product involving RCA derived primer.

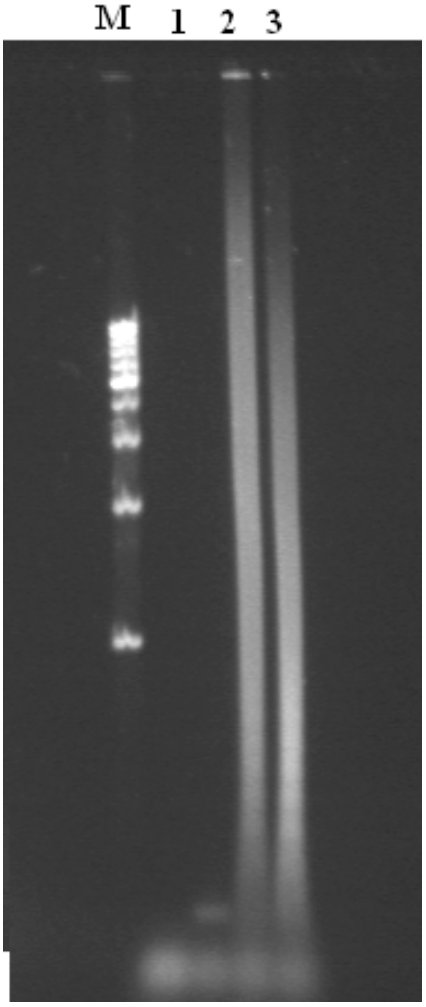

Figure 2.12: PCR of RCA product analyzed by 1% non-denaturing agarose gel electrophoresis showing increased in length when one primer is used. Lane M, 1 Kb ladder; lane 2 and 3 PCR of RCA product using one and two primers, respectively.

The goal of this study is to generate high MW product of predictable sequence from a particular circle template; the cleavage experiments are just evidence that the circle acts as a true template for the rolling synthesis. In addition, for other applications it might be advantageous to cleave the long repeating multimeric copies into unit-lengths since oligonucleotides of defined length and sequence have many uses.

Fig. 2.13 shows the banding patterns produced during cleavage, with an enzyme with a periodic location of recognition site that occurs once per unit. Furthermore, the time course of the reaction defined the size of digested product. Note that successively smaller

product results as incubation time increases. The enzymatic reaction was carried out in ice to reduce the activity of the endonuclease. The combination of efficient RCA synthesis and optimum cleavage strategy will be a useful method for preparing oligonucleotides of defined length and sequence.

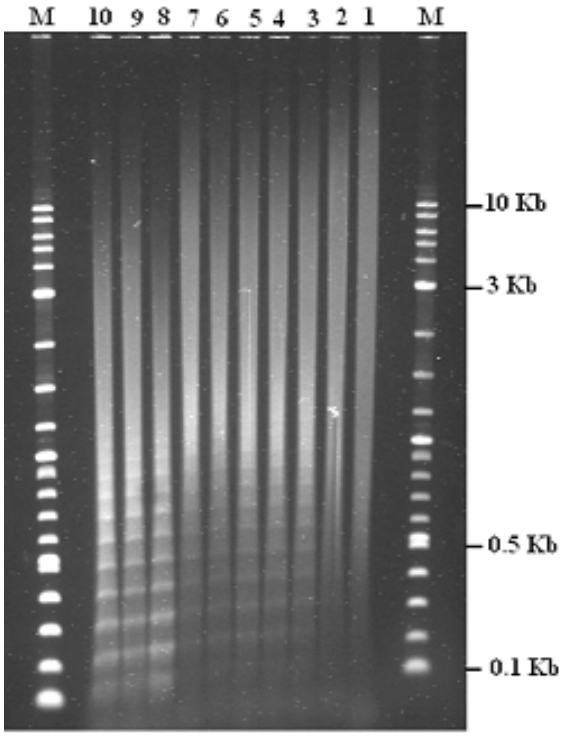

Figure 2.13: Partial digestion of multimeric products with restriction endonuclease *CfoI*. Gel images shown is for a 1% non-denaturing agarose gel. Note banding patterns produced. Lane M 1 Kb ladder; successive lines from 1 to 10 represent aliquots of cycle time digestion products taken consecutively from 0 to 45 min.

Fig. 2.14 shows the complete digestion of multimeric RCA product. *Cfo I* is a restriction enzyme with double stranded activity, so we had to double strand our sample in a separate enzymatic polymerization. The gel analysis shows an extra band in lane 1; compared with lanes 2 and 3 we see that the extra band is the remaining PCR primer. In addition, complete digestion serves as a further proof that the enzymatic synthesis is a true rolling progression of the enzyme around the circle.

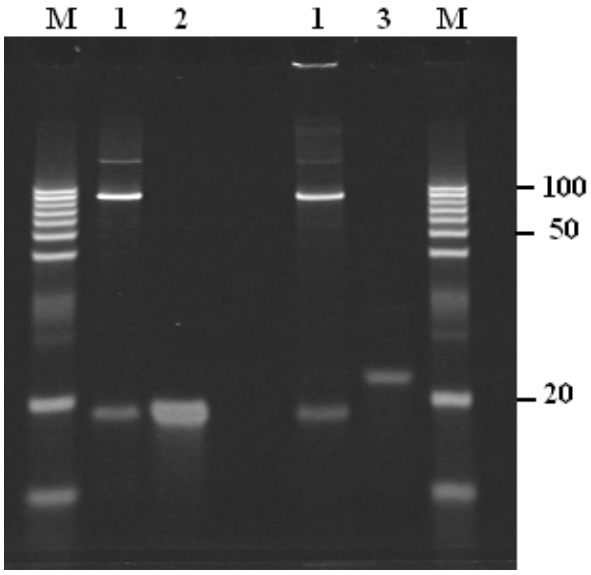

Figure 2.14: Complete digestion of multimeric products analyzed by 10% precast TBE-Urea gel Electrophoresis. Lane 1, unit-length oligonucleotides produced by complete digestion; lane 2 and 3 represent the 2 PCR primers.

CONCLUSIONS

RCA is a molecular amplification method with the unique property of generating long repetitive on localized (surface bound) primed. Unlike other amplification techniques, such as PCR, RCA produces a single-stranded DNA molecule that is composed of tandemly repeated copies of the complement to the template circle that remains linked to the DNA primer. RCA has been widely used in DNA microarrays and disease diagnostics. In RCA microarrays RCA primer is immobilized to a surface from its 5'-end leaving 3'-end free to which the circle hybridizes. The linear product is detected by hybridization of short oligonucleotides containing fluorescent labels. (7). It is now possible to detect as few as 150 molecules bound to the microarrays using RCA. In addition, as an isothermal amplification technique, RCA is well suited for generating localized signals at specific microarray locations by on-chip amplification. By its nature, isothermal amplification excludes the complications caused by high and widely varying temperature (protein denaturation).

In the other hand, producing tandem repeats of the template copy itself represents a big advantage for DNA based nanostructure fabrication. It is clear that repetition is an intrinsic property of the array structure. This component of the project demonstrated the possibility of producing multiple copies of long ssDNA, using RCA technique. We also verified that the circle DNA was a true template of the generated product.

Two further problems need to be solved. First, to benefit from this amplification technique, we need to be able to control the size of the DNA produced. Ideally, an integral number of copies will be most useful. Second, adding two unique, specific ends will enable us to hybridize the synthesized DNA to the surface. In the next section of the project these two problems will be addressed.

3) DESIGN AND INTEGRATION OF SPECIFIC ENDS TO PRODUCE NANOSTRUCTURED MACROMOLECULES

As described above, we succeeded in producing a long strand of DNA consisting of multiple copies of the blue strands of block A and block B. This DNA will be used as a director strand or nucleator in future studies. This strand will be attached to a substrate via thiol and isocyanide modified oligonucleotides respectively linked to gold and platinum dots on the surface of a substrate. The main purpose of the component of the work described here was to ensure specific attachment at each location. The later is not guaranteed unless two specific ends are incorporated into the multimeric DNA. Our approach involves two major steps. The first is to add 18 bases to the primer used for the rolling circle amplification reaction. The sequence of this tail is unique and provides control over one end of the RCA-synthesized DNA. The second step is to use PCR to integrate another specific, unique sequence at the other end of the DNA strand. This PCR procedure is somewhat complicated and three primers were used instead of the more common two primers.

I. Tailed-primer RCA

We increased the length of the sequence of the rolling circle amplification reaction primer from 24 to 42 bases, keeping the same binding site formed by the original 24 bases. The extra 18 bases form a tail that will remain attached to the long synthesized

sequence. As shown in Fig. 3.1 each synthesized multiple copy oligomer has this tail. For later uses we designed the extra 18 bases sequence so that it includes a specific restriction enzyme site.

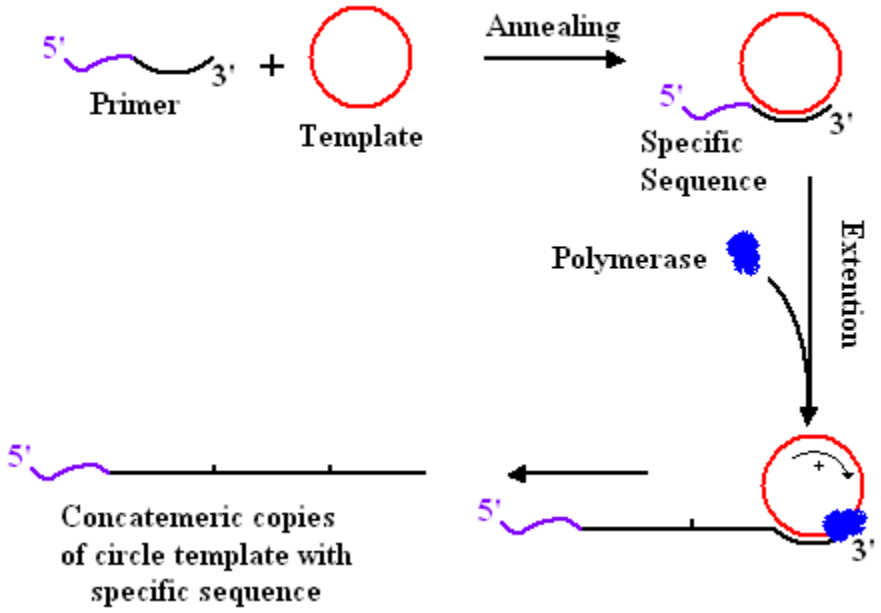

Figure 3.1 Scheme of Tailed-primer Rolling Circle Amplification reaction
The extra 18 bases (purple color sequence) appears in all the new synthesized multiple copies

METERIALS AND METHODS

- RCA primer sequence: 42 bases

5'-CATGTGACCTCTTCTAGATCGGACAGCAGCCTGACGCTGGTT-3'

The red sequence denotes the extra 18 bases; this sequence will be dissimilar to the rest of the synthesized DNA. The 42 base oligonucleotide was ordered from **IDT** (HPLC purification), diluted in water to the same concentration as that of the primer used for the normal RCA reaction previously described.

A mixture of 1 pmol of pure circles (same single stranded circle used in the previous Rolling Circle Amplification reactions), 10 pmol of the new primer, 20 μL of 5X reaction buffer (supplied with the polymerase), and 76 μL of water was heated at 80 ^{o}C for 3 min then allowed to cool to room temperature. Then 10 μL of 100 mM DTT, 4 μL of a mixture containing all four dNTPs (25 mM each), 2.5 μL of SSB protein, from **USB**, and 4 μL of Sequenase 2.0 (13U/μL), from **USB**, were added and the reaction mixture was incubated over night at 37 ^{o}C. Finally the reaction mixture was extracted by phenol/chloroform/isoamylalcohol (25:24:1), ethanol precipitated, then dissolved in either water or TE buffer.

- The DNA product was analyzed using a 1% non-denaturing agarose gel (1X TBE running buffer). A 25 cm gel was used at a field of 6.7V/cm, for a total running time of ca 4 hours.

RESULTS AND DISCUUSION

We designed the extra 18 bases of the sequence to contain the **XbaI** restriction site. This restriction site provides more control over the entire sequence. We inserted the restriction site sequence at the beginning of the original sequence so that if we digest the product, we recover the same starting material. The recognition site for the restriction enzyme is shown in blue below.

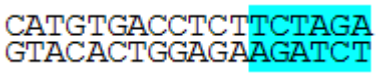

Figure 3.2 displays a gel image documenting success in production of long strands of DNA consisting of multiple tandem copies of 95 base pair repeats plus the 18 extra unique bases that are not repeated in the rest of the sequence. There does not appear to be any significant difference in the yield of the reaction compared to the previous RCA reaction at the same conditions. These 18 bases will form a recognition site with high importance for both PCR and for cloning. The length of the product ranges between 1 and 10 Kb, with high yielded near the 7 Kb range. We also see some product that did not run through the gel; this product seems to be much higher in molecular weight than 10 Kb. Not necessarily longer than the rest of the product, the sticking of the DNA to the well might be explained by the existence of double stranded DNA in the sample. It was suggested that the RCA might produce double stranded DNA as a result of the nonspecific DNA binding. This has the appearance of a ladder like RCA product (6). In our research we have other evidence for the formation of double stranded DNA in the normal Rolling circle Amplification reaction.

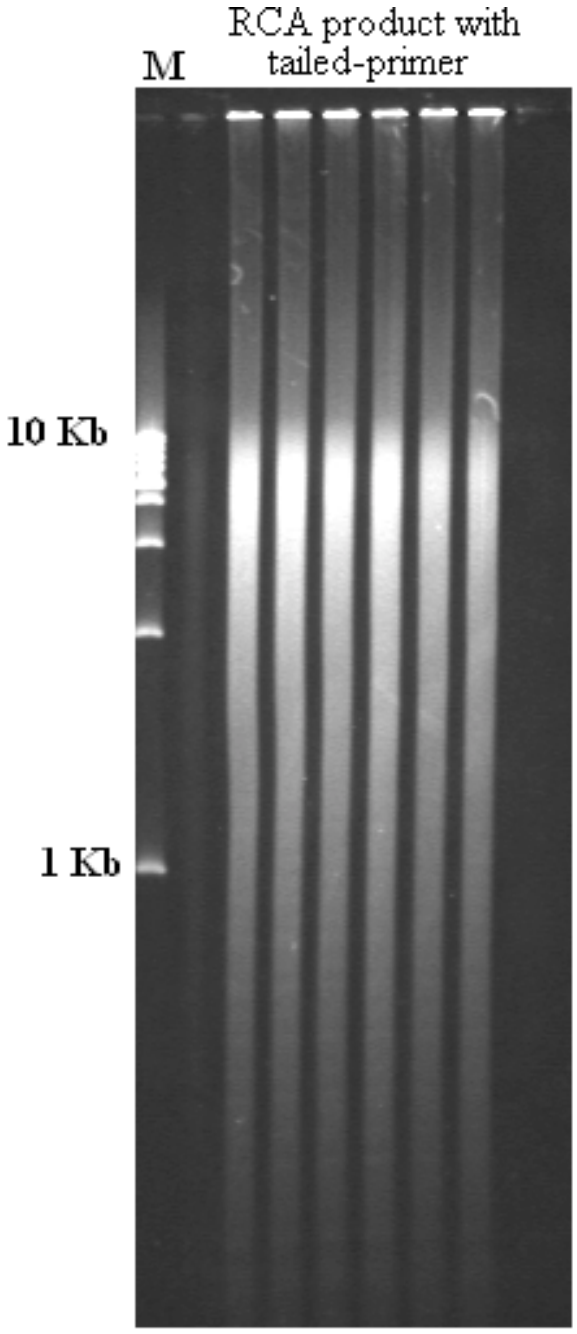

Figure 3.2: Gel Analysis of RCA products by 1% non-denaturing agarose gel electrophoresis. Reaction was performed as described in the experimental section. Lane **M**, 1 Kb marker; all the other lanes, RCA products using tailed-primer.

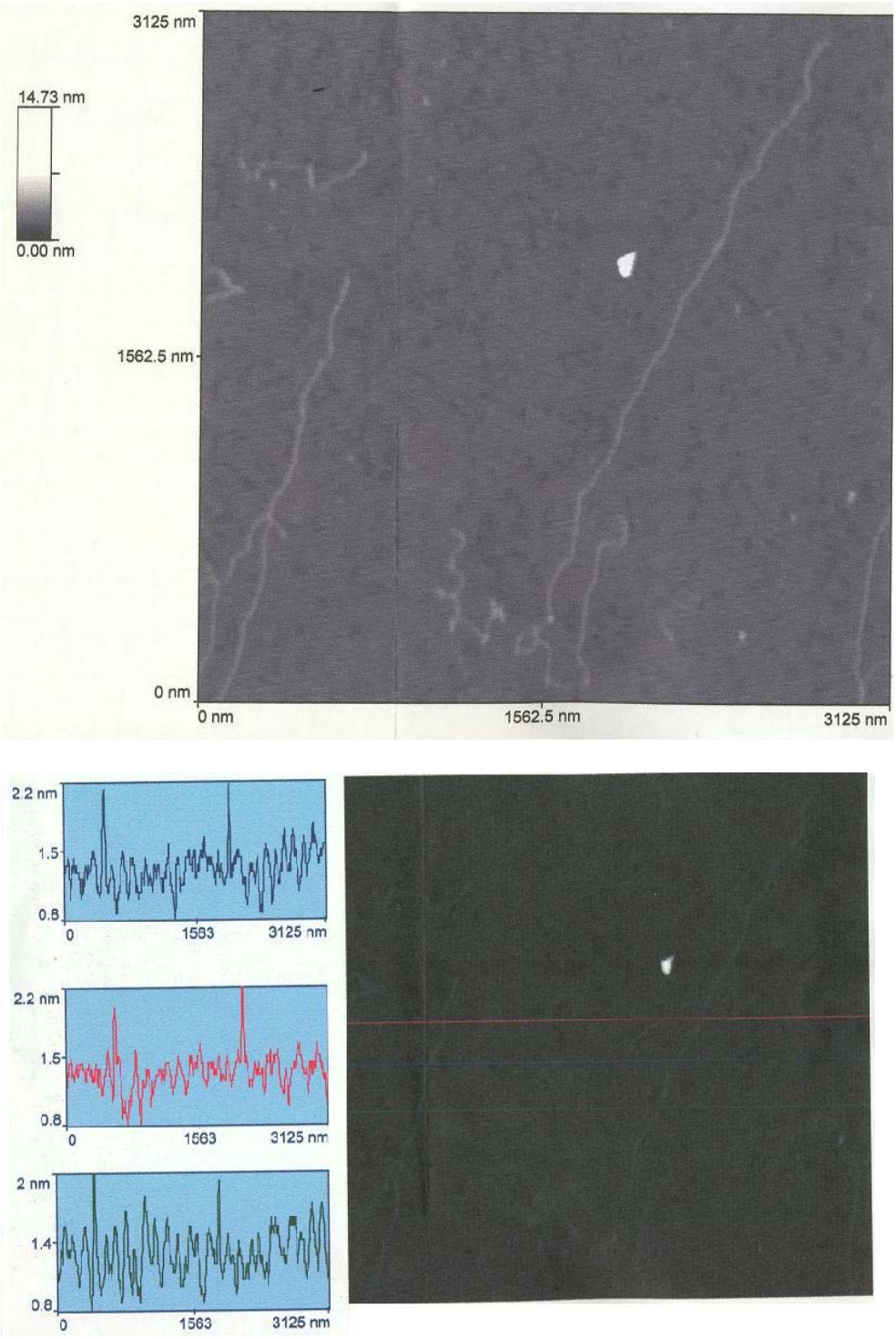

Figure 3.3: AFM image of RCA product previously described. The image shows a relatively long strand of DNA (ca 4 μm, higher than 10 kb). On the bottom analysis of the image shows that the average height of single stranded DNA is ca 1 nm.

II. Incorporation of a second end using a PCR reaction

MATERIALS AND METHODS

In this reaction we used a long PCR protocol. Unlike the normal PCR reaction, the effectiveness of long PCR results from the use of two polymerases: a non-proofreading polymerase is the main polymerase in the reaction (**Tth** polymerase in this case), and a proofreading polymerase (3' to 5' exonuclease activity, **Vent** in this case) is present at a lower concentration.

The reaction mixture composition and the PCR program are provided below

<u>50 microliter sample reaction in 1X Long PCR buffer</u>

10 µl of 5X buffer (recipe is given below)

5U **Tth** (1 µl if the concentration is 5U/µl)

0.02U **Vent**

0.4 µl of 25mM dNTP

1 µl forward primer (40 pmol/µl)

1 µl reverse primer (40 pmol/µl)

10 µl template (concentration empirically determined)

25.5 µl water

<u>10 ml 5X buffer</u>

4.25 ml of 1M KOAc

1.25 ml of 1M Tricine, pH8.7 at 25 degrees C (pH adjusted with KOH)

4.00 ml glycerol

0.50 ml DMSO

120 µl of 500 mM $Mg(OAc)_2$

Cycle times and temperatures

Initial melting 94 degrees C for 2 min.

Cycles 94 degrees C 15 sec, 72 degrees C for a variable time as indicated in the text (20 times).

Extension at 72 degrees C for 10 min.

The annealing temperature was determined using gradient-block PCR; we ran the reaction at annealing temperature between 45 degrees C and 60 degrees C with ca 1.2 degrees increment. This optimization is discussed on page 44.

Primers sequence

Primer 1: 5'-CATGTGACCTCTTCTAGATCG-3' (21 bases)

Primer 2: 5'-GCCATCCTCACTCGGAATTCTGCGGTCACTGGTTAGTCCA-3' (40 bases)

Primer 3: 5'-GCCATCCTCACTCGGAATTC-3' (20 bases)

Primer 2 and primer 3 have EcoRI restriction sites as indicated in red below.

```
5'-GCCATCCTCACTCGGAATTCTGCGGTCACTGGTTAGTCCA-3'
3'-CGGTAGGAGTGAGCCTTAAGACGCCAGTGACCAATCAGGT-5'
```

The three primers have the same annealing temperature (60 degrees C). Note that only 20 bases of primer 2 bind to the repetitive sequence.

All primers were checked for self-priming and self-dimerization using Oligo software. They do not show any serious design flaws (result not shown).

RESULTS ANR DISCUSSION

At this point we have a multiple tandem repeat DNA strand with one specific end. The goal is to produce two specific ends that can function differently as two different recognition sites. Having the first specific end at the 5' end of our strand makes it possible to monitor the other end using the PCR reaction. Fig. 3.4 shows the scheme of the PCR process.

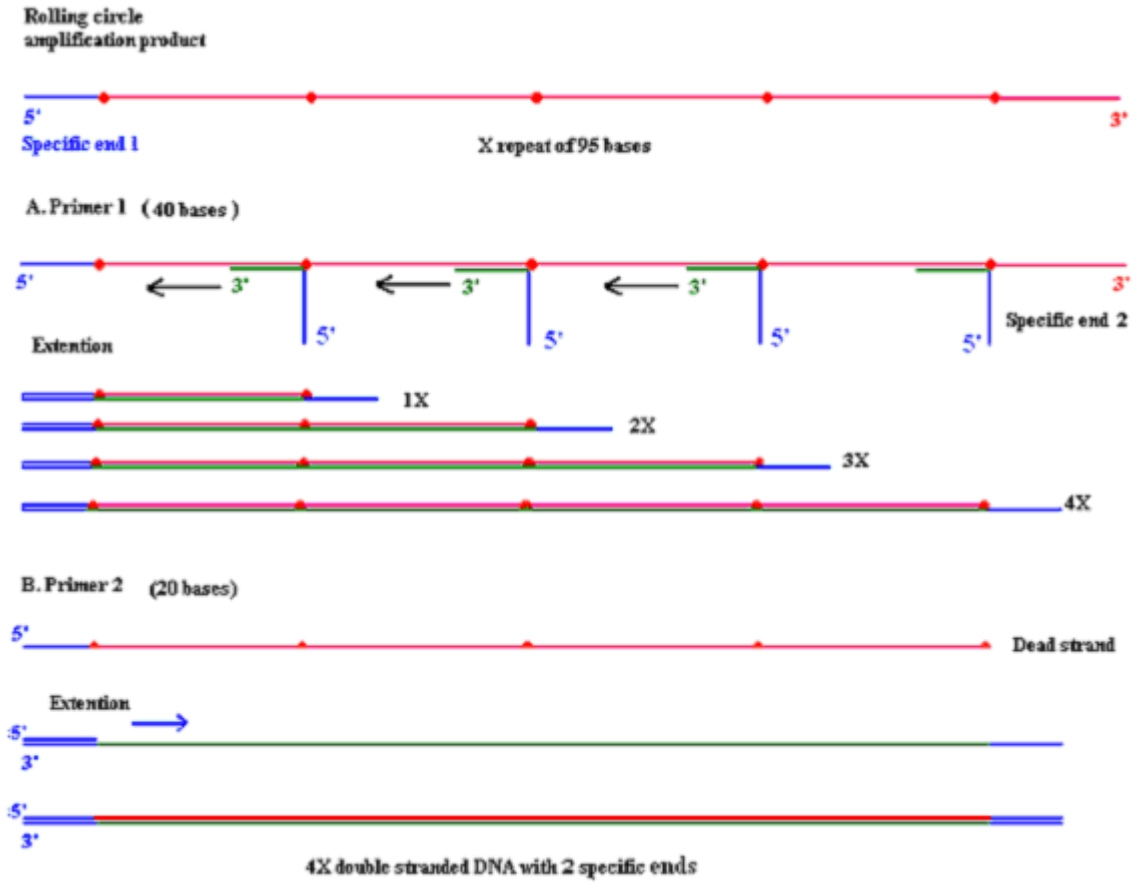

Figure 3.4: Scheme of the PCR reaction. The starting material which is long blue with a specific, unique end on the 5'is treated with long primer (40mers). The long primer has 20 base binding site, the remaining 20 form the specific end. Ideally after the first cycle this second end is incorporated into all products. Finally one strand can be chosen and amplified with two specific primers (1 and 3). This PCR amplification should yield mono-length product.

Based on the scheme shown in Fig. 3.4 we expect a ladder-like product to result from the first PCR (PCR of the RCA product using the long primer). We also expect no amplification if we use primer 1 and primer 3, because the binding site of primer 3 does not exist in the RCA product, it should be incorporated after amplification with primer 1. Amplifying the PCR product with primer 1 and primer 3 should make the bands more intense, ideally it will just amplify the strands that have the extra 20 bases in the 5'end. In addition, theoretically, extracting mono-length strands from the first PCR (by cutting a band) and amplifying it with primer 1 and primer 3 should give the same mono-length strands, however, amplifying it with primer 1 and primer 2 should yield multiple bands lower in molecular weight than the origin band extracted.

First PCR (PCR of RCA product)	Primer 1	Primer 2	Primer 3
Primer 1		Ladder-like product	No product
Primer 2	Ladder-like product		No product
Primer 3	No product	No product	

Table 1: Possible results of PCR of RCA product using different primer combinations.

Second PCR (PCR of an extracted band	Primer 1	Primer 2	Primer 3
Primer 1		Multiple bands lower in MW than the template	One product equal to the template MW
Primer 2	Multiple bands lower in MW than the template		No product
Primer 3	One product equal to the template MW	No product	

Table 2: Possible products of PCR of an extracted band from the first PCR using all the primer combinations

Table 1 and table 2 describe the nature of the theoretical products generated from PCR of respectively Rolling Circle Amplification and a selected band from the first PCR using all the possible primer combinations. It is clear from this theoretical result that we should have full control over the reaction; however, the experiments show different results. Fig. 3.5 shows a gel of the DNA resulting from the PCR using primer 1 and primer 3, PCR of RCA using primer 1 and primer 3, PCR of RCA using primer 1 and primer 2, and RCA, respectively in lanes 1, 2, 3, and 4. A first observation is that no bands are present at all. The most surprising result was that amplification of the RCA product with primer 1 and primer 3 (lane 2) did occur. The purpose of that lane was to prove that the amplification does not occur unless the specific end exists in the template, but the result was totally the opposite.

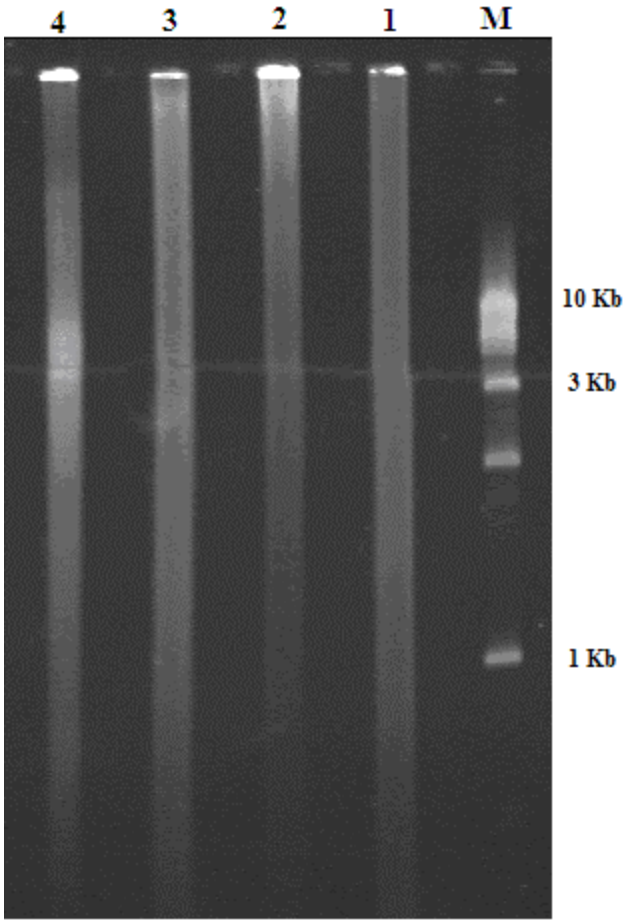

Figure 3.5: Analysis of PCR products using 1% non-denaturing agarose gel electrophoresis. Reaction was performed as described in the experimental section, 60 degrees annealing temperature. Lane **M**, 1 Kb marker, lanes **1**, **2**, **3**, and **4** represent **1)** PCR of first PCR using primer 1 and primer 3, **2)** PCR of RCA using primer 1 and primer 3, **3)** PCR of RCA using primer 1 and primer 2, and **4)** RCA product

The gel shows unexpected amplification in lane 2 with more material that is higher in molecular weight than the rest of the lanes. To further investigate the system, we performed a reaction in which RCA product would be amplified without any primer. The result was quite unexpected, the amplification still occurs. Many causes for this amplification were considered, such as the possibility of amplifying external DNA from

contamination. To test our hypotheses we ran new PCR reactions, figure 3.6 shows the results of these control reactions; the first lane was a control PCR sample with no template, lane 2 is PCR of RCA product without any primers, lane 3 is PCR of RCA product with primer 1 and primer 2, and finally lane 4 represents another negative control in which we used the same quantity of DNA as was used in the experiment in lane 2 before amplification.

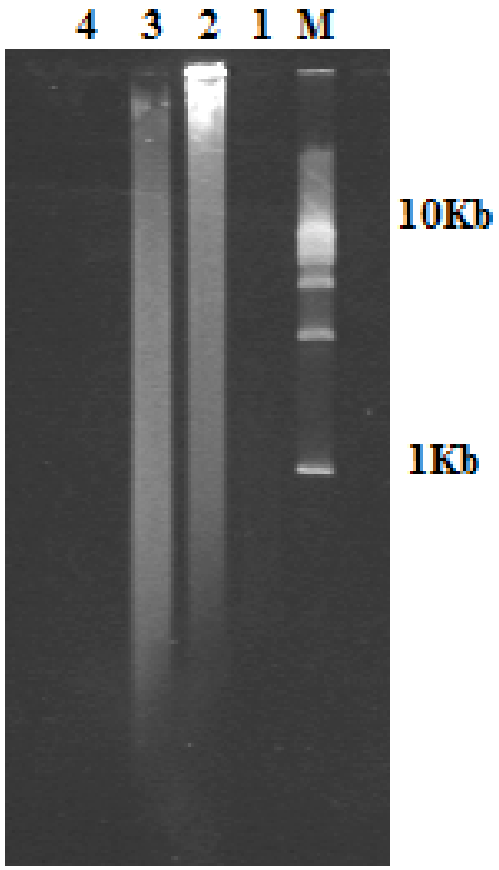

Figure 3.6: Analysis of PCR products using 1% non-denaturing agarose gel electrophoresis. Reaction was performed as described in the experimental section, 60 degrees annealing temperature. Lane M, 1 Kb marker, lane**1** reaction sample without DNA lane**2** PCR of RCA without any primers, lane**3** PCR of RCA with primer 1 and primer 2, finally lane 4 represents same amount of DNA as in lane 2 before amplification.

We demonstrate here that the amplification of the RCA product takes place without any primers. This finding implies that we have some double stranded DNA in the RCA product. Although we had considered the presence of double stranded DNA in the RCA product previously mentioned Fig. 2.7**, t**hese experiments provide the first solid evidence.

The question that should be answered now is how the PCR reaction, being a primer-dependent reaction, might amplify RCA double stranded DNA leading to higher molecular weight product. We feel that the most likely explanation is that during the PCR reaction nonspecific binding might happen, and due to the unusual nature (multiple tandem repeat copies) of the product, the double stranded RCA product can rebind in each cycle and continue being amplified. The RCA product acts as template and primer at the same time, yielding a much more complicated system. This process is schematized in Fig. 3.7.

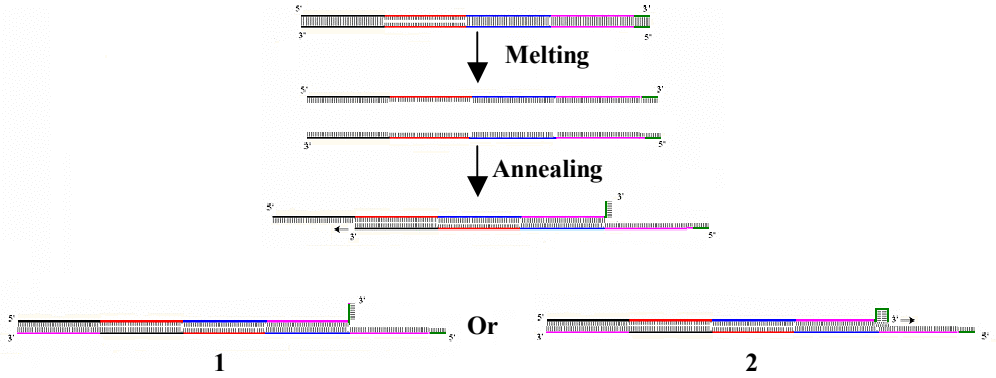

Figure 3.7: This scheme shows how multimeric double stranded DNA product with one specific end can leads to a higher molecular weight result. In product 2 the specific end or part of it is introduced to the PCR product.

This amplification occurs independently of added primers, it leads to much higher molecular weight and irresolvable product. In the product 1 there is a mixture of double and single stranded DNA, which complicates the resolution via gel. In product 2, due to

the presence of the hydroxyl group that will initiate the polymerization, the 18 bases may bind back to itself and the extension can start again.

The next step was an attempt to optimize the annealing temperature of the PCR of RCA reaction (primer 1 and primer 2). We ran a gradient block PCR, with the annealing temperature ranging between 45 and 60 degrees C. We also decreased the extension time from 5 min to 2 min. The product was then analyzed in 1% non-denaturing agarose gel electrophoresis Fig. 3.8.

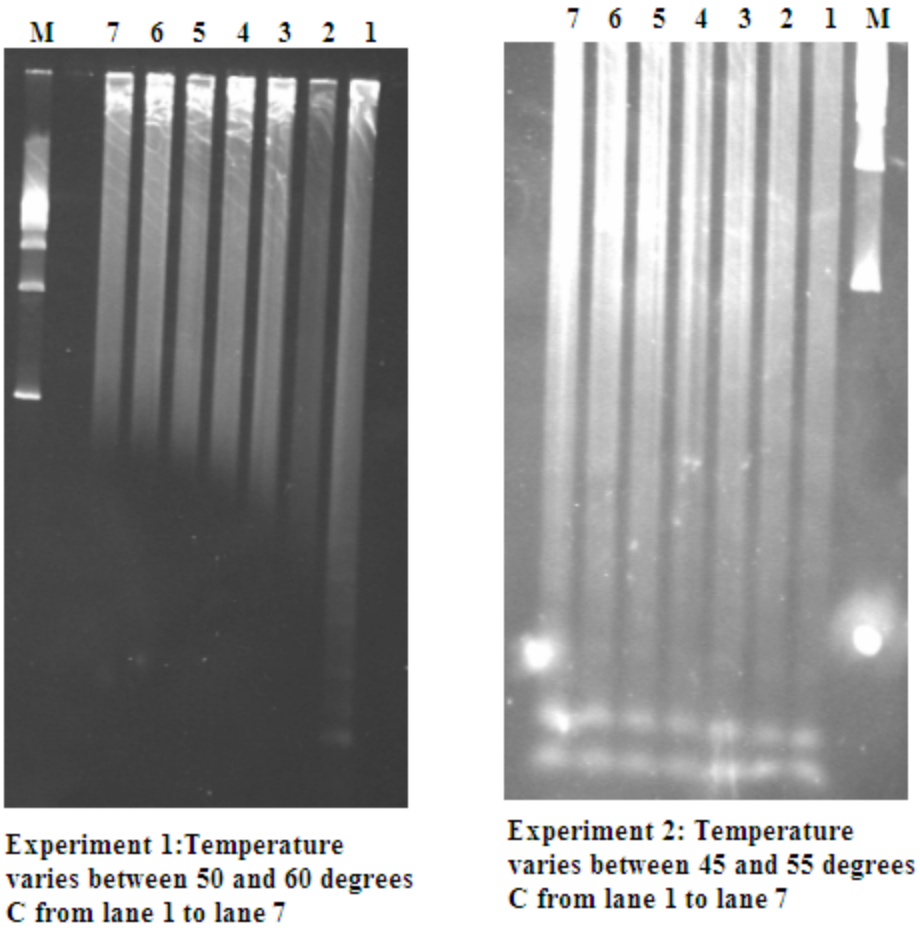

Figure 3.8: These images show two gradient block PCR reaction. Same sample preparation for both reactions. The temperature varies entirely from 45 to 60 degrees. The lower annealing temperature shows better result. In lane 1 experiment 1 some low MW bands are shown, lane M 1 Kb ladder . Product analyzed with 1% agarose gel, 6.7 V/cm, 4 hours.

These experiments showed much more promising results. At 50 degrees C annealing temperature we see 5 clear bands nicely resolved. The extension time in both experiments is 2 min, considering 25bases/sec average speed for the polymerase (*) we estimated the number of bases extended in the 2 min as 3000 bases. We observe that a majority of the product is more than 10 kb in length in both experiments. These long DNA strands must be produced as a result of the self-amplification previously discussed. The five bands of relatively short product result from specific priming.

Another question may be asked: where does this double stranded self priming DNA come from?

The Rolling Circle Amplification reaction starts with a circular single stranded DNA and a primer. The polymerase extends that primer giving single stranded DNA product. With time, miss-priming occurs and double stranded DNA is formed. One expects the RCA reaction to start with single stranded DNA, thus time may be a critical factor in controlling the reaction. All the RCA reactions described so far have been incubated over night at 37 degrees C. In the next set of experiments the incubation time was reduced to 4 hours instead of over night. The result is shown in Fig. 3.9.

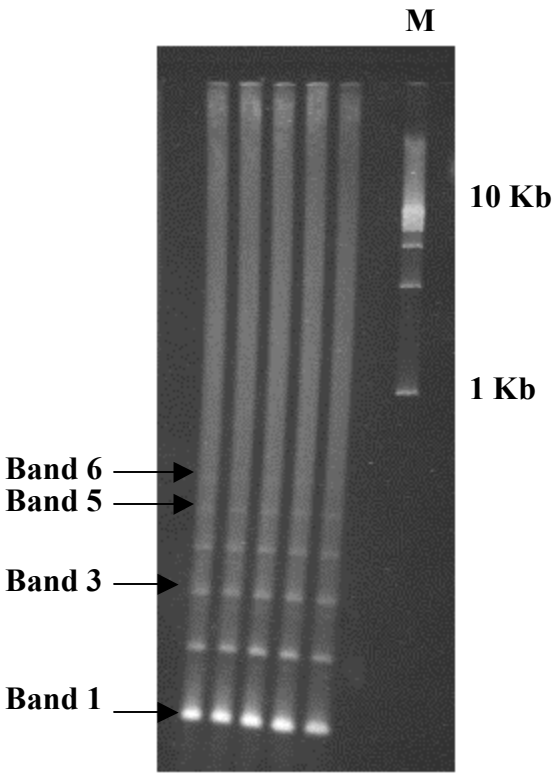

Figure 3.9: PCR of RCA (primer 1 and 2) product. The RCA was incubated 4 hours instead of over night, PCR conditions: annealing temperature 50 degrees C, extension time 2 min. the image shows nicely resolved bands at the bottom of the gel. The bands are 95 bases apart.

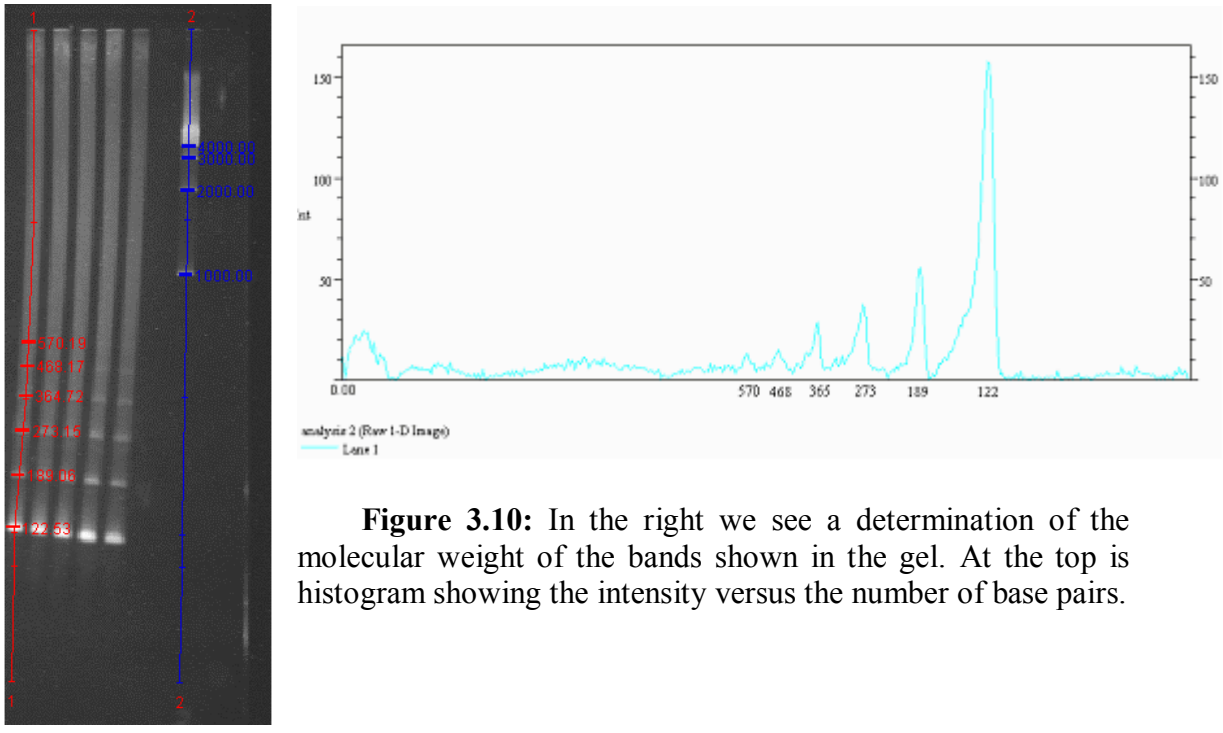

Figure 3.10: In the right we see a determination of the molecular weight of the bands shown in the gel. At the top is histogram showing the intensity versus the number of base pairs.

We used Quantity 2.2 software to determine the size of the DNA molecules in the bands (result shown in Fig. 3.10). Here we give the calculation of the real bands and a comparison between the two calculations

Ln=95n+18+20 (Ln is the length of the PCR product sequences, n is number of band)

L1=95+18+20=133

L2=190+18+20=228

L3=285+18+20=323

L4=380+18+20=418

L5=475+18+20=513

L6=570+18+20=608

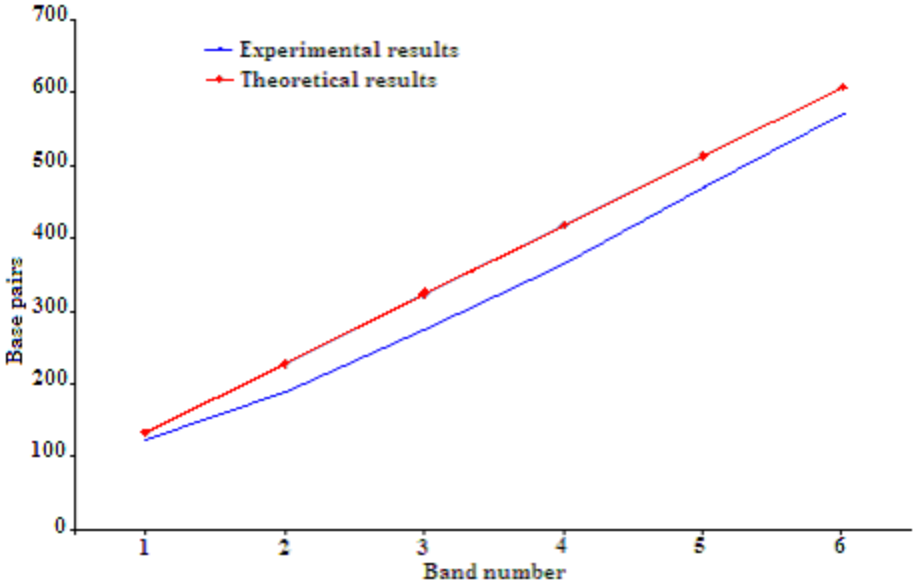

Graph 3.1 Plot of theoretical and experimental expected product size. The graph shows that the experimental results are in close agreement with the theoretical results

The plot above shows that the experimental results are in close conformity with the theoretical calculations. The slight difference, we believe, is explained by the errors due to software analysis of gel image.

The last two gel images (Fig. 3.10 and Fig. 3.11) show very clear bands at the bottom of the gel, as was expected. By looking at the diagram of the PCR (Fig. 3.4) we can see that the primers may bind to different binding sites in the same template. This priming pattern leads to product of varying lengths with the smallest molecule being 133 bases long and other major products being longer in increments of 95 bases (133, 323, etc). Statically we expect the low molecular weight product to be more abundant. In addition, in the gel it is much easier to resolve bands with low molecular weight.

To verify this assumption we cut two bands from the previous gel, and then the DNA was extracted and amplified with different primer combinations listed in Table 2.

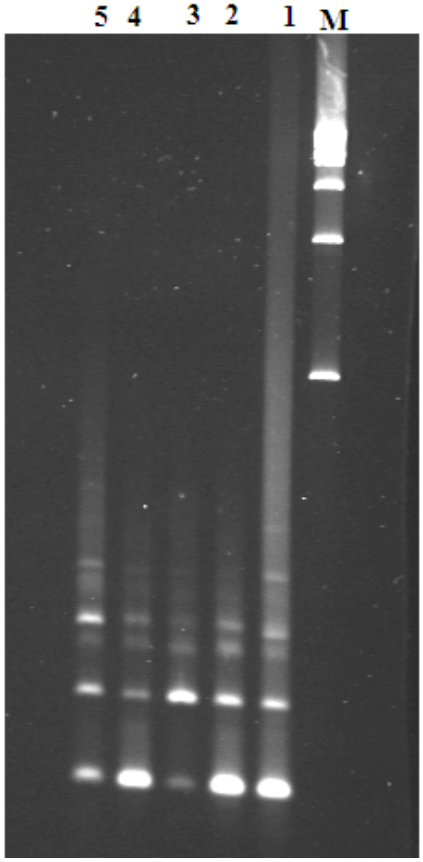

Figure 3.11: Gel image shows the different PCR products resulting from amplifying 228 base pairs with different combinations of primers. The amplified DNA product was purified from the second band from the bottom of the previous gel.

In Fig. 3.11 lane 1 is PCR of RCA product (primer 1 and 2), lanes 2 and 3 present the PCR products of band 2 (228 base pairs) respectively by long and short primer. Lanes 4 and 5 represent the PCR of band 3 (323 base pairs) respectively by short and long primers.

- Lane 2: we suppose to see here band 1 and band 2 (because we are using the long primer), with band 1 being higher in intensity (major product). The experiment shows exactly the same results, band 3 is explained by the miss-amplification explained in Fig. 3.7; it is lower in intensity.

- Lane 3: PCR of the band 2 with short primer. Theoretically the product will have the same molecular weight as the template. The experiment shows the expected result, the most intense band is the 228 band (same as template). Other bands are due to miss-priming.

- Lane 4: PCR of the third band with the long primer. In comparison to lane 3, this product should have ample quantities of shorter bands. The experiment shows the expected result, first band is the higher in intensity with some product in band 2 and band 3.

- Lane 5: PCR of the same third band with short primer. Hypothetically we expect to see just the third band. Experiment shows almost same intensity for all bands 1, 2 and 3, this supports our explanation of the long product being harder to amplify even with short primer.

We observe in the gel image some double-bands, such as in band 3 (all lanes). More investigations are needed to determine the possible causes.

CONCLUSIONS

RCA is a molecular amplification method with the unique property of producing a single-stranded DNA molecule that is composed of tandemly repeated copies of the complement to the template circle which remains linked to the DNA primer. Even though this property seems very exciting for DNA-based nanotechnology applications, the RCA technique has not been used in nanotechnology applications. We believe that a big disadvantage of the RCA amplification method is the non-specificity for manipulation. This means that we have no control over the synthesized DNA sequence because they are tandem repeats of the same subunit sequence. Any manipulation, such as digestion, ligation or hybridization can not be fully localized in one specific site of RCA produced sequences. In order to make the RCA technique useful for nanotechnology this problem should be overcame, full control over the RCA product should be realized. This will enable us to further manipulate the RCA product such as, self-directing the RCA product to be placed in determined locations on a surface or incorporation of the RCA product in a plasmid vector for cloning.

In this component we developed a technique to add two specific ends to the RCA product. These two ends will give us good control over the product, which will enable us to use the repetitive nature of the RCA product to great advantage. The RCA product will be used as a scaffold for a one dimensional nano-array using the fact that the sequence repeats every 30 nm, and we know the complementary sequence of the DNA. In addition, all our gel experiments showed that the resolution of the PCR of RCA product is limited to only a few copies (6 copies), so a new isolation technique is required. In the next part

of the project we will discuss the possibility of using cloning, a common biological amplification technique, as an isolation technique. We will also demonstrate that cloning has many more advantages than just an amplification or isolation technique.

4) CLONING OF NANOSTRUCTURED MACROMOLECULES INTO *E.COLI*

INTRODUCTION

We demonstrated in the previous section that the PCR technique is not able to specifically amplify the DNA structure needed. That DNA sequence should have multiple copies of the 95 base sequence with two unique, specific ends. Even considering the repetitive nature of these DNA strands, the PCR technique does provide a possible technique for introducing the second end, but it has not proven suitable for amplification and isolation of mono-length DNA fragments as large as a few kilobases in length. An alternative technique was necessary. Cloning is a very common amplification technique in biology; in which a specific sequence of DNA is isolated and placed into a DNA molecule (called a vector). The result is a recombinant molecule or molecular clone, composed of the DNA insert linked to the vector DNA sequence. Large quantities of the inserted DNA can be obtained if the recombinant molecule is allowed to replicate in an appropriate host. The DNA fragments used to create recombinant molecules are usually generated by digestion with endonucleases. Many of these enzymes cleave their recognition sites in a staggered configuration, leaving cohesive single stranded tails that can associate with each other by complementary base pairing. The association can be established permanently by treatment with DNA ligase. Thus, two different fragments of DNA prepared by digestion with the same restriction endonucleases can be readily joined

to create a recombinant DNA molecule. Depending on the size and the purpose of the experiment, many different types of cloning vectors can be used for the generation of recombinant molecules. In our particular experiment a plasmid vector was used to produce the desired recombinant molecule due to its ease of manipulation.

One may expect that cloning will play a potential role in DNA-based nanotechnology as a large-scale DNA production technique; however, cloning has been barely used in nanotechnology (14). The topologies contained in the DNA sequences used in the construction of DNA objects, particularly three-dimensional geometric DNA objects, prevent them from being cloned. This may be explained by the nature of the cloning. In contrast to PCR, which is more considered a chemical amplification technique, cloning involves the direct use of a living system (the bacteria). This living system has some complicated mechanisms, such as repair mechanisms, that will reject particular sequences in the vector. In addition, the inserted DNA should be compatible with the bacterial system; other wise the bacteria will not grow.

In our project the cloning plays a double role, first as a selective technique, and second as an amplification mechanism. We designed the two specific ends to have two restriction sites for EcoRI and XbaI, two restriction enzymes that exist in the pGEM vector, a commercial vector from **Promega**. Thus the inserted DNA fragments will certainly have the two specific ends. Other fragments that lack one or both ends will not be able to be ligated into the bacterial vector. Moreover, it is known that in each individual colony the inserted DNA fragments will be exactly identical, which means that one DNA length will be amplified per colony. Consequently a cloning library can be formed, where all the DNA lengths that correspond to the different copy numbers will be available (the DNA

fragment length is related to the copy number by N=26+95n, N is the number of bases in the DNA fragment and n is the copy number). By providing a wide variety of material, this library is considered an immense advantage. Second, the director strand is described as a single stranded sequence. So, cloning will also ensure the production of single stranded DNA out of the bacterial vector, due to the f1 origin. By intentionally putting the DNA fragment in the correct orientation into the vector one of the two strands could be generated after treating the bacteria with the helper phage. Alternatively, we are developing other methods for single stranded DNA extraction, such as magnetic beads, and direct removal of single stranded DNA out of the bacterial vector.

In addition, having the desired DNA fragment inside the vector will give us more flexibility to incorporate parts of the vector sequence into the director strand. This will enable us to achieve our goal to have 1 micron DNA fragment, even with less than a copy number of 30.

Plasmid Vector for Recombinant DNA

Plasmids are small circular DNA molecules that can replicate independently, without being associated with chromosomal DNA, in bacteria. All that is required on the plasmid DNA is an origin of replication, the DNA sequence that signals the host cell DNA polymerase to replicate the DNA molecule. In addition, plasmid vectors carry the genes that give resistance to antibiotics (ampicillin resistance), so bacteria carrying the plasmids can be selected. To be cloned into a plasmid vector, a fragment of the desired DNA is

ligated to an appropriate restriction site in the vector and the recombinant molecule is transformed into *E. coli.* The bacteria are then plated on medium containing ampicillin, so that only the bacteria that are ampicillin-resistant because they carry plasmid DNA are able to form colonies. Individual colonies can then be isolated and grown in large quantities for isolation of recombinant plasmids. The small plasmid circles can then be isolated from the bacterial genome yielding pure recombinant molecules, which are suitable for enzymatic restriction to get the DNA fragments, or for further exploitation. Finally we note that the plasmid vectors usually consist of only 2 to 4 kb of DNA, in contrast to the 30 to 45 of phage DNA present in lambda vectors. This will facilitate the analysis of the inserted DNA fragment; however, it limits the size of the insert to ca 10 kb maximum.

The figures below show the main steps in the plasmid vector cloning process. Different DNA inserted fragment colors represent different DNA lengths, which mean different numbers of copies. It is clear here how the cloning is used in this application as an isolation technique.

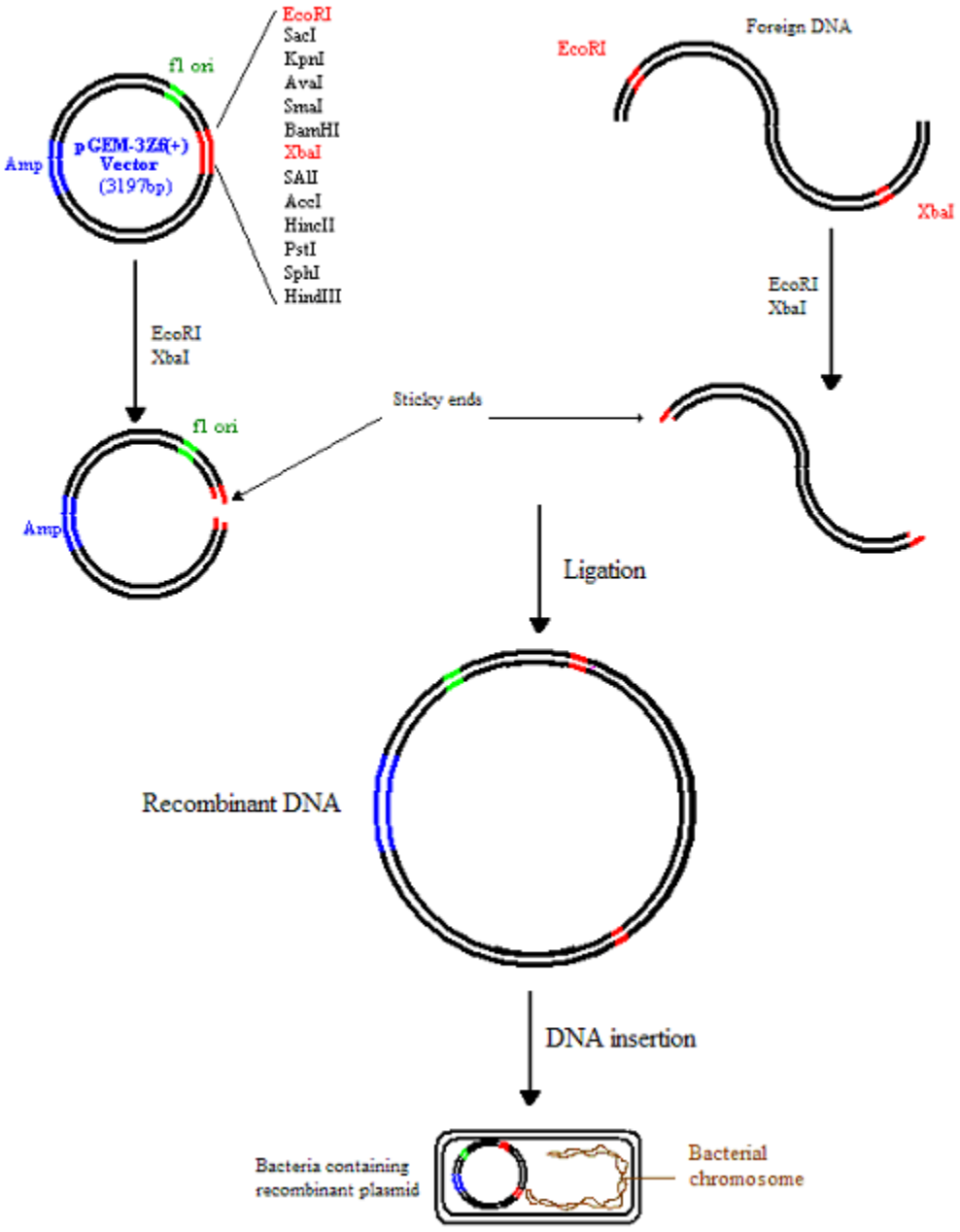

Figure 4.1: Process of preparing plasmid vectors and transforming bacteria.

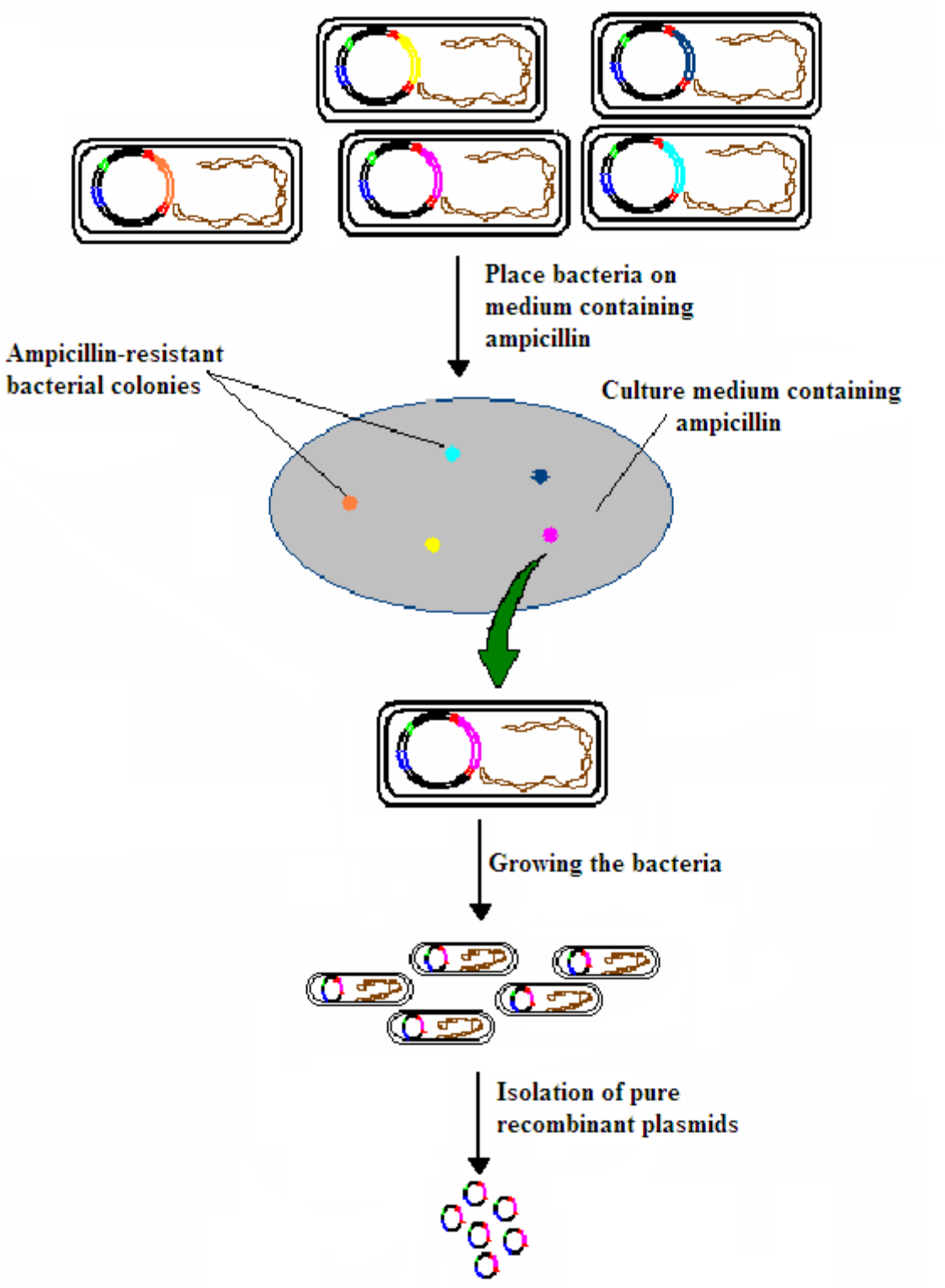

Figure 4.2: Process of selecting a clone and isolating recombinant plasmids

MATERIALS AND METHODS

- pGEM-3Zf(+) vector from *Promega.*
- UltraMax™ DH5α-FT™ Competent Cells from *Invitrogen.*
- EcoRI, XbaI, and HaeII from *Promega.*
- Ampicillin, IPTG (isopropyl-beta-D-thiogalactopyranoside), and Xgal (X-galactose) from *Sigma.*
- DNA rapid ligation kit from *Roche.*
- Miniprep kit from *Qiagen*
- TOPO TA Cloning® Kit (TOP10F') form *Invitrogen.*

1. Cloning with pGEM vector:

- RCA product is PCRed with primers (primer 1 and primer 2). The PCR product is analyzed with gel electrophoresis, and then higher molecular weight product was purified.
- DNA digestion with EcoRI and XbaI (see Appendix A).
- The vector is digested with same two enzymes (see Appendix A).
- Ligation of the DNA fragments with the digested vectors (see Appendix A).
- Put 3 μl of ligation solution in one bacteria aliquot (competent cell should be stored at -80 degree. When used, aliquot must be thawed and manipulated in ice. Ligation solution can be stored at -20 for further uses)
- Leave the mixture 30 min in ice.
- Put the tube mixture at 42 degree (heat block or water bath) for 30 seconds, then back to ice for 2 min.

- Add 250 µl of SOC, and then put the tube in 37 degree shaker for 1 hr.
- In the mean time get the plate ready (see appendix A).
- After the hour take the tube mixture from the shaker, spread X µl into the plate then incubate the plate overnight at 37 degrees. (X volume may vary from one experiment to the other depending on the concentration of the original ligation solution. As a consequence, plating several plates with different volume of solution is more convenient. In this particular experiment, I used 50 µl of solution, since the concentration of DNA fragments was very low. It had been gel purified and the ligation efficiency was expected to be low).
- Next day, blue/white colonies should be observable on the plates. Choose the plate that has the colonies evenly distributed on the surface of the plate. Highly condensed plates are not advisable to use.
- Prepare some 12 ml tubes containing 2 ml LB + ampicillin. Then pick the white colonies from the plates and transfer them into the tube. For colony picking a 10 µl micropipette tip can be used. Gently touch the colony, then place the whole tip in the tube, leaving the tip in the tube is suggested to ensure transfer of the colony. For control purposes, one blue colony is always picked.
- Shake the 12 ml tubes overnight at 37 degrees (shaking speed 225).
- Next day, transfer 1.5 ml into microcentrifuge tube, spin at 14 000 rpm for 1 min, discard the supernatant.
- The recombinant plasmids are extracted using the Miniprep kit.

2. Cloning with the PCR cloning Kit

This kit is suitable for direct cloning of PCR product. *Taq* polymerase has a nontemplate-dependent terminal transferase activity that adds deoxyadenosine (A) to the 3' ends of PCR product. The linearized vector supplied in this kit has single, overhanging 3' deoxythymidine (T) residues. This allows PCR insert to ligate efficiently with the vector. The ligation is maintained by Topoisomerase I (seeAappendix A). If proofreading polymerase is used in PCR insert amplification, such as *Vent* in our case, direct cloning is often difficult because the proofreading enzyme removes the 3'A-overhangs necessary. In this case the A-overhangs should be added separately to the PCR insert.

- Add 3' overhang (see Appendix A).
- Mix 4 µl of previous solution, 1 µl of salt solution (Topo cloning Kit), and 1 V (vial) of TOPO vector. Incubate the mixture 5min at room temperature.
- 2 µl of the mixture was mixed with 1 vial of competent cell, handled the same as the cells in the first cloning
- All the other steps are similar to those for cloning with the plasmid vector.

Gel analysis:

After isolation of pure DNA recombinant, the plasmids were cleaved with EcoRI and XbaI restriction enzymes. The size of inserts was then determined using 1% agarose gel. Quantity 2.2 Bio-Rad software was used for gel image analysis.

DNA sequencing

All our DNA sample were sent for sequencing at the Integrated Biotechnology laboratories facility at the University of Georgia

Riverbend Research Lab Room 161. 110 Riverbend Road. Athenis, Georgia 30602.

Tel: (866) 410-6935

Fax: (706) 542-6414

RESULTS AND DISCUSSION

Cloning with pGEM vector:

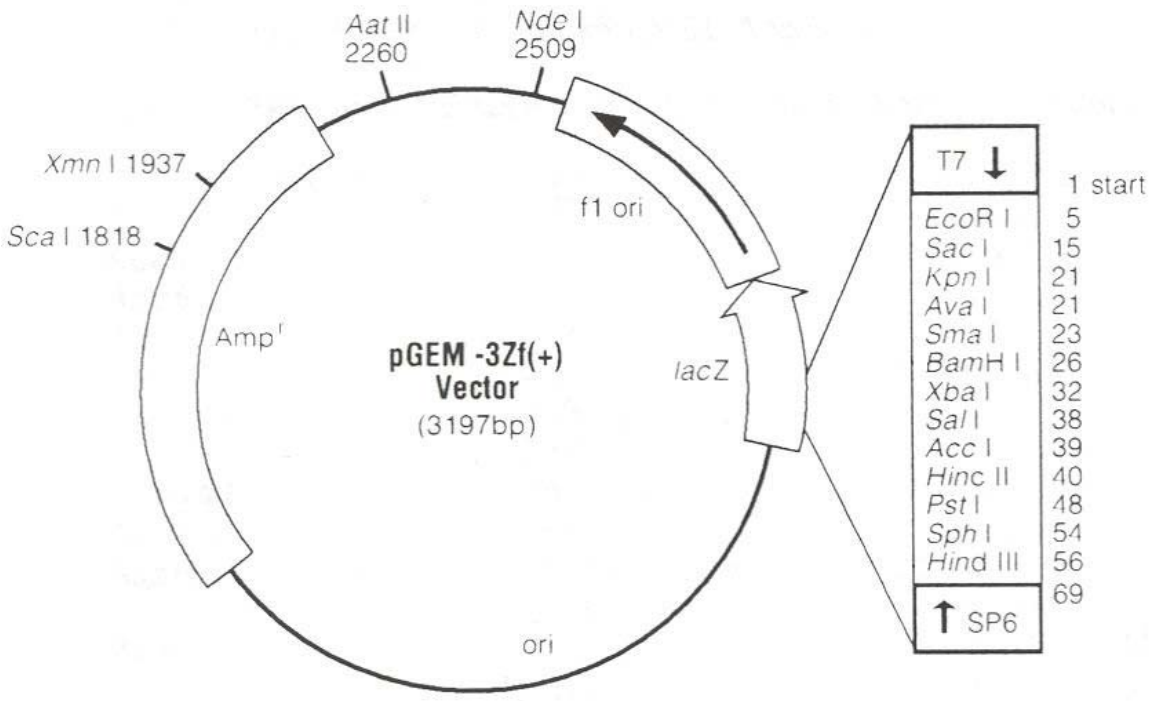

Figure 4.3: pGEM® _3Zf(+) Vector circle map and sequence reference points

Fig. 4.3 shows the vector circle map, where multiple restriction sites are shown. EcoRI and XbaI are restriction sites earlier introduced in the double stranded synthesized long blue fragments. We start by running a gel, and then purifying long DNA fragments (3kb to 10 kb) from the PCR product previously prepared. By treating simultaneously both, vector and DNA fragments with EcoRI and XbaI, we will generate two overhanging tails that can be readily joined together to create recombinant DNA molecules. The paired complementary ends were then ligated using a ligase enzyme. The created recombinant molecules were chemically transferred into competent *E. coli* cells. *E. coli* cells are chemically pretreated to take in the foreign DNA. The cells are suitable for blue/white screening of colonies on bacterial plates containing X-gal and IPTG. The purified cloned plasmids are digested simultaneously with EcoRI and XbaI, the resulting product was analyzed with 1% gel electrophoresis to verify the size of the inserts. The double digested plasmids were expected to be 3170 bp (3190-27), the inserted fragments are supposed to be 95xn bp, where n is the number of copy.

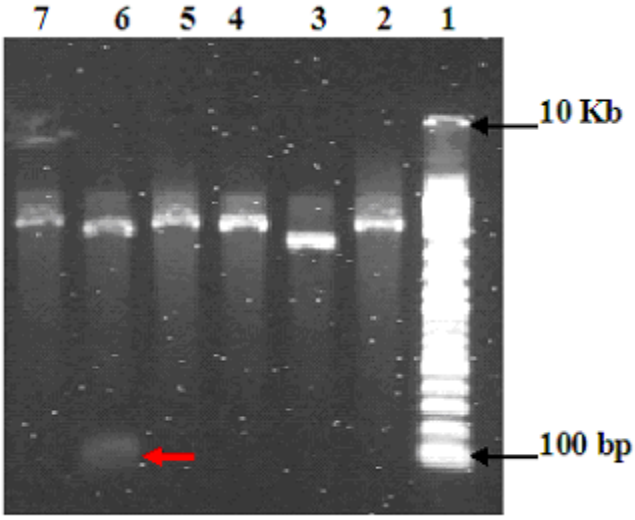

Figure 4.4: Image of plasmid gel. Purified plasmids were digested with EcoRI and XbaI, and then analyzed with 1% agarose gel electrophoresis. The upper bands represent the linearized plasmids vectors. The red arrow indicates the only DNA insert shown in the gel. Lane 1: 10 kb DNA ladder. Lane 2 to 7 different purified colonies.

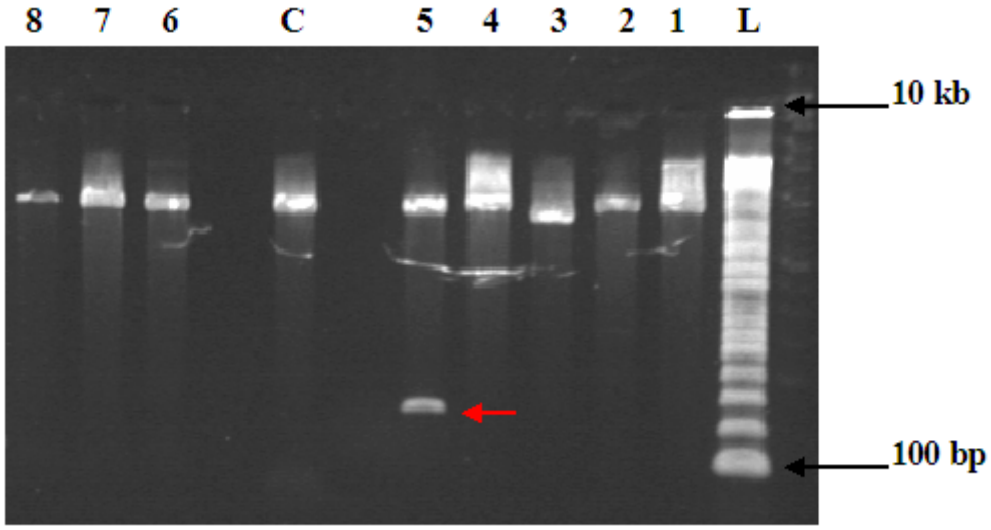

Figure 4.5: 1% agarose gel analysis of different sampled colonies.

Fig. 4.4 and Fig. 4.5 show the result of the gel analysis. The only DNA inserted fragment seen in the gel images are indicated with red arrows.

To further investigate the size of the inserted DNA fragments some of the gel images were analyzed using the Quantity 2.2 software. This tool permits us to determine the actual size of the DNA bands shown in the gel image based on the migration of the ladder bands. Due to the weak resolution in the upper part of the DNA ladder, we believe that the sizes of the lower molecular weight bands in the gel are more accurate than the upper ones.

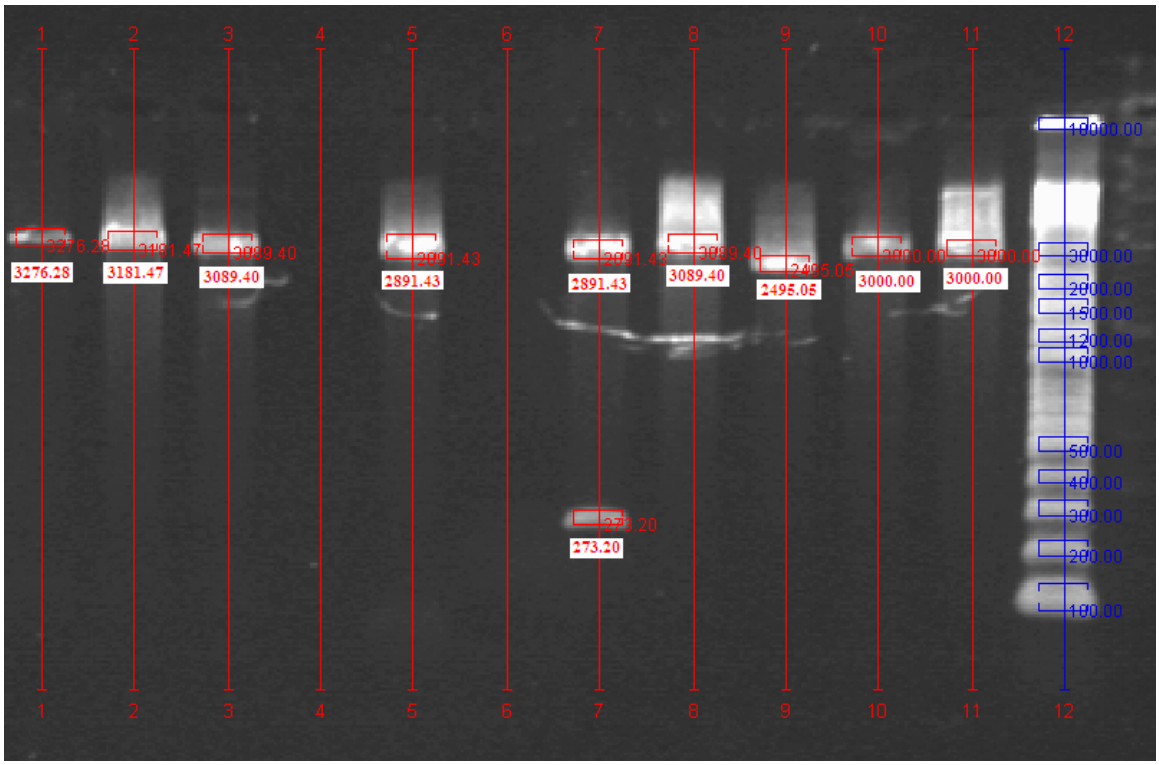

Figure 4.6: Quantity 2.2 software was used to determine the band size based on the migration of the ladder bands. The size of the insert is determined to be 273 bp; this number is close to the 285 bp size of three copies.

This result was not sensible because the linearized plasmids did not run at the same level in the gel as expected (after the double digestion they should have the same size). In addition, the yield of the cloning, referring to the gel results, is very low for a normal cloning reaction. It is known that in some cases the efficiency of a restriction enzyme may dramatically decrease with a particular DNA sequence. We believe that, for some reason, one of the restriction enzymes used did not properly digest the DNA fragment, so a poorer yield resulted. To verify this hypothesis we proposed a new reaction, in which the recombinant molecules were digested with a Hae II restriction enzyme. This restriction enzyme was chosen because it has one recognition site in the 95 bp sequence. Thus, when the recombinant plasmids are treated with the Hae II the inserted DNA fragments, which already exist in the plasmid, will be chopped up into their 95 bp subunits. The same enzyme has 4 recognition sites in the plasmid vector. The original distribution of DNA fragment lengths expected to result from the Hae II treatment is indicated in Fig. 4.7.

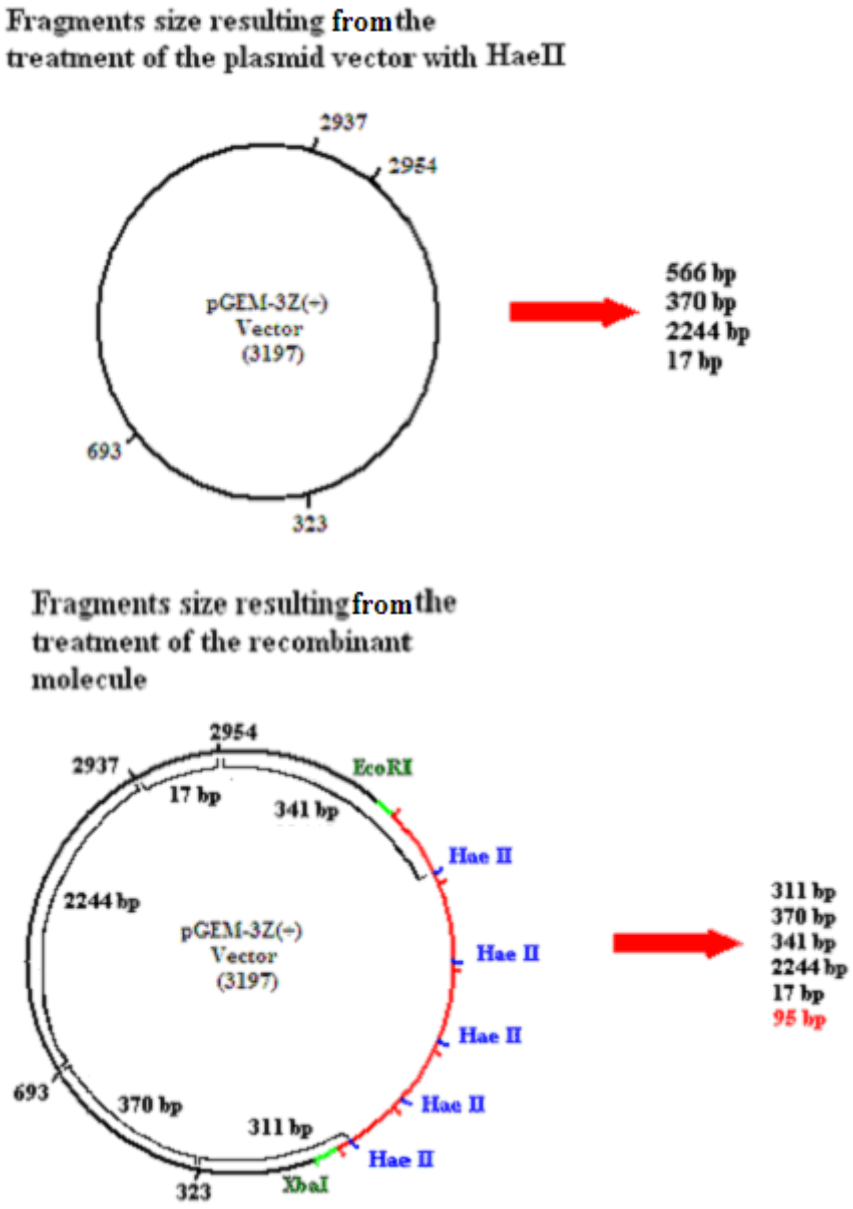

Figure 4.7: Scheme showing the expected DNA fragments resulting from the treatment of respectively, plasmid vector and recombinant molecule with Hae II restriction enzyme

Fig. 4.8 is an image of a gel run on the digested recombinant molecules. It shows the actual size of the fragments obtained. We ran a control sample, which is the plasmid vector extracted from a blue colony then treated with the Hae II restriction enzyme. By

showing 95 bp fragments in almost all of the analyzed samples, the gel data proved that, accidentally, one of the two restriction enzymes, EcoRI or XbaI, did not efficiently cleave the recombinant molecules.

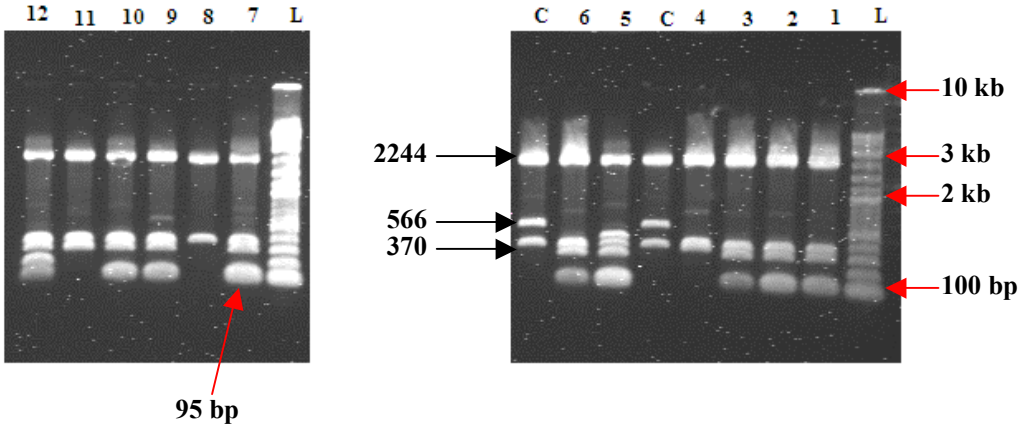

Figure 4.8: Gel analysis of DNA fragments resulting from the treatment of the recombinant molecule with Hae II restriction enzyme. Lanes 1 to 12 represent an assortment of analyzed colonies. Lane C: control sample (plasmid vector isolated from blue colony). Lane L: 10 kb DNA ladder.

For the control samples, the gel shows three bands with the expected base pair numbers. The 17 bp DNA fragment is too low in molecular weight to be seen in this gel. The 2244 bp ran exactly at the same level for control and experimental samples. For the experimental samples, we expected to see three bands at respectively 311, 341 and 370 bp; however, in most cases just two bands are detected. This may be explained by the limited resolution of the gel, which renders it unable to distinguish DNA fragments of relatively close molecular weight; although in lane 5 the three anticipated bands are clear. In total, 9 samples out of 12 showed successful cloning, as proven by the 95 bp DNA

fragments seen in the bottom of the gel image. It is noticeable that the intensities of these bands are different from one sample to the other. The band intensity should correlate with the number of 95 bp copies inserted in the analyzed sample colony. We attempted unsuccessfully to determine the size of the inserted DNA fragments by comparing the intensities of the higher band (the 2244 bp band) and the lower band (the 95 bp band) .

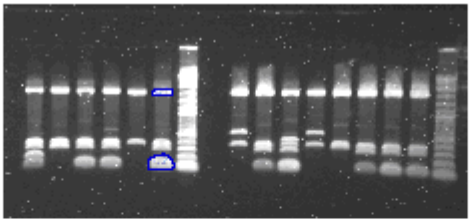

Index	Name	Type	Volume CNT*mm2	Concentration	Density CNT/mm2
1	U1	Unknown	331.7382813	N/A	307.8343363
2	U2	Unknown	1628.613281	N/A	578.8897627

Figure 4.9: Quantity 2.2 software was used to determine the intensity of two selected bands from lane 7 of the gel image on Fig. 4.8.

To verify the size of the DNA fragments inserted in the cloning experiment, we sent five selected samples for sequencing. The chosen samples are samples correspond to lanes 2, 5, 7, 9, and 10 from the gel documented in Fig. 4.8. The sequencing results revealed that the DNA fragment sizes ranged between 2 and 6 copies (result shown in table 3). Figure 4.10 displays the sequence for the 6 copy insert, cloned into the plasmid vector.

Lane number	Copy number
2	4
5	6
7	4
9	4
10	3

Table 3: Copy number from sequencing result (see Appendix B for the rest of the sequencing result)

(Q230:12)A1/160G-34:Plasmid DS:GC Rich +++ M13-48 REVERSE (24)/MGIF-0:Primer:N : 204004699

CTTGACCTGATTCGCCAGCTATTTAGGTGACACTATAGAATACTCAAGCTTGCATGCCTGCAGGTCGAC
TCTAGATCGGACAGCAGCCTGACGCTGGTTGCATCGGACGATACTACATGCCAGTTGGACTAACGGCT
CTACCGTGCATCATGGACTAACCAGTGACCGCATCGGACAGCAGCCTGACGCTGGTTGCATCGGACGA
TAATACATGCCAGTTGGACTAACGGCGCTACCGTGCATCATGGACTAACCAGTGACCGCATCGGACAG
CAGCCTGACGCTGGTTGCATCGGACGATACTACATGCCAGTTGGACTAACGGCGCTACCGTGCATCAT
GGACTAACCAGTGACCGCATCGGACAGCAGCCTGACGCTGGTTGCATCGGACGATACTACATGCCAGT
TGGACTAACGGCGCTACCGTGCATCATGGACTAACCAGTGACCGCATCGGACAGCAGCCTGACGCTGG
TTGCATCAGACGATACTACATGCCAGTTGGACTAACGGCGCTACCGTGCATCATGGACTAACCAGTGAC
CGCATCGGACAGCAGCCTGACGCTGGTTGCATCGGACGATACTACATGCCAGTTGGACTAACGGGCGC
TACCGTGCATCATGGACTAACCAGTGACCGCAGAATTCGCCCTATAGTGAGTCGTATTACAATTCACTG
GCCGTCGTTTTACAACGTCGTGACTGGGAAAACCCTGGCGTTAC

Figure 4.10: Sequencing result. Each copy is depicted in a different color; the red color shows the EcoRI and XbaI restriction sites introduced into the DNA fragment.

All of our sequencing results showed that the inserted DNA fragments are composed of multiple copies of the 95 bp unit. These subunits are nicely arranged between two restriction enzyme sites; however, the number of copies is not quite as high as expected. Even though we purposely selected long DNA fragments isolated from gels for cloning, the sequencing results show relatively short fragments. It is known that long DNA

fragments are much more problematical for cloning than short fragments. Especially during the ligation step, short DNA pieces are more probable to become ligated to the plasmid vector than long pieces. To overcome this problem we changed from the plasmid vector, where the digestion and ligation are critical steps, to the TA cloning, where no digestion or ligation are required.

Cloning with PCR cloning kit

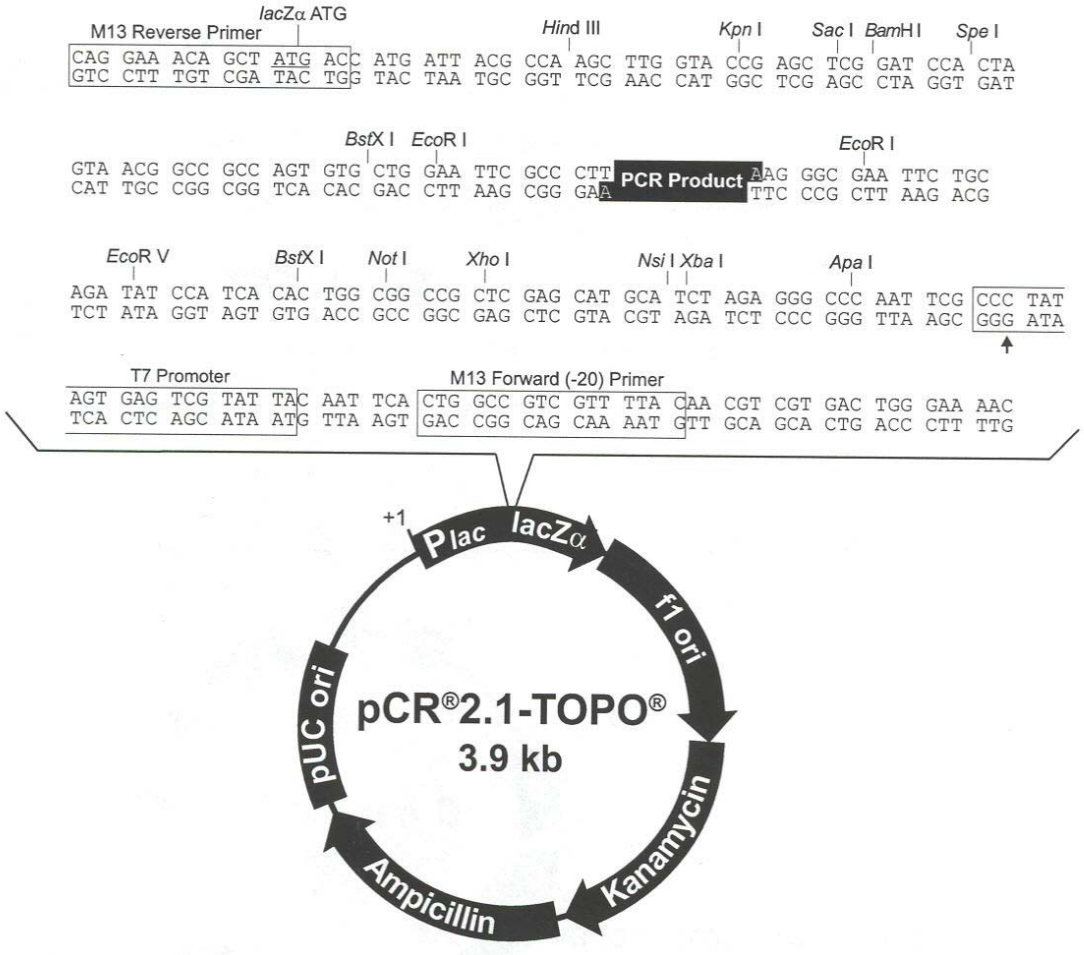

Figure 4.11: Map of PCR® II-TOPO® . The map shows the sequence surrounding the TOPO® Cloning site. Restriction sites are labeled to indicate the actual cleavage site.

In TA cloning, the PCR product is directly inserted into the plasmid then transformed into the bacteria cell host. The same long DNA fragments, gel purified, were used for insertion. After recombinant molecules were purified, they were treated with EcoRI restriction enzyme, and then gel analyzed to verify the size of the insert.

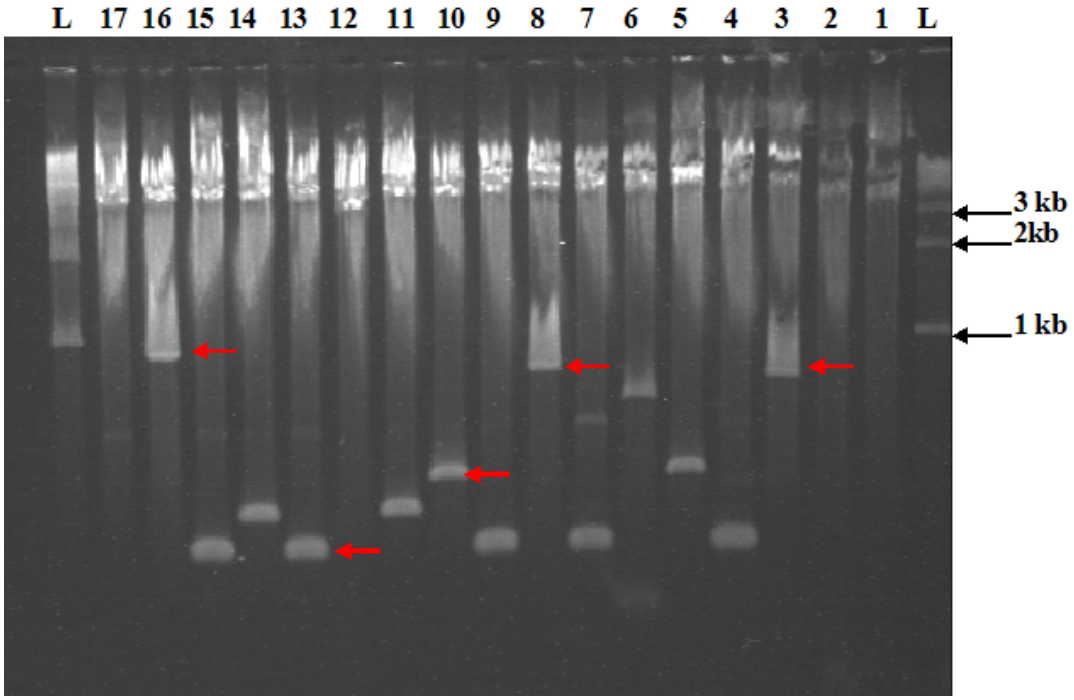

Figure 4.12: Purified plasmids were digested with EcoRI, and then analyzed with 1% agarose gel electrophoresis. The upper bands represent the linearized PCR TOPO plasmids. The red arrows indicate the DNA inserts shown in the gel. Lane L: 10 kb DNA ladder. Lane 2 to 17 different colonies purified.

Fig. 4.12 shows that the new cloning reaction was more efficient than the previous one. All the samples showed inserts. The size of the TOPO plasmid should be the same after the EcoRI digestion, which is 3.9 kb. Some bands are as high as 1 kb, corresponding to ca 9 or 10 copies. To verify the insert size, we analyzed this gel image using the quantity 2.2 software. Result of the analysis is displayed in the next figure.

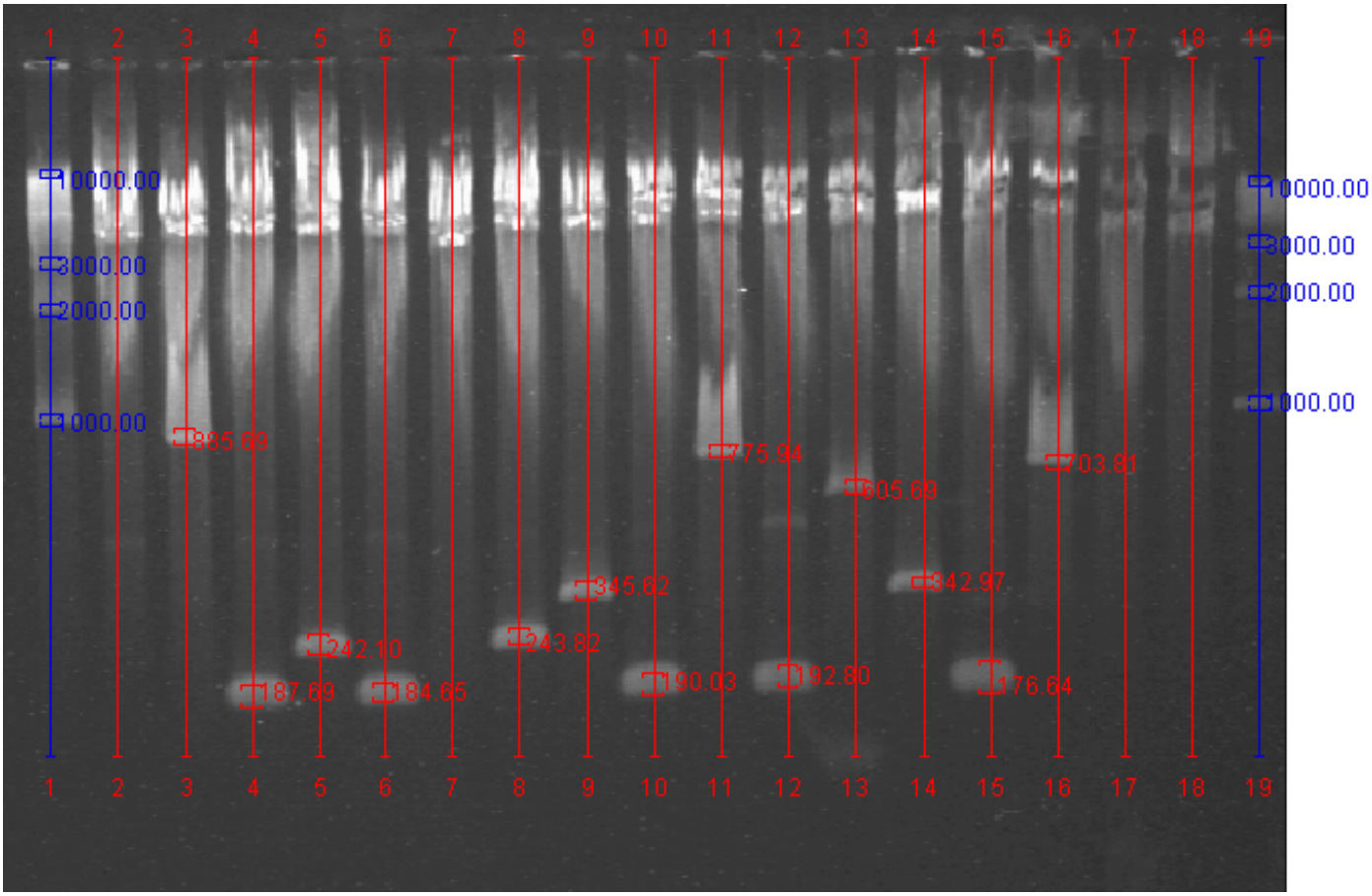

Figure 4.13: Quantity 2.2 Bio-Rad software was used to analyze the previous gel image (Fig. 12.4). The band sizes were determined using the known ladder bands as calibration standards.

The gel analysis shows a distribution of band sizes ranging between 176 bp (probably 2 copies) to 885 bp (probably 9 copies). We successfully increased the size of the inserted DNA fragments by changing the insertion technique. We believe that this is a very important result; however, we are still searching for a method which will yield a bigger insert.

It is known that the *E. coli* in particular and bacteria in general use many repair mechanisms in order to preserve the integrity of their bacterial genome. These repair mechanisms are mainly divided into two categories, replicative DNA repair and post-

replicative DNA repair. It has also been reported that, in the genomes of many organisms, deletions arise between tandemly repeated DNA sequences of lengths ranging from several kilobases to only a few nucleotides (15). In *E. coli*, spontaneous deletion often occurs at tandem repeats. These repeats may initiate genetic rearrangements by formation of hairpin secondary structures that block DNA polymerases. It is believed that this process may be initiated as post-replicational DNA repair.

A reason for not getting the expected DNA fragments cloned might be the repair mechanism of the *E .coli* host cells. To overcome this ambiguity we have chosen a new cell host. SURE cell is a genetically modified bacteria strain commercially available from Stratagene. This cell is designed to facilitate cloning of DNA containing irregular structures, such as repeats and secondary structures. By removing genes involved in the rearrangement and deletion of these structures, the stability of DNA containing long inverted repeats is increased 10- to 20-fold.

CONCLUSION

In this section of the project we demonstrated success in designing, synthesizing and cloning of tandemly repeated DNA sequences. The sequencing results represent strong evidence of the repetitive nature of the RCA synthesized DNA. It also proves that we effectively incorporated two pre-designed specific ends into the RCA product. This will provide us considerably greater control over the repeated sequence. Now, the self direction of these long repeats towards specific spots on the surface has become possible. In addition, we synthesized and cloned an assortment of different DNA fragments sizes, as high as ca 885 bp corresponding to 9 copies, 95 bp per copy. After being transformed into bacterial cells, the regeneration of this product is readily possible at any future time.

One more advantage of having the DNA fragments inserted into plasmid vectors is that we have the choice of using the DNA target as double or single stranded material. By simply treating the recombinant molecules with the appropriate restriction enzymes, the target DNA can be easily isolated. We can manage the size of the isolated DNA fragments by choosing the restriction enzymes. For examples, if we need to add 1kb to one end of the inserted fragment we can do so by selecting a restriction enzyme that cleaves the plasmid vector 1 kb upstream to the end of the inserted DNA fragment. Some one may argue that restriction sites are not provided all over the plasmid, this is true but we can always introduce a restriction site using the commercially available change cloning kits. This way the 1 micron DNA fragment, with the desired copies located anywhere in the sequence, can be obtained.

5) ASSEMBLY OF GOLD NANOPARTICLES

INTRODUCTION

Methods for patterning materials at the nanometer scale have advanced tremendously in recent years (16). One of the most important achievements is the synthesis of assemblies of metallic, magnetic, or semiconducting nanocrystals with a controlled spacing (17). The importance of these systems is motivated by the fact that at the nanometer scale, the properties of materials depends strongly on the size (18). Optical, electronic and magnetic properties may totally change depending on the size of the particles investigated. A system consisting of patterned nanoparticles will have many potential applications as chemical sensors, spectroscopic enhancers, and optical or electronic processors (19, 20, 21). Alternatives methods must be developed soon to meet the need for further miniaturization of electronic components. This is not possible with today's top-down lithography techniques.

Many techniques such as colloidal crystallization (22, 23), monolayer deposition (24, 25), multilayer casting (26), molecular crosslinking (27, 28), and synthesis of nanoparticles in patterned etch pits (29) have been used to pattern nanocrystals into superlattice structures. Recently, methods which use DNA to assemble nanocrystals in a controlled pattern have been thoroughly investigated. For example, two complementary single stranded DNA, each derivatized with Au nanocrystals can be hybridized to form a

periodic array (19). Also, nanocrystals modified with ss-DNA were arranged into homodimeric, homotrimeric (16), heterodimeric and heterotrimeric (17) assemblies in which the Watson-Crick base pairing interactions were used to control the relative spatial arrangement of gold nanoparticles.

In contrast to all previous work reported, where at most three Au-nanoparticles are arranged by design, in this project we describe a method for patterning a single strand of DNA, used as a scaffold, with several 5 and 10 nm gold nanoparticles. Using repetitive single stranded DNA, we hybridized 5 and 10 nm nanocrystals modified with, respectively, 32 and 50 base oligonucleotides complementary to the repeats. The spacing between the nanoparticles in the system generated is ca 32 nm, making the technique promising for nanostructure fabrications (one and two dimensional patterning) and for the study of nanoparticle interactions at the nanometer scale (electronic properties).

We choose DNA to be both template and director material for its high stability in a given solution buffer, ability to form well-defined secondary structure, the property of self addressing to specific sites in the template and its small size relative to the nanogold crystals. In order to implement these experiments, we applied three techniques that have been developed by Alivisatos and his co-workers (16). The Au nanocrystals are chemically coated by complexation with dipotassium bis(p-sulfonatophenyl)phenyl-phosphane dihydrate (30) to prevent aggregation at high concentration in aqueous buffer. Single stranded oligonucleotides are thiol modified in their 5' ends in order to bind to the complexed nanocrystals. The ssDNA-Au nanocrystals are thereby addressed to specific sites in the template. Finally, the ssDNA-Au nanocrystals complex is purified from all

other undesired materials (Au nanocrystals bonded to more than one oligoniceotide, unbounded ssDNA and plain gold particles) using gel electrophoresis for separation.

Alivisatos and co-workers demonstrated in previous reports that thiol groups in the thiol-modified ssDNA can penetrate the shell of the coated particles and react with the gold surface forming gold-sulfur covalent bonds. Derivatized gold particles migrate slightly slower than their counterparts, plain particles, in gel electrophoresis. AFM was used to characterize the assemblies produced. Herein the decoration of the director strand was attempted using different conjugates, such as gold streptavidin coated nanoparticles, nanogold crystals and double labeled oligonucleotides. AFM was the main technique used to characterize the nanostructures produced.

I Streptavidin Coated Gold Nanoparticles

MATERIALS AND METHODS

- 32 base 5' biotinalyted single stranded DNA from *IDT* (Integrated DNA Technology). Oliginucleotide is HPLC purified, BioTEG linker (6 carbon atoms spacer)
- DNA sequence:

5'-/5BioTEG/AACGATGCAACCAGCGTCAGGCTGCTGTCCGA-3'

- Streptavidin coated 5 nm gold particles from *Ted Pella*. 1.7 10^{14} particles/ml.
- All steps in sample preparation for AFM were performed in a humid chamber. The freshly cleaved mica disk (V1 mica from SPM, approx. 1cm diameter) was

pretreated for 1 minute with 3 µl of 10x TAE / Mg^{++}. The mica was rinsed three times with deionized water, the water was allowed to drain off and the final rinse was wicked away with a Kim-wipe. The sample solution was added (different volumes were used to achieve a variety of surface coverage densities) and allowed to incubate on the mica for 3 minutes. Finally, the water was blown off the mica with a steady, light jet of argon gas. The sample was imaged using the ThermoMicroscopes Explorer scan head and analyzed with the SPMlab software package also from TM. Images were acquired in non-contact mode. We used a variety of set points (30-70% of free oscillation amplitude) and feedback parameters in response to imaging conditions which change with time.

EXPERIMENTAL DESIGN

Streptavidin is a tetrameric protein (4 x 13kDa) that has various biochemical applications. Each monomer of streptavidin binds one molecule of biotin with high binding affinity (Ka ~ 10^{13} M^{-1}). This high affinity and the tremendous stability over a wide range of temperature and pH make the biotin/streptavidin system of special interest (31). In the first part of this work a complex DNA nanostructure was formed by hybridizing a 32 base single stranded DNA oligomer derivatized with 5nm streptavidin coated gold particles with the director strand. The 32 bases single stranded DNA are synthesized with biotin at the 5' end. The biotin-DNA linkage is purposely chosen to be through a 6 carbon atom linker. In addition the 32 base ssDNA has 30 bases

complementary to the director strand and 2 extra bases. This extra space is meant to increase the binding capacity between the DNA oligomers and the Au particles by providing enough space between the gold particles and the DNA. The increase in binding capacity is provided by both decreasing the electrostatic repulsion between the Au particles and the DNA (both are negatively charged), and minimizing the steric hindrance. Fig. 5.1 depicted the DNA-nanogold particle complex structure.

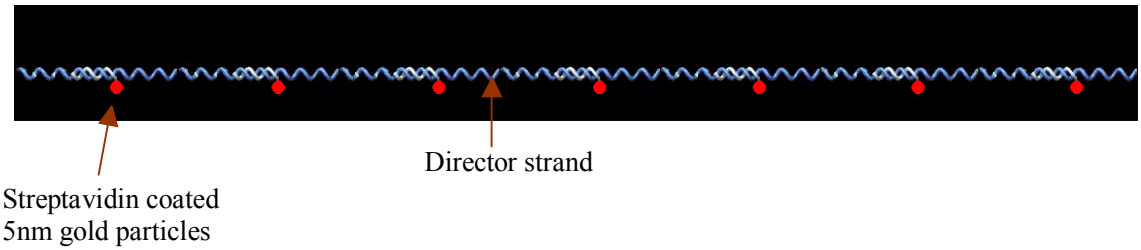

Figure 5.1: Complex DNA nanostructure composed of the director strand hybridized with oligonucleotides derivatized with 5 nm Au nanocrystals.

The nanogold particles are supplied in 20 mM Tris (tris-hydroxymethyl-aminomethane), 20 mM sodium azide, 154 mM NaCl, 1% BSA, and 20% glycerol pH 8.2. We first used the same buffer as a reaction buffer for DNA annealing and AFM imaging. Because of the high viscosity and the fairly high salt concentration, the buffer was not appropriate for direct use. In addition, preliminary experimental results showed that the gold nanoparticles need to be further concentrated to the appropriate working concentration. Also the separation of particles according to the number of oligonucleotides attached to them is a critical step, as the main goal of the experiment is

to have a highly controlled structure. A 5nm particle has 5 proteins per particle, which mean 20 biotin binding sites per particle. In the first experiment we studied the number of oligonucleotide distributed on the gold particles. An excess of 32 base ssDNA was incubated over night on a shaker with the 5 nm streptavidin coated gold particles in the supplied buffer. The mixture was characterized with 15% PAGE (Poly Acrylamide Gel Electrophoresis), Cyber green stained then imaged with Bio-Rad imaging system. The image shows the DNA bands (Fig. 5.2).

RESULTS AND DISCUSSION

The gel image, which shows the DNA bands, is provided on Fig.2.5

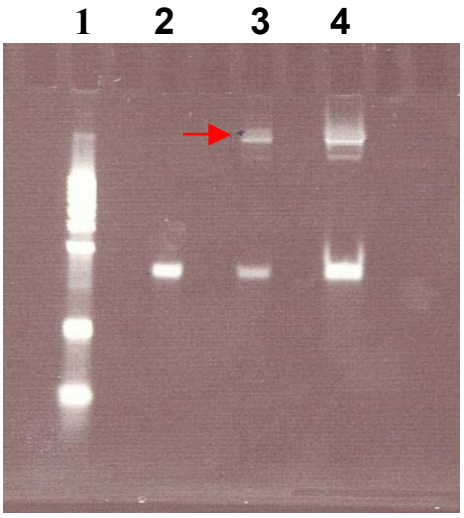

Figure 5.2: Gel image of derivatized 5 nm streptavidin coated nanogold particles. An excess of 32 bases biotinalyted single stranded DNA was incubated with the particles, the mixture was then resolved in 15% TBE Urea `gel. Red arrow indicates the major band, which corresponds to the saturation state (highest ratio of particles/DNA). Lane 1, 10 base DNA marker, lane 2, DNA oligomer, used as control, lane 3 and 4 mixture of derivatized particles at different concentrations.

There is one bright band that migrated slower than the plain DNA which was used as a control. The result allows us to draw two conclusions; the first is that in excess, the 32 base single stranded DNA binds specifically to the particles with a determined number of oligonucleotides per particle. The ratio of DNA to particles was not determined in this experiment, as we were not able to see multiple bands corresponding to different numbers of oligonucleotides per gold particle. There is a very light band lower than the main band, which may correspond to a lower DNA to particle ratio. Due to the quite large difference in migration between the plain DNA (control) and the main band, which is believed to be more than the shift produced by one or two extra DNA strands on the particles, we consider that the main band represent the state of saturation. However, we are not able to demonstrate how many oligonucleotides were bound per single particle in that state. Secondly, this image shows that the dye fluorescence is not quenched by the gold particles. In contrast to other DNA/nanogold particles experiments we have performed, here we can directly see the stained DNA.

The gold/fluorescence quenching is expected to be distance dependent. The closer the DNA is to the surface, the greater is the quenching. Being able to detect DNA bound particles by simply staining the gel represents a great advantage provided by the streptavidin coated particles. It is believed that the streptavidin protein spaces the DNA sufficiently far from the gold to inhibit quenching.

Some attempts were made to extract the derivatized nanogold from the gel using traditional freeze thaw methods, but none of them were successful. One reason could be the sensitivity of the streptavidin coated particles towards the low temperature (freezing temperature) which is called for in many gel extraction protocols.

We then tried to isolate the nanogold particles from the buffer by centrifugation. 20 µl of 5 nm streptavidin nanoparticles were centrifuged for 1 hour at 14,000 rpm, then the supernatant was discarded, particles were suspended in 50 µl of 1X TAE/Mg^{2+} buffer. The appropriate quantity of DNA linker was added for a 1 to 1 DNA/particle ratio.

The mixture was incubated overnight with the director strand then AFM imaged (Fig. 5.3). The image shows an excess of DNA linker. The director strand is pretty much decorated with the 32 base single stranded DNA (shown as dots on the long template). The 5 nm gold particles (white spots) are not attached to the DNA. This may be explained by the change of buffer that may affect the streptavidin/biotin binding capacity. The binding capacity is decreased many folds according to our AFM images. The distance between two consecutive binding sites might be argued to be ca 32 nm (95 bases between two binding sites); however the AFM data Fig. 5.4 shows a higher value. This higher distance obtained by the AFM is due to the single stranded nature of the director strand. That makes the distance between two bases greater than 0.34 nm (distance between two bases in double stranded B-form DNA). To the best of my knowledge the distance between two bases can not be precisely determined for single stranded DNA; it might vary strongly with the pH and salt concentration of the buffer. Our data here shows one dimensional patterning of single stranded DNA, used as scaffold, by a 32 base complementary strand.

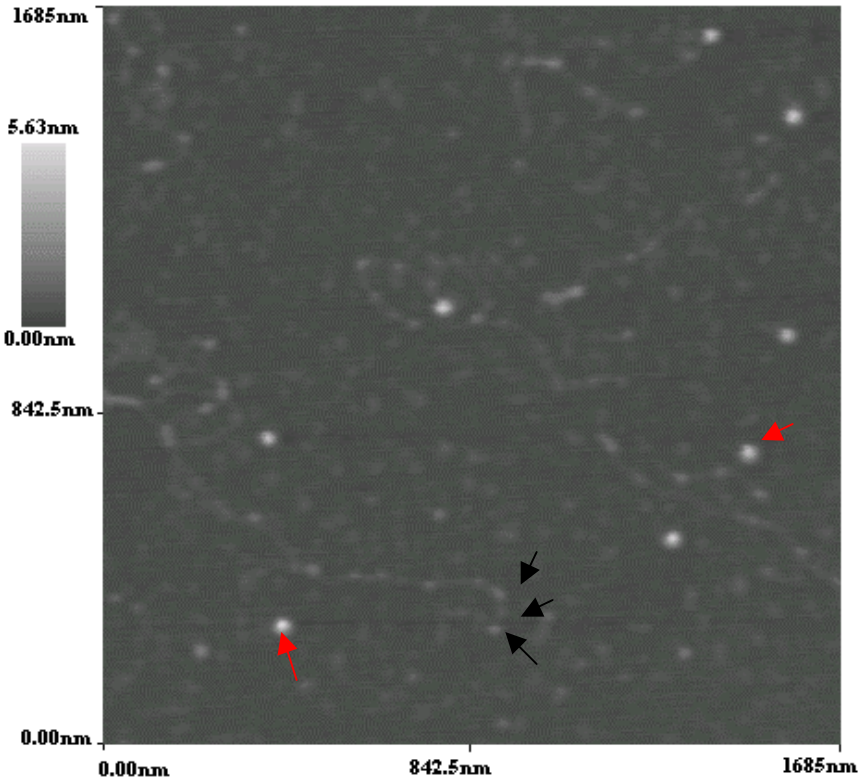

Figure 5.3: AFM image of blue strand used as scaffold for 5nm streptavidin coated gold particle patterning. The image shows that the particles did not efficiently bind to the long strand; however the 32 base complementary strand is demonstrated to form a pattern of ca 40 nm spacing. Red arrows show the 5 nm particles, black arrows show the successive pattern formed by the 32 base complementary strands.

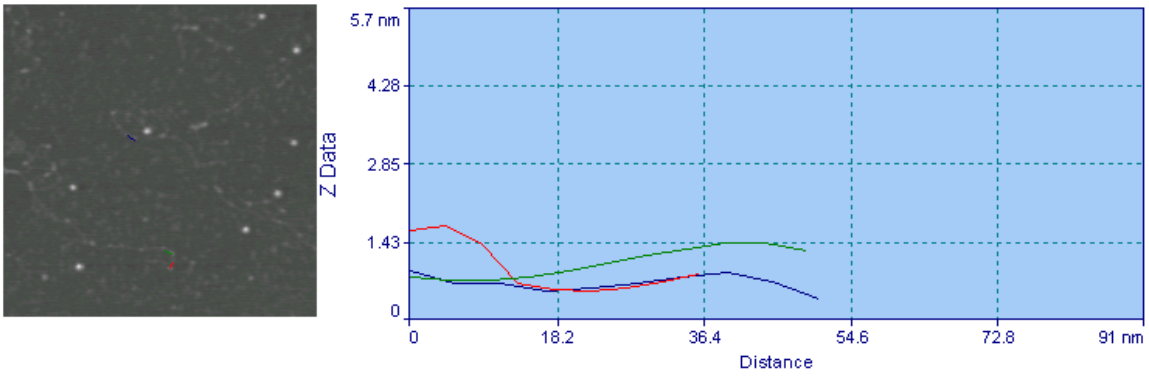

Figure 5.4: Line scan plot showing the average spacing between two consecutive dots.

In a next series of experiments the director strand was first annealed with the DNA linker then mixed with the appropriate amount of nanogold particles to make a 1 to 1 DNA to gold particle ratio. The mixture was incubated overnight in the supplied buffer. A Spin column (5500) from *Amersham* was used to separate the DNA nanostructure from the undesired material. The sample was vigorously rinsed before any image could be obtained. The quality of the images (Fig. 5.5) was much lower than the AFM images obtained with the first process (Fig. 5.3). It is clear that the particles are irregularly distributed on the template. In some images a pattern with a spacing distance of ca 45 nm, can be seen, but the director strand is not obvious.

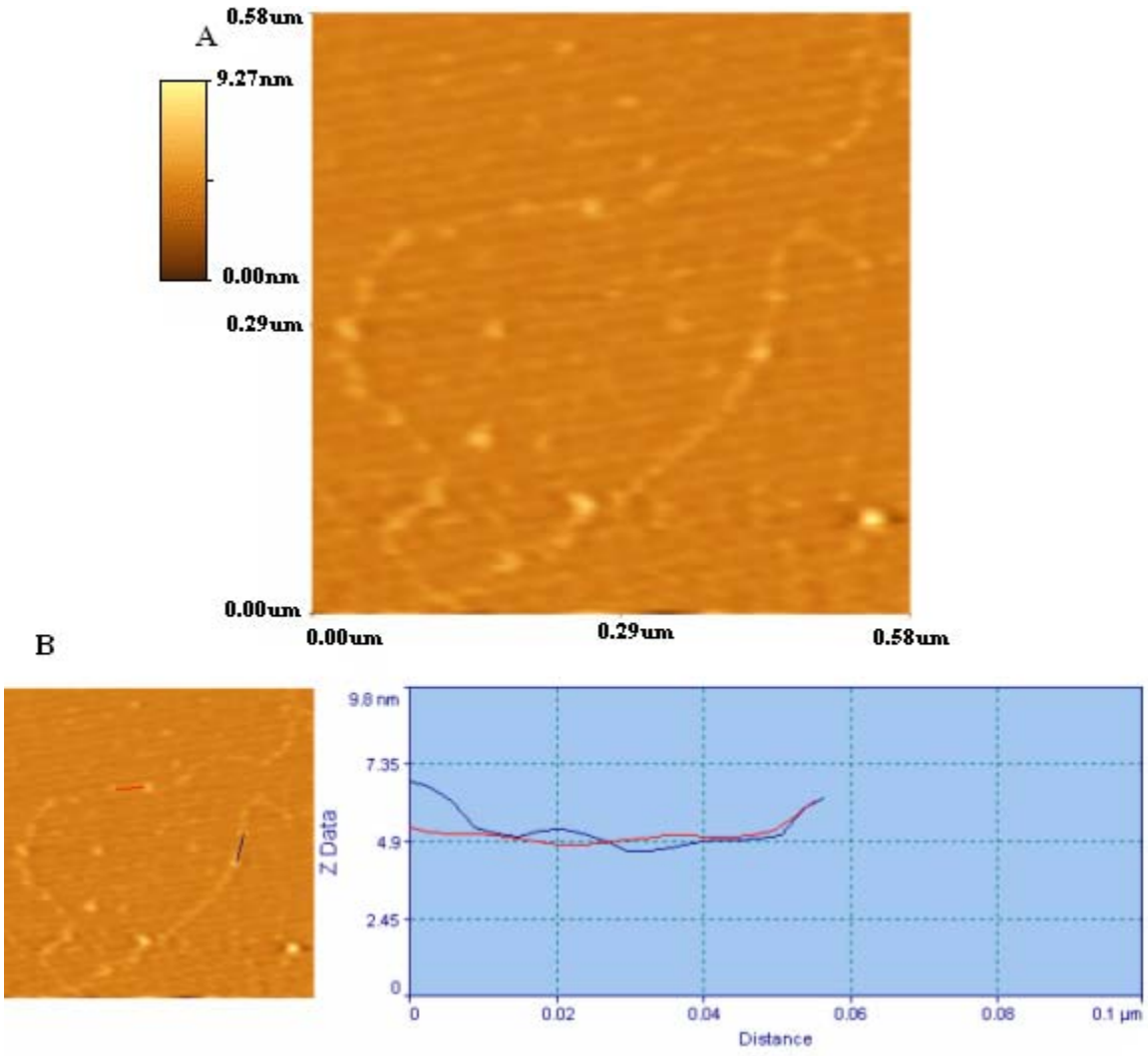

Figure 5.5: AFM image showing a single stranded DNA strand semi-patterned with 5 nm streptavidin coated gold nanoparticles. The sample was purified using 5500 spin column before imaging.

II Director Strand Patterned by Cyan Strand

Here we will refer to the central strand of block A (block A and B are two components of the DNA nanoarrays previously discussed) as the cyan strand. The cyan strand is 42 bases long, with the arms complementary to the unit copy of the director strand, as shown in Fig. 5.6. The cyan forms a very unusual shape in the nanoarrays; it has 21 bases complementary to the red strand, and two arms that bind to the blue strand requiring a 180 degree rotation. The cyan strand has the shape of a circular strand, but it is nicked in the middle of the side complementary to the blue strand. We emphasize the study of this structure because we believe that the stability of the bond between the two arms and the blue strand will play a critical role in determining the stability of the entire nanostructure. Fluorescence Resonance Energy Transfer (FRET) was used to study association of the cyan strand with the director strand.

Fluorescence Resonance Energy Transfer (FRET)

Briefly, Fluorescence Resonance Energy Transfer is a distance-dependent interaction between the electronic excited state of one dye molecule (a donor) and the ground state of another dye molecule (acceptor). In FRET, excitation is transferred from the donor molecule to the acceptor molecule without emission of a photon. The efficiency of FRET is dependent on the distance separating the donor and acceptor, typically between 1 and 100 angstroms (18). The donor is usually exited at a given wavelength, different than the acceptor excitation wavelength. The later is excited due to the overlap in the absorption

spectrums of the acceptor with emission spectrum of the donor. By measuring the efficiency of the energy transfer, the donor/acceptor distance can be determined with high accuracy. Qualitatively, relative changes in acceptor emission can be interpreted in terms of relative positions of the donor/acceptor molecules.

The ends of the cyan strand were labeled with fluorescein at one end and rhodamine near the other. When integrated into the block structure the distance between the two dyes is ca 1 nm (3 bp x 0.3 nm/bp). We studied this director strand cyan assembly system with Confocal microscopy (as discussed in the next section).

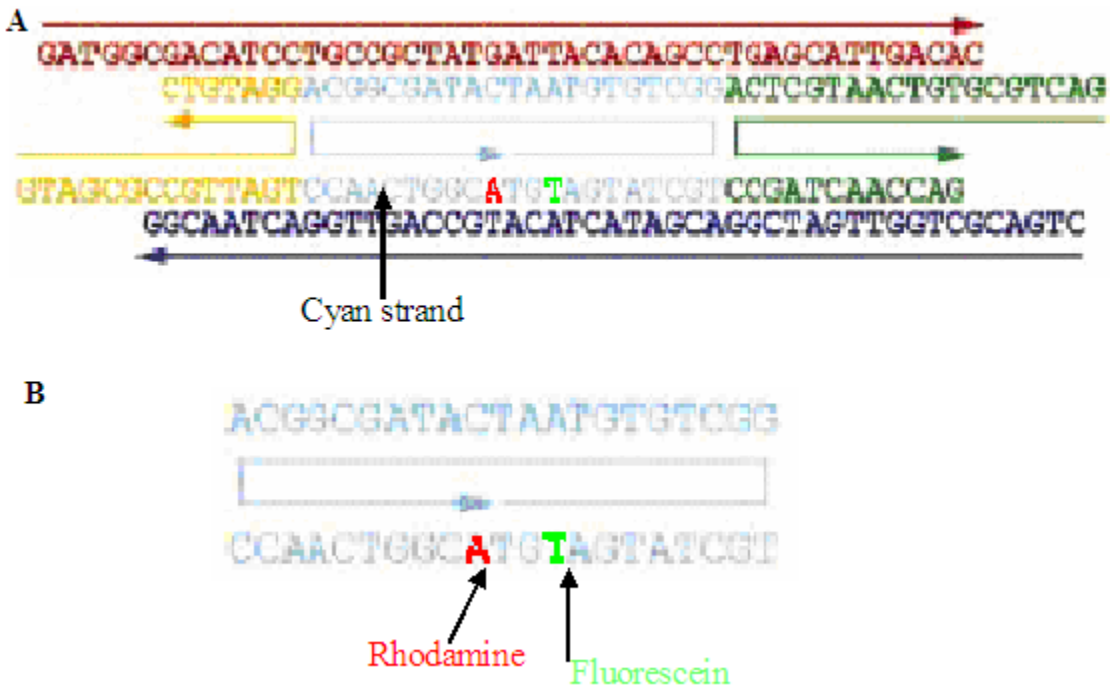

Figure 5.6: A. Scheme showing the structure of Block A. B. The structure of the Cyan strand. The sequence is continuous forming two 180^{o} angles. Rhodomine and Fluorescein are shown respectively in red and green. The energy transfer between the two labels reflects the distance between them.

AFM studies of the system were performed to verify appropriate assembly. We annealed the director strand with the cyan at the appropriate concentration (1:1 ratio). The annealing was performed by heating the mixture in TAE/Mg^{++} at 90 degree for 5 min. Then the mixture was slowly cooled down to room temperature.

The AFM images show continuous punctuation evenly distributed over the template. We believe that the AFM height measurements are more accurate than the observed distances separating two consecutive cyan strands. This may be explained by tip broadening. Tip broadening arises when the radius of curvature of the tip is comparable with, or greater than, the size of the feature imaged. The diagram in Fig. 5.7 illustrates this problem; as the tip scans over the specimen, the sides of the tip make contact before the apex, and the microscope begins to respond to the feature. This is what we may call tip convolution.

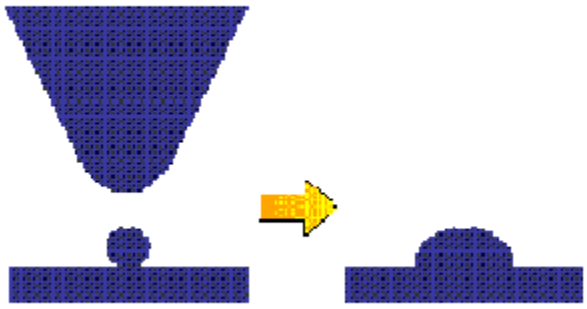

Figure 5.7: Diagram showing the broadening caused by the tip shape on the specimen features. Tip convolution is particularly observed when the size of the tip is comparable to or greater than the size of the features studied.

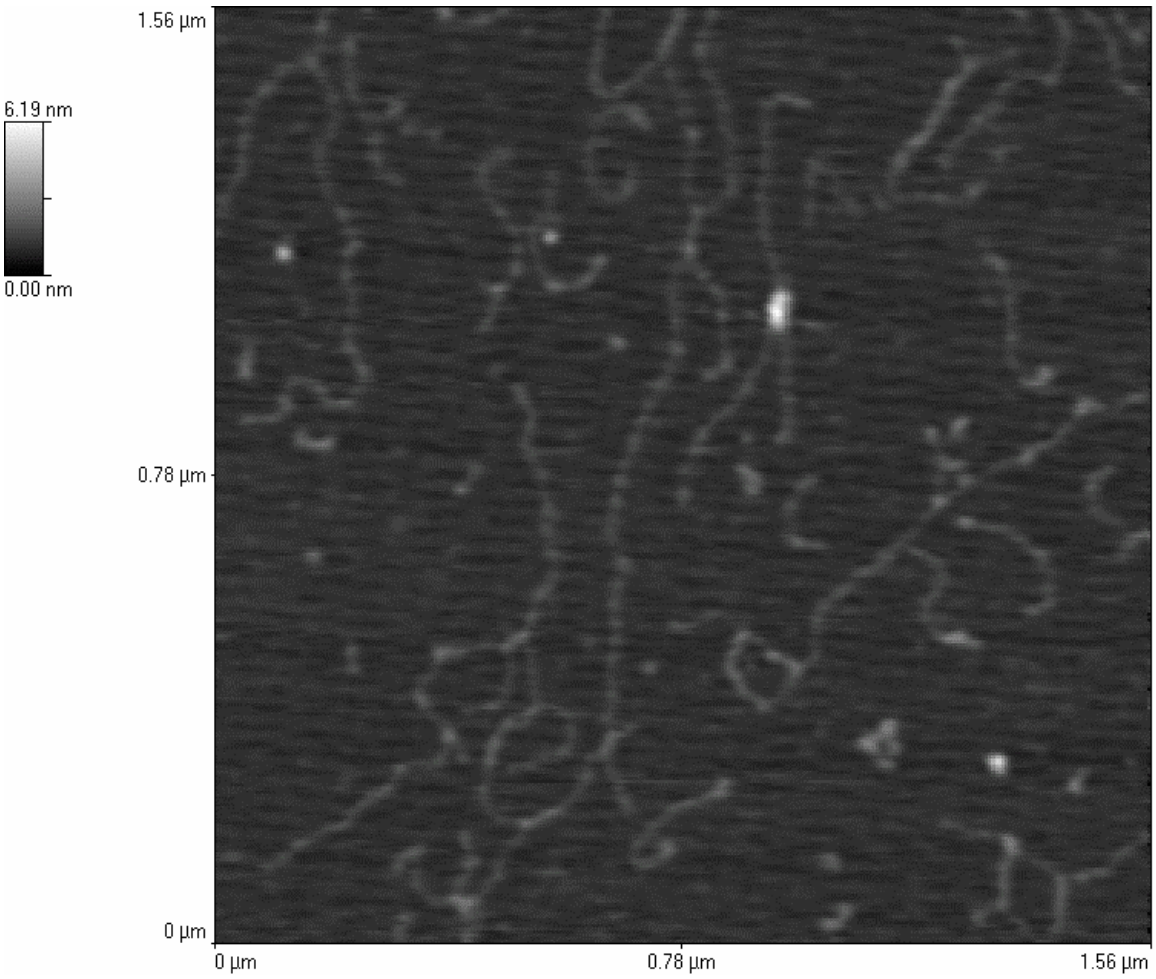

Figure 5.8: AFM micrograph of Cyan strands hybridized with synthesized blue strands. The cyan strand is represented by the consecutive punctuation on the DNA scaffold. Image was acquired in non-contact mode.

Fig. 5.8 shows blue strands decorated with cyan strands. The blue strands are composed of multiple copies of a 95 base sequence, an intrinsic component of the DNA nanoarrays. The noise level in these images does not allow us to determine the Cyan strand distribution on the blue strands. This may be explained by the environmental conditions, rather than by the sample preparation (DNA hybridization and AFM sample preparation).

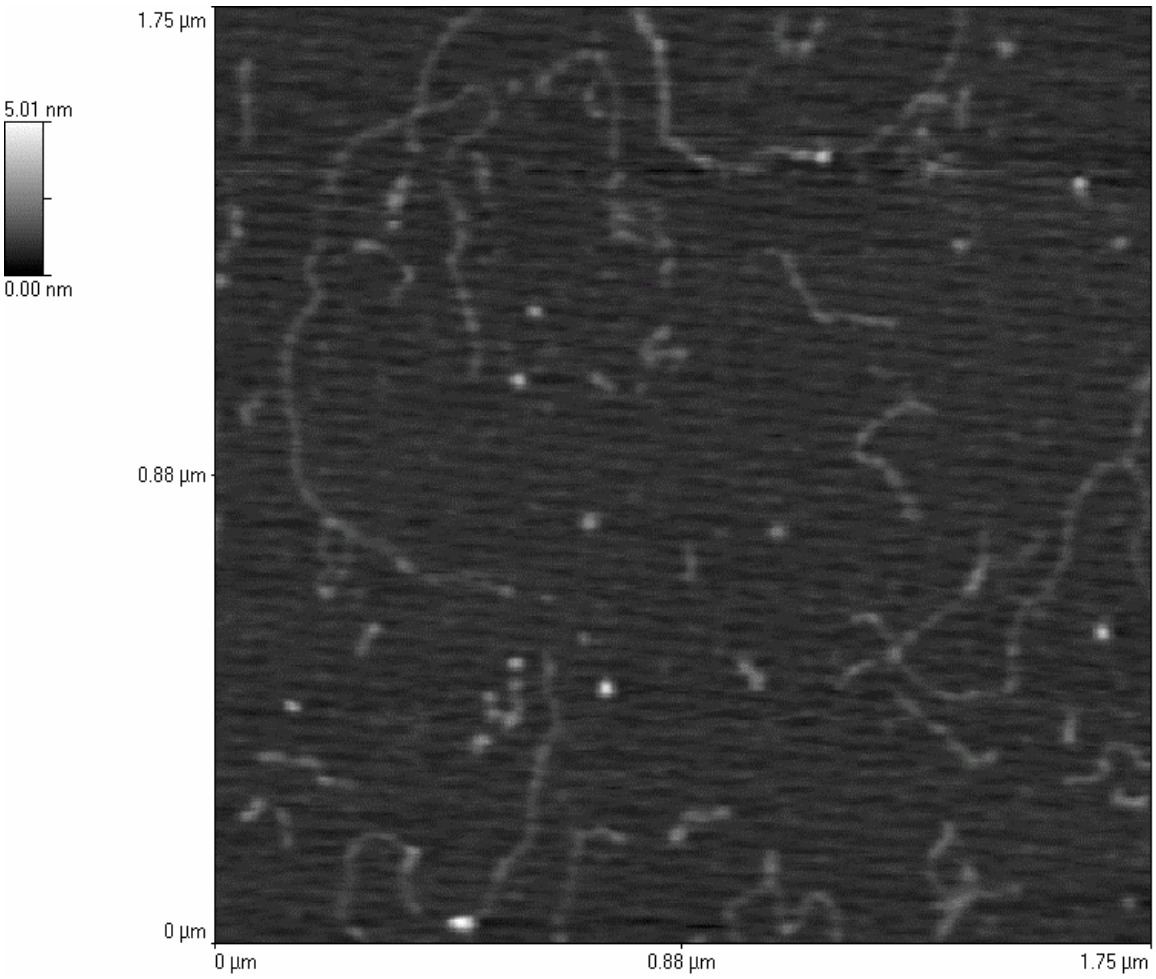

Figure 5.9: AFM micrograph of the same sample showing the Cyan pattern on the blue strands

a)

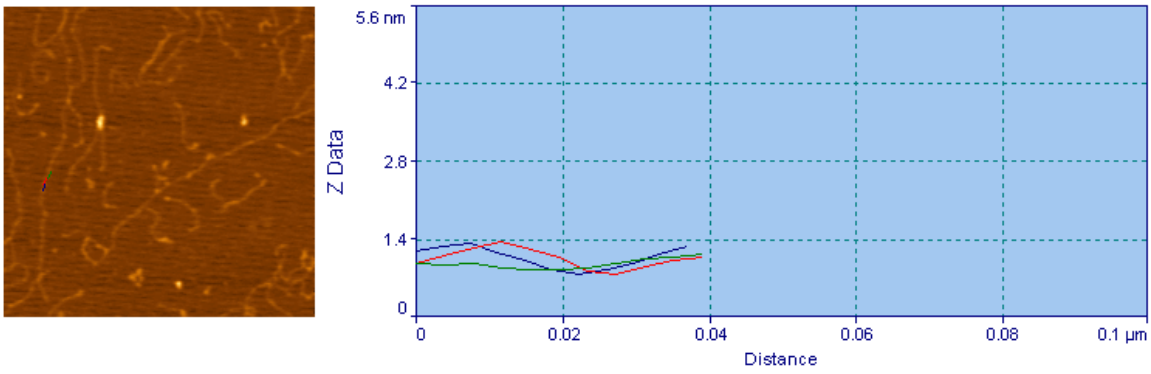

b)

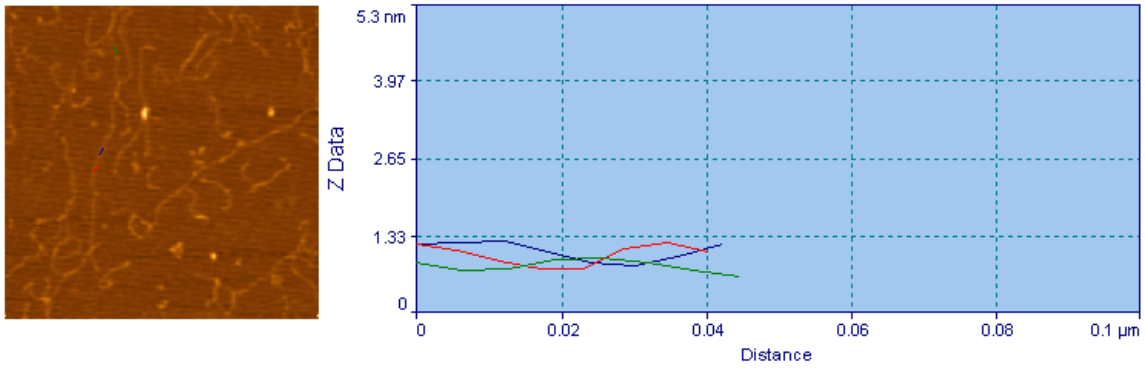

c)

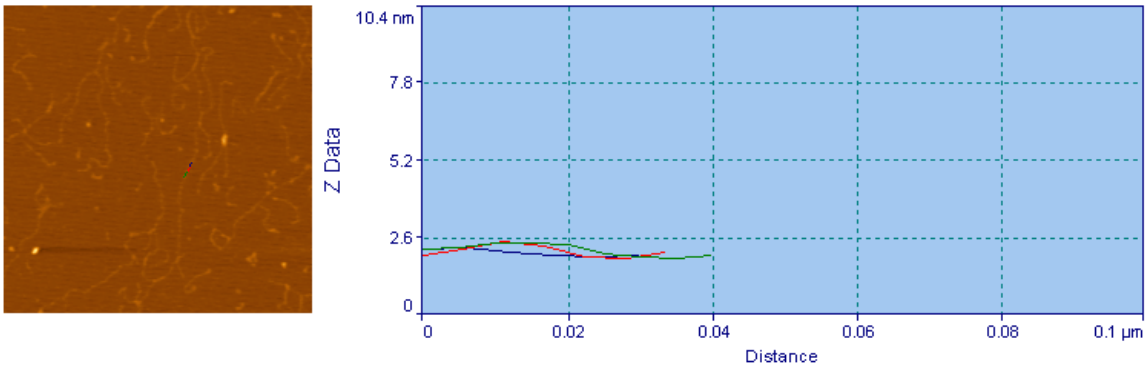

Figure 5.10: a, b and c represent three AFM images of the blue strand-Cyan hybridization. The distance between two consecutive Cyan strands is measured.

It is worth note here that the spacing between two cyan strands is 95 bases (the periodicity of our structure); this is equal to 30.4 nm if it is double stranded DNA. In our case the DNA is single stranded, so the distance is anticipated to be greater. To the best of my knowledge the distance between two bases in single stranded DNA is variable, although it is predicted to be between .32 nm and .6 nm per base. Our result is in close agreement with these predictions. We would predict the distance between to consecutive cyan strands to be ca 51 nm (21x0.32nm/bp + 74x0.6nm/base).

III Biotinalyted DNA Surface Chemistry on Magnetic Beads Coated with Streptavidin

In this part of the project we studied the binding efficiency of biotinalyted RCA product, produced with a biotinalyted primer, on streptavidin coated magnetic beads. Also we studied the energy transfer in the double labeled cyan strand. As we previously indicated when the cyan binds to the blue strand the two ends are separated by approximately 1 nm. In this case a high FRET efficiency is anticipated. In order to detect this energy transfer we used confocal microscopy. It is known that the resolution of the confocal microscope is above single molecules. To overcome this problem we used multiple copies of the blue strand synthesized by Rolling Circle Amplification as a scaffold. In addition, a large amount of DNA can be attached to a single magnetic bead, which makes the detection using the confocal microscope achievable.

One goal of this part of the project is to study the potential of using such a system for DNA mismatch detection. We believe that under certain conditions, complete base pairing is needed to obtain maximum FRET. If a mismatch exists in the target, no energy transfer will be observed. By designing the appropriate double labeled probe, which is the cyan strand here, mismatches could be detected easily based on the different emission wavelengths of the two fluorophores. Confocal has multiple advantages over other techniques such as fluorimetry. Particularly, confocal is easier to use and less time consuming. Also, since this is an imaging technique, multiple results can be depicted in one image, with different colors, which make them easier to interpret.

One control probe was designed where the two fluorophores were kept away from each other. By exciting the fluorescein at 488 nm wavelength the control sample should strongly emit at ca 522, the emission wavelength of fluorescein, indicating no energy transfer. Under the same conditions the control sample should emit weakly at ca 598 nm, the emission wavelength of rhodamine. Fig. 5.11 displays the control and experiment schemes.

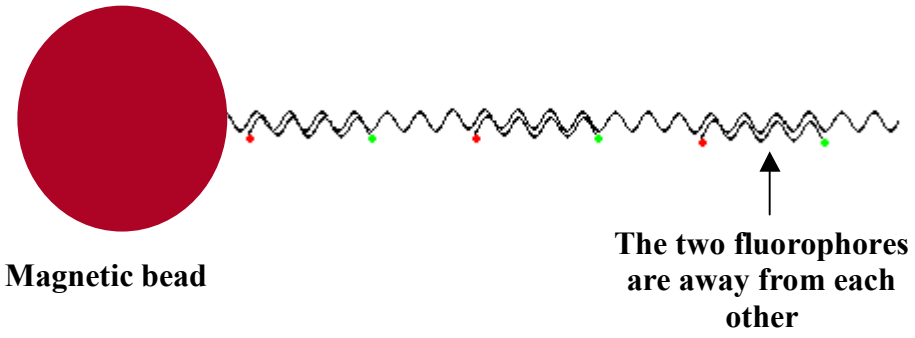

A- Control: No FRET

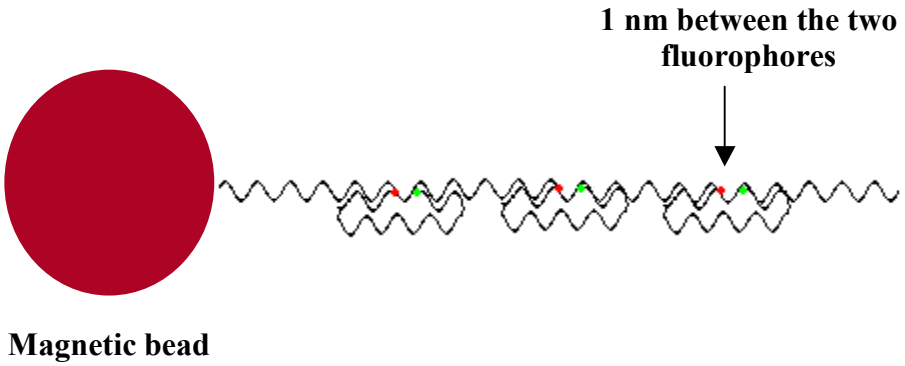

B- Experiment: high FRET efficiency

Figure 5.11: Scheme of the confocal experiment

MATERIALS AND METHODS

- Two different beads are used, 2.8 μm streptavidin coated magnetic beads from *Dynabeads* (M-280) and 0.8 μm streptavidin coated magnetic beads from *Sera-Mag microparticles.*
- Biotinalyted RCA is prepared using TEG-biotinalyted primer, so all the product will have biotin on the 5'end. Primer ordered from *IDT*, HPLC purified.
- Cyan sequence: 5'TGT(Fdt)AGTATCGTGGCTGTGTAATCATAGCGGCACCAACTGGCA(TAMARA)3' from *IDT*, HPLC purified
- Control cyan sequence: 5'(ifluorT)CCAACTGGCATGTAGTATCGT(36-TAMTph)3' from *IDT*, HPLC purified
- Sample preparation for Dynabeads.

1. Resuspend the beads by shaking the vial to obtain homogeneous suspension.
2. Transfer 5 μl (50 μg) resuspended beads to 1.5 ml microcentrifuge tube, place the tube in magnet 1 to 2 min until the beads settle on the wall of the tube.
3. Remove the supernatant (tube remain in the magnet)
4. Remove the tube, add 20 μl of binding solution then gently resuspend them by pipetting.
5. Take 5 μl of the previous solution and add 18 μl of binding solution.
6. Put it in the magnet and take off the supernatant.
7. Add 20 μl of binding solution and 20 μl of biotinalyted RCA.
8. Incubate at room temperature for 3 hours on a roller (shaker).

9. Put the tube back on the magnet remove the supernatant and add 40 µl of washing solution, resuspend by pipetting then remove the supernatant (repeat it twice).
10. Wash the beads one more time with 40 µl of water, the excess RCA will be discarded.
11. Resuspend the beads in 20 µl of 1X TAE/Mg^{++}, add 5 µl of cyan and incubate for 30 min at room temperature.
12. Put the tube back on the magnet and remove the supernatant, the excess of cyan will be discarded, add 40 µl of 1X TAE/Mg^{++}.
13. Finally heat up the tube at 45 degree then discard the supernatant, add appropriate volume of 1X TAE/Mg^{++} for confocal imaging. This step will insure that no unspecific binding cyan will interfere in the experiment.

RESULTS AND DISCUSSION

The relationship between the transfer efficiency and the distance between the two probes is given by the equation:

$$E = \frac{R_o^6}{R_0^6 + R^6}$$

where R_0 is the Forster distance between the donor and the acceptor probes at which the energy transfer is (on average) 50% efficient (Fig. 5.12). R is the real distance between the two fluorophores.

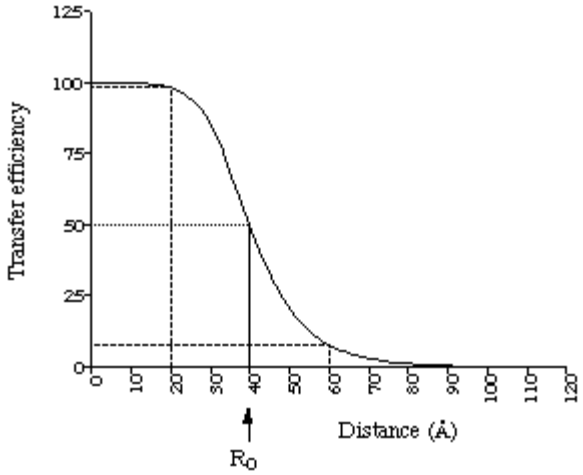

Figure 5.12: The solid curve represents the relationship between the efficiency of the fluorescence resonance energy transfer and the distance separating the donor and the acceptor. The importance of this relationship is that there is a limited range of donor-acceptor distances which can be probed by any particular donor-acceptor pair.

In our experiment the distance between the two fluorophores is ca 1.2 nm (3 bases apart) so the efficiency should be high, calculated to be 0.98 (Ro = 5.5 nm for fluorescein-TAMARA). In the control experiment the distance is 7.14 nm (21 bases) the efficiency will be low, calculated to be 0.17. It is worth noting here that we kept the same binding site for both cyan and control. This will assure the same binding condition (temperature, buffer etc).

Fig. 5.13 summarizes the result of the first set of experiments using the Dynabeads. Column 1 and column 2 show images of beads and beads with labeled cyan oligomer. Images show similar uniform distribution of autoflluorescence. Adding the cyan to the pure beads does not affect the emission intensity. When cyan is added to the bead/RCA complex a halo of fluorescence is seen, it is attributed to the long RCA product binding from one end to the beads and having the other end extending into the solution. The

detection of a small variation in the emission could not be detected due to the autoflluorescence activity of the beads.

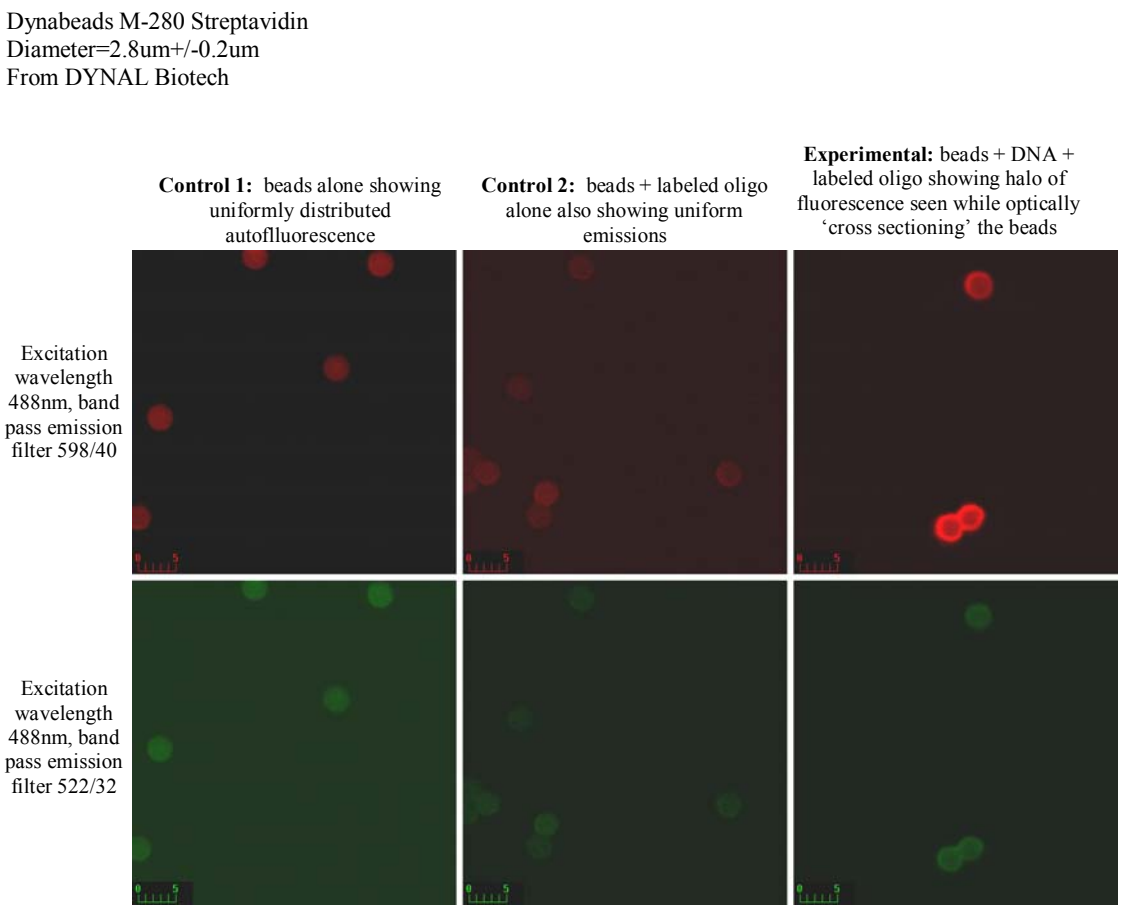

Figure 5.13: Experiments shows emission when the cyan is added to the RCA product. The 2 controls (beads and beads plus cyan) show only the bead auto-fluorescence

In the next set of experiments we changed from the Dynabeads to the Sera-Mag beads (beads used in this experiment Sera-Mag streptavidin magnetic microparticles from seradyn Bead size 0.737 um (nominal)); the latter did not show any autoflluorescence activity. As seen in Fig.5.14 controls showed virtually no signal. Experiments were performed with the two different double labeled oligomer, one

designed to bring the 2 fluorophores into close proximity (<3nm), the other to keep them apart (>6nm). The confocal images in Fig. 5.14 show two higher rhodamine emission with the first oligomer as expected. With the second oligomer we see very weak rhodamine emission even after data normalization.

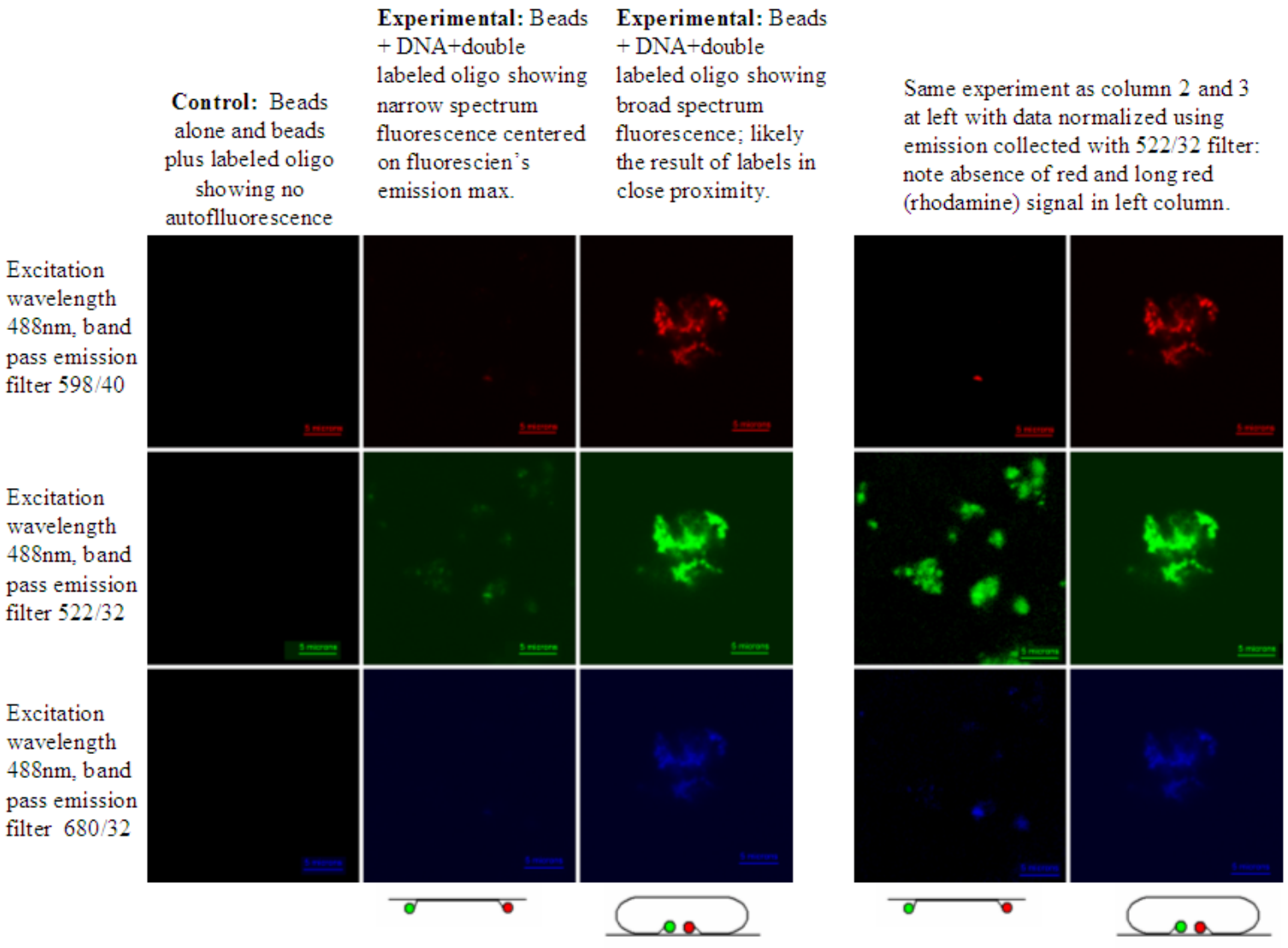

Figure 5.14: Confocal images of assemblies at three different emission wavelengths. Control probe shows higher fluorescein emission with respectively small rhodamine emission. In the case of cyan higher rhodamine emission is observed. The plain beads display no autoflluorescence.

We believe that by properly designing labeled oligomers, we can study their interactions with complementary DNA strands by analyzing differential fluorescent emissions that can result from FRET. By using solid substrates (beads), we hope to better probe the 3D conformation of the DNA/oligo/fluorophore complexes. In addition the experiments suggest that the rhodamine emission is an appropriate reporter for determining if any FRET occurs in this system.

VI DNA Assembly of Gold Nanoparticles

INTRODUCTION

The capability of generating assemblies of metallic nanocrystals, in which the relative spatial arrangement of crystals is well controlled, would provide new opportunities for experimentation. Such a system will allow for a methodical study of the magnetic, optical and physical properties of the arranged crystals. Unlike all reported work, we attempted here to produce a structure of multiple 10 nm nanogold crystals at ca 32 nm spacing, DNA was used as both scaffold and carrier. In order to achieve that highly organized nanostructure many preliminary steps had to be taken. We started with designing the appropriate complementary strand that will address the nanocrystals to the desired location on the long blue scaffold. It has been demonstrated that for 10 nm diameter gold nanocrystals with only a few DNAs per nanocrystal, fragments of oligonucleotide are nonspecifically attached to the Au particle surface (34). We designed our complementary

strand to be 50 bases long in order to avoid this complete wrapping of oligonucleotides around the nanocrystals. Then the gold nanocrystals were phosphine coated to avoid aggregation at high concentration. Finally a separation technique based on the difference of the electro-mobility was used to extract mono-hybridized nanocrystals from undesired material.

By coating the gold nanoparticles with negatively charged triphenyl phosphine sulfonate their charge density becomes similar to that of DNA. Thus when oligonucleotides are attached to the gold, through a thiol attachment, the first effect will be a change on the size of the system rather than change the charge density. As a consequence the electrophoretic mobility is size based. Gel electrophoresis was used to separate different DNA to gold ratio structures due to its sensitivity to conformation variation and its ease of use.

MATERIALS AND METHODS

- Gold nanocrystals with a diameter of 10 nm were purchased from *Ted Pella* (Redding, CA). dipotassium bis(p-sulfonatophenyl)phenyl-phosphane dehydrate fromStrem Chemicals (Newburyport, MA).
- 50 base thiol oligonucleotides: 5'-/5ThioMC6-D/AAAACTGGCATGTAGTATCGTCCGATGCAACCAGCGTCAGGCTGCTGTC-3' from *IDT*, HPLC purified.
- Gold complexation:

1. Aqueous solution of 100 ml of 10 nm nanocrystals (used directly as supplied) was stirred with 30 mg of dipotassium bis(p-sulfonatophenyl)phenyl-phosphane dehydrate at room temperature for more than 10 hours.
2. Add solid NaCl to the reaction mixture until the color change from burgundy to red blue.
3. Centrifuge the sample 5 min at 500 x g blue pellet should be seen on the wall of the tube.
4. Remove the supernatant.
5. Redissolve the pellet in an aqueous solution of dipotassium bis(p-sulfonatophenyl)phenyl-phosphane dehydrate (30 mg in 100 ml).

EXPERIMENTAL

- Nanocrystals molecule purification:
    1. 2% agarose gel was used to analyze and isolate the desired structure (DNA monohybredized nanocrystals). Glycerol (6X) as used as loading buffer and 0.5X TBE buffer was used as running buffer.
    2. After electrophoresis, samples were isolated by slicing the gel in front of the desired band and inserting glassfiber microfilters (Whatman GF/C) that were backed with dialysis membranes (Spectra/Por, MWCO: 10000).
    3. Gel with was run with filter/membrane inserted for 3 to 5 min, or until the desired bands incorporated into the glassfiber filter.

4. The filter/membrane pieces were then taken out of the gel and placed into microcentrifuge tubes (Ultra free-MC centrifugal Filter Devices from Millipore) and centrifuged for 1 min (1400 x g).

- Nanocrystals-DNA structure assembly: the gel isolated DNA monohybridized nanocrystals were added to RCA product (the concentration of RCA was approximately determined to have one nanocrystal for each binding site.
- All steps in sample preparation for AFM were performed in a humid chamber. The freshly cleaved mica disk (V1 mica from SPM, approx. 1cm diameter) was pretreated for 1 minute with 3 µl of 10x TAE / Mg^{++}. The mica was rinsed three times with deionized water, the water was allowed to drain off and final rinse was wicked away with a Kim-wipe. The sample solution was added (different volumes were used to achieve a variety of surface coverage densities) and allowed to set on the mica for 3 minutes. Finally, the water was blown off the mica with a steady, light jet of argon gas. The sample was imaged using the ThermoMicroscopes Exploreer scan head and analyzed with the SPMlab software package also from TM. Images were acquired in non-contact mode. We used a variety of set points (30-70% of free oscillation amplitude) and feedback parameters in response to imaging conditions which change with time.

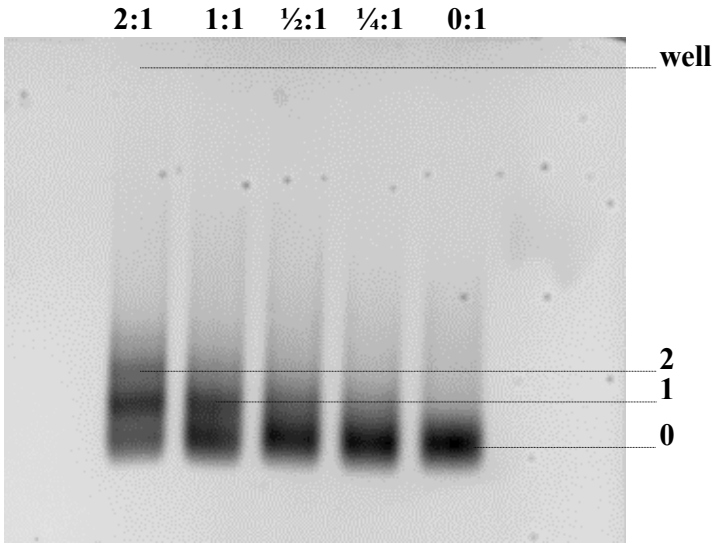

Figure 5.15 2% agarose gel loaded with different DNA/Au conjugates after 1 hour at 200 V in 0.5X TBE buffer. 50-base DNA with 5' thiol modification was added in different ratios (DNA to gold listed on the top of the image) to phosphine coated Au nanocrystals of 10 nm diameter and incubated for 2 hours in 50 mM NaCl on a rocking platform at room temperature. To obtain the different DNA/gold ratios, the DNA concentration was reduced successively by a factor of 2 by dilution with H_2O, before the DNA was added to the nanocrystals. Depending on the DNA/Au ratio bands with a discrete number of DNA molecules (1, 2 and 3) attached per nanocrystals can be resolved.

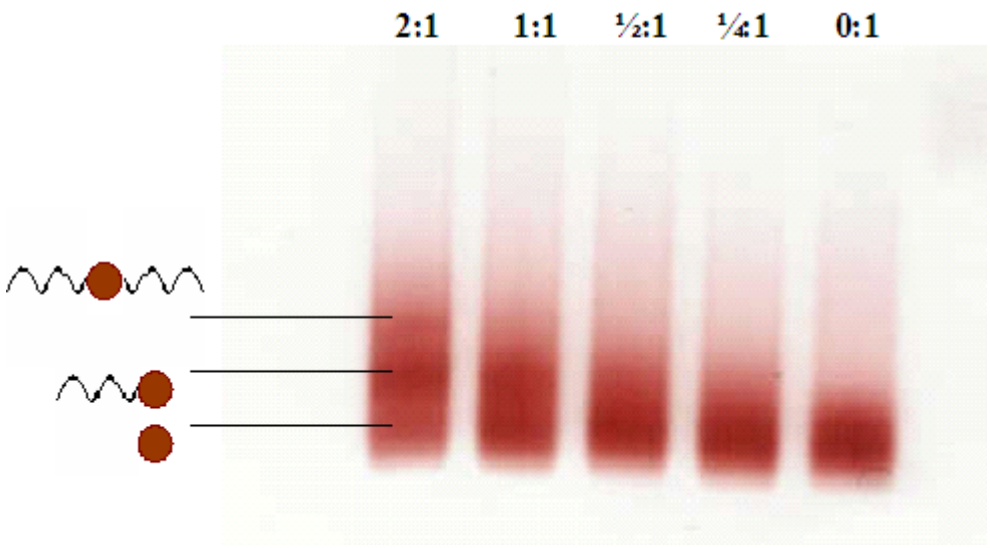

Figure 5.16: Same gel image as above with natural color. Reddish color is due to the gold nanocrystals. Image was taken with a scanner.

Fig. 5.15 shows that the mobility of gold nanocrystals is retarded by the addition of oligonucleotides. By running different DNA/gold ratios through gel electrophoresis we were able to distinguish between gold nanocrystals with different numbers of DNA molecules attached. Mono-derivatized particles were then extracted. It is worth noting that, in contrast to our case where the mobility retardation increases upon addition of DNA, in many other cases the mobility increases by adding more DNA. For example, for silica coated nanocrystals with low charge density compared to DNA, the mobility increases with DNA addition (34). In that case DNA may be considered to be driving the nanoparticles through the gel.

Due to the gold fluorescence quenching, the use of a staining dye is not recommended. Instead the red color of the gold makes the detection of the different bands possible with the unaided eye.

It has been demonstrated by Alivisatos and co-workers that for 10 nm diameter Au nanocrystals, the inner part of about 30 bases of the oligonucleotide is fully stretched, whereas the outer part has a coil conformation, in the case of saturated nanoparticles. The outer part of the DNA can adopt a random coil conformation, most like free DNA molecules, and should be very accessible for DNA hybridization. As a consequence, using DNA sequence higher than 30 bases may be effective in using nanoparticles as building blocks. In the case of only having a single DNA molecule attached to a nanoparticle, the DNA strand can be expected to be nonspecifically attached to the gold surface. It is then suggested that one should use a dense layer of short oligonucleotides (30 bases at least), and one single, long DNA molecule for which only the outer part codes for hybridization. In addition to preventing the nonspecific binding of the DNA molecule to the nanoparticle surface, the dense DNA coating ensures excellent stability even for high salt concentration. Further efforts include attempting the hybridization of mono-derivatized 10 nm gold nanocrystals with the RCA product and the characterization of the nanostructure with AFM.

CONCLUSION

Molecular electronics currently consists of only the formation of single molecule based electronic devices. But it can also be generalized to the area of science and technology that studies the electronics and sensors based on molecular recognition. We believe that DNA will play a major role in the toolkit of molecular electronics. DNA can be combined with basically any chemical side group. For example, single stranded DNA can be attached to electrically active molecular elements, such as nanocrystals, carbon nanotubes, or molecular switches. The self assembly proprieties of DNA will self-direct the modified DNA sequences to well determined sites. This way the DNA can be at the same time the driving material and the scaffold. We demonstrate here the synthesis of tandemly repeated strands of DNA. We also had some success hybridizing complementary sequences with a spacing of 32 nm. We also effectively isolated mono-derivatized gold particles. There are 10 nm gold nanocrystal bound to a single DNA molecules. These nanocrystals should be able to hybridize to the long DNA scaffold, enabling us to pattern matter at the nanometer scale.

This work gives entry to a new area of DNA/nanoparticles assembly. These nanostructures will have useful electrical, optical and structural properties by controlling the nanoparticle size and the distances that separate them. We believe that this work can be extended easily to hybridize other active molecules or molecular elements, such as carbon nanotubes, molecular switches or other noble-metal or semiconductor colloidal nanoparticles. Unlike all previously reported work, where at maximum three nanoparticles were patterned on a DNA scaffold, this strategy will enable us to pattern as

high as 9 particles on a precisely designed, synthesized DNA scaffold. Increasing the number of derivatives and precisely controlling the distance between them will give rise to a new class of materials particularly attractive for molecular electronics fabrication. Further improvements in the cloning strategy, especially the isolation and amplification of longer DNA fragments (more copies), is required before the Rolling Circle Amplification can be the technique for synthesis of complex mixtures of different molecular element that is limited only by the extent of control over the DNA template.

6) CONCLUSION

In this work we addressed the challenge of growing DNA nanoarrays composed of two blocks (block A and block B) on pre-determined sites on a surface. Block A and block B are each formed of five different DNA strands. The five strands are called blue, red, cyan, yellow and green strands. In particular the blue strands extend horizontally through the DNA crystal. Our approach consists of the synthesis of multiple copies this "blue" DNA strand. The subunit itself is composed of the two blue strands, one from block A and one from block B. The synthesized DNA sequence will first be attached to gold and platinum dots produced on a surface 1 micron apart. This DNA attachment is maintained via two oligonucleotide anchors complementary to the two ends of the tandemly repeated sequence. The two anchors are selectively bounded to the platinum and gold dots through pre-established surface chemistry. Then, the two blocks will be sequentially added to grow the DNA crystals. The long blue strand will be a nucleation site for growing and placing the DNA nanoarrays.

In order to do that, Rolling Circle Amplification technique was used to generate the long DNA repeats. The RCA product consisting of multiple copies, is complementary to the single stranded circular DNA used as template. As a nonthermal amplification technique, this technique produces an assortment of different length single stranded DNA products. A 95 base single stranded DNA oligomer, complementary to the two blues was first circularized and used as a RCA template. We successfully produced, then verified the repetitive nature of the synthesized DNA. Our RCA product appears to be as long as 10 kb when analyzed by both gel electrophoresis and AFM. To increase the usefulness of

this DNA we had to incorporate two specific ends. We used the PCR technique to add the two specific, unique ends. By doing so, we produced a double stranded DNA composed of multiple copies with two specific ends. This product was then cloned into host bacterial cells. This cloning step serves as an amplification and isolation technique.

The sequencing results of our DNA fragments demonstrated that the cloned DNA pieces are, as planned, true copies of the 95 bp long blue strand with the two pre-incorporated specific ends. We believe that having our DNA target inserted in a plasmid vector has many advantages. First of all, the recombinant molecules represent a DNA material supply that can last forever. Secondly, this makes the manipulation of the target DNA more feasible, in terms of adding more DNA bases to one or both sides of the inserted DNA fragment. In addition, the plasmid sequence upstream and downstream of the DNA target represents a specific sequence that can be used as a hybridization objective if the placement of the DNA target is desired.

By further developing this technique, especially with regard to the challenging objective of obtaining more copies, we believe that Rolling Circle Amplification can contribute as a new tool in addition to the DNA-based nanotechnology techniques already established. In contrast to its tremendous advantages, production of multiple copies as high as 100, the only shortcoming of the RCA technique is the uncontrollable product size and the lack of specific ends. By developing a strategy to overcome these two problems, we consider RCA a potentially very important technique in the future of nanotechnology.

We also pioneered the assembly of DNA/nanoparticle nanostructures. We used the self recognition properties of DNA and the repetitive nature of the DNA scaffold to construct

a pattern of 10 nm nanocrystals. We believe that this new generation of material, controlled at the nanometer scale, will play a critical role in molecular electronics fabrication. By transferring this nanostructure from DNA to the surface, this work may introduce a new DNA-based lithography technique. The size of the nano-features will be controlled only by the size of the nanoparticles and the distance between them. This spacing is actually the size of the repeat sequence, in our case it is 32 nm (95 bp). This distance can be easily downsized to less than 10 nm. We note here that other active molecules or molecular elements may be also patterned the same way. It is known that chemistry of DNA allows for a broad range of manipulations. Thus carbon nanotubes, other nanoparticles (for example, Ag, Pt), semiconductors (for example, CdSe, CdS), or electronically active molecules (for example, molecular diodes, molecular switches) can also be patterned in one dimension on a synthesized DNA scaffold.

APPENDIX A: Recipes & Protocols

1 DNA digestion with EcoRI and XbaI:

The enzymes must be handled in ice. Do not take them out of ice. After use store the enzymes at -20 degrees.

Mix:

1. 50 µl of DNA (DNA should diluted in water; avoid DNA dilution in buffers containing EDTA. EDTA will enhance many enzymatic reactions.
2. 7 µl of 10X buffer H. buffer H is compatible with both restriction enzymes. For other enzymes check the buffer compatibility.
3. 7 µl of 10 X BSA.
4. 1.5 XbaI and 1.5 µl of EcoRI.
5. 3 µl of water.

The total volume is 70 µl. Incubate the mixture 2 hrs at 37 degrees. Heat block or water bath can be used. The mixture should be then purified with *Qiagen* PCR purification Kit. If one enzyme is used the same protocol is kept, but substituting the volume of the unused enzyme with water.

2. Vector Digestion with EcoRI and XbaI:

the vector must be stored frozen.

Mix:

1. 2 µl of the vector.
2. 1 µl of 10X buffer H.
3. 1 µl of BSA.

4. 0.5 µl of EcoRI and 0.5 µl of XbaI.
5. 5 µl of water.

The mixture should be then purified with *Qiagen* PCR purification kit.

3. Ligation of the DNA fragments with the digested vectors using the rapid ligation kit

When tow different fragment of DNA prepared by digestion with the same restriction enzymes, they can be readily joined together.

Mix:

1. 10 µl of ligation buffer from the rapid DNA ligation kit
2. 2 µl of dilution buffer from the rapid DNA ligation kit.
3. 0.5 µl digested, purified vector.
4. 7.5 digested, purified DNA
5. 1 µl T_4 DNA ligase.

DO NOT vortex the mixture. Incubate 5 min at room temperature.

3. Plate preparation for storage:

1. Make 40g/l LB agar media (the LB agar is powder).
2. Autoclave
3. when the media is warm add ampicillin 50 to 100 ng/l
4. Add 15 ml media per plate; leave the plate at room temperature until solidification.
5. Store the plates in a clean place at 4 degrees.

4. Plate preparation for use:

1. Pre-warm the plate at least 30 min at 37 degree before use (this is if the plates are taken from the 4 degree storage, if not no need for pre-heat).

2. Add 40 µl of Xgal (20 mg/µl) and 4 µl of IPTG (200 mg/µl) per plate. Xgal and IPTG are used for blue/white screening. Remember that the normal color of colonies is blue, just colonies with positive insert are white.
3. Gently spread the Xgal and the IPTG through all the surface of the plate. Use a metallic stick to spread the solution on the plate. The stick must be damped in pure ethanol and heated to keep it sterilized.
4. Put the plate back at 37 degrees. After 20 min the plate are ready for use.

P.S. If the plates are quite bit old (more than 1 month) it is suggested to add some ampicillin. Ampicillin can be added as desired (ca 50 ng per plate) before adding the Xgal and the IPTG.

5. LB solution:

Same concentration as LB agar media (40 g/l). Make sure you Autoclave the solution before use.

6. Protocol for adding the 3' overhang:

Mix:

1. 1 µl dATP (just the A).
2. 0.5 *Taq* polymerase.
3. 2.5 10X PCR buffer.
4. 20 µl DNA. (PCR product amplified with proofreading enzyme).
5. 1 µl water.

The total volume is 25 µl. incubate the mixture 15 min at 72 degrees (we suggest the use of thermo-cycler to adjust the temperature).

7. How pCR® II-TOPO® or pCR® 2.1-TOPO® works

Topoisomerase I from *Vaccina* virus binds to duplex DNA at specific sites and cleaves the phosphodiester backbone after 5'-CCCTT in one strand. The energy from the broken phosphodiester backbone is conserved by formation of covalent bond between the 3' phosphate of the cleaved strand and a tyrosyl residue (Tyr-274) of topoisomerase I the phospho-tyrosyl bond between the DNA and enzyme can subsequently be attacked by the hydroxyl of the original cleaved strand, reversing the reaction and releasing topoisomerase.

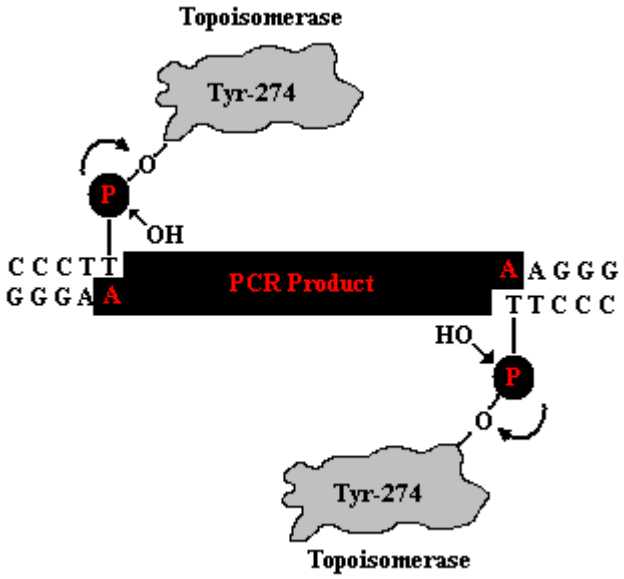

8. Phenol extraction

Phenol: Chloroform: Isoamyl Alcohol 25:24:1 is used

1. Add 1 volume of phenol to 1 volume of DNA solution.
2. Vortex for 30 sec.

3. Spin the mixture (top speed) 10 min.
4. Transfer the top layer (aqueous phase that has the DNA) to a fresh tube.

When the top layer is transferred be careful NOT to pull out the interface layer, where all the protein is laid. It is better to lose some DNA than contaminate your product.

The proteins which were initially in the DNA solution will be unfolded in reacting with phenol. When unfolded the proteins move to the interface where its hydrophobic parts face the organic phase (bottom phase) and the hydrophilic parts face the aqueous phase (top phase).

9. Ethanol precipitation:

1. Add 1/10 of DNA solution volume of 5M NH4OAc (Ammonium acetate). To your DNA solution
2. Add 2.5 volume of 100% ethanol.
3. Vortex 10 sec.
4. Store at -80 degrees for at least 3 hours (alternatively solution may be stored overnight at -20 degree).
5. Spin for 30 min (top speed, at 4 degree), smaller DNA pieces or lower concentrations require longer spinning time.
6. A white pellet sticking to the wall of the tube should be seen, then carefully remove the supernatant. (if you are not very familiar with ethanol precipitation technique we suggest to keep the supernatant so DNA can be recovered)
7. Add 1 ml of 70% ethanol, mix by inverting twice, DO NOT vortex.
8. Spin for 10 min (top speed, at 4 degree).

9. Discard the supernatant.
10. Let the DNA pellet air-dry at room temperature for 10 min.
11. Resuspend DNA in the appropriate buffer.

10. 0.5 M EDTA solution

EDTA solution is a pH-dependent solution and it is a stop solution for most enzymatic reactions

1. Dissolve 186.1 g of (Na_2 EDTA, $2H_2O$) in 700 ml water.
2. Adjust the pH to 8.0 with 10M NaOH (ca 50 ml).
3. Add water to 1 liter.

Smaller volume can be prepared by adjusting the given volume above.

11. Exonuclease VII buffer:

Below is the recipe for the Exonuclease buffer

1. 70 mM Tris, pH 8.0.
2. 8 mM EDTA.
3. 10 mM ß-Merceptoethanol.

For Exonuclease reaction mix:

1. 1 µg DNA.
2. 2 U Exo VII.
3. 50 µl buffer.

APPENDIX B: Sequencing Results

(Q230:11)C2/160G-33:Plasmid DS:GC Rich +++ M13-48 REVERSE (24)/MGIF-0:Primer:N : 204004699

TTGNNTGATTCGCCAGCTATTTAGGTGACACTATAGAATACTCAAGCTTGCATGCCTGCAGGTCGACTC
TAGATCGGACAGCAGCCTCACGCTGGTTGCATCGGACGATACTACATGCCAGTTGACTAACGGCGCTA
CCGTGCATCATGGACTAACCAGTGACCGCATCGGACAGCAGCCTGACGCTGGTTGCATCGGACGATAC
TACATGCCAGTTGGACTAACGGCGCTACCGTGCATCATGGACTAACCAGTGACCGCATCGGACAGCAG
CCTGACGCTGGTTGCATCGGACGATACTACATGCCAGTTGGACTAACGGCGCTACCGTGCATCATGGA
CTAACCAGTGACCGCATCGGACAGCAGCCTGACGCTGGTTGCATCGGACGATACTACATGCCAGTTGG
ACTAACGGCGCTACCGTGCATCATGGACTAACCAGTGACCGCAGAATTCGCCCTATAGTGAGTCGTATT
ACAATTCACTGGCCGTCGTTTTACAACGTCGTGACTGGGAAAACCCTGGCGTTACCCAACTTAATCGCC
TTGCAGCACATCCCCCTTTCGCCAGCTGGCGTAATAGCGAAGAGGCCCGCACCGATCGCCCTTCCCAA
CAGTTGCGCAGCCTGAATGGCGAATGGACGCGCCCTGTAGCGGCGCATTAAGCGCGGCGGGTGTGGT
GGTTACGCGCAGCGTGACCGCTACACTTGCCAGCGCCCTAGCGCCCGCTCCTTTCGCTTTCTTCCCTTC
CTTTCTCGCCACGTTCGCCGGCTTTCCCCGTCAAGCTCTAAATCGGGGGCTCCCTTTAGGGTTCCGATT
TAGTGCTTTACGGCACCTCGACCCCAAAAAACTTGATTAGGGTGATGGTTCACGTAGTGGGCCATCGCC
CTGATAGACGGTTTTTCGCCCTTTGACGTTGGAGTCCACGTTCTTTAATAGTGGACTCTTGTTCCAACTG
GAACACACTCACCCTATCTCGGTCTATTCTTTTGATTATAAGGGATTTGCCGATTNCGNCTATGGGTNAA
AATGAGCTGATTACAAANTTANCGCGANTTTACAAATATAACGCTACATTTCTGATGCGNATTTCTCTTA
CCATCTTGCGGATTCCCCGCAATGGGCCTTCANAANTTGTTGAGCCCAANTAGCANCCNAACCGCAAA
CCGTANNGCCTGAGGNTGTTGTCCGNTCNTNNAAANTGACNTCCGGNTNTGGTAAGTTNCNTTNNCNA
CNGGNAAANGCNCGACCATTTTAGGNAGCAGAAAGGTNTAACCGGGGCTTGGATGNGACCTTTTTTNA
ATAATTTCCNCGAAACNAAGTAAATNAAAAAATNATTCGNCTTTCTTGGTTCCTTTTNCAACGGAAANNA
ATGGCNGTNNAGTNGANTNTCCAATTNATATTTGGNTNTTNGAACNCCTTAAGTACCAATNGNATG

(Q230:9)3/160G-31:Plasmid DS:GC Rich +++ M13-48 REVERSE (24)/MGIF-0:Primer:N : 204004699

GCTTGACCTGATTCGCCAGCTATTTAGGTGACACTATAGAATACTCAAGCTTGCATGCCTGCAGGTCGA
CTCTAGATCGGACAGCAGCCTGACGCTGGTTGCATCGGACGATACTACATGCCAGTTGGAAACGGCGC
TACCGTGCATCATGGACTAACCAGTGACCGCATCGGACAGCAGCCTGACGCTGGTTGCATCGGACGAT
ACTACATGCCAGTTGGACTAACGGCGCTACCGTGCATCATGGACTAACCAGTGACCGCATCGGACAGC
AGCCTGACGCTGGTTGCATCGGACGATACTACATGCCAGTTGGACTAACGGCGCTACCGTGCATCATG
GACTAACCAGTGACCGCATCGGACAGCAGCCTGACGCTGGTTGCATCGGACGATACTACATGCCAGTT
GGACTAACGGCGCTACCGTGCATCATGGACTAACCAGTGACCGCAGAATTCGCCCTATAGTGAGTCGT
ATTACAATTCACTGGCCGTCGTTTTACAACGTCGTGACTGGGAAAACCCTGGCGTTACCCAACTTAATC
GCCTTGCAGCACATCCCCCTTTCGCCAGCTGGCGTAATAGCGAAGAGGCCCGCACCGATCGCCCTTCC
CAACAGTTGCGCAGCCTGAATGGCGAATGGACGCGCCCTGTAGCGGCGCATTAAGCGCGGCGGGTGT
GGTGGTTACGCGCAGCGTGACCGCTACACTTGCCAGCGCCCTAGCGCCCGCTCCTTTCGCTTTCTTCCC
TTCCTTTCTCGCCACGTTCGCCGGCTTTCCCCGTCAAGCTCTAAATCGGGGGCTCCCTTTAGGGTTCCG
ATTTAGTGCTTTACGGCACCTCGACCCCAAAAAACTTGATTAGGGTGATGGTTCACGTAGTGGGNCATC
GCCCTGATAGACGGTTTTTCGCCCTTTGACGTTGGAGTCCACGTTCTTTAATAGTGGACTCTTGTTNCAA
ACTGGAACANCACTCAACCCTATCTCGGGCTATTCTTTTGATTTATAAGGGATTTTGCCGATTTCGGCCT
ATTGGTTAAAAATGAGCTGATTAACAAAAATTNACGCGAATTTTACAAATATNACGCTTACANTTCCTGA
TGCGGATTTTTTCTTANCATCTGTGCGGATTTCAACCNNAAATGGGGNACTTTCAGNANANTTGTTTGA
TGNCNAAANTTANNCAGCCCNAACCCGCAAACCCGNTAANNGCCTGANGGNTTGTTGTTCCGGATCCT
TTAAAAAANNTNGACGTTCNGGACTCTGGNNNAGTTTCCCNNTNCCAACCNGAAAAAGGGCCGGACCC
NTTTAGGTAAGNCGAAATGTTTANGCNGGNCTTNGGANGGGGAACCTTNTTTTNAANTAATTTCCCCGA
AACNGANGTTAATGAAGAAGGNGTNATTCGGGCTTCTTGGGTTCNCTTTTCNACTGGAAAANNAATTG

(Q230:10)4/160G-32:Plasmid DS:GC Rich +++ M13-48 REVERSE (24)/MGIF-0:Primer:N : 204004699

CTTGACATGATTACGCCAGCTATTTAGGTGACACTATAGAATACTCAAGCTTGCATGCCTGCAGGTCGA
CTCTAGNATCGGACAGCAGCCTGACGCTGGTTGCATCGACGATACTACATGCCAGTTGGACTAACGGC
GCTACCGTGCATCATGGACTAACCAGTGACCGCATCGGACAGCAGCCTGACGCTGGTTGCATCGGACG
ATACTACATGCCAGTTGGACTAACGGCGCTACCGTGCATCATGGACTAACCAGTGACCGCATCGGACA
GCAGCCTGACGCTGGTTGCATCGGACGATACTACATGCCAGTTGGACTAACGGCGCTACCGTGCATCA
TGGACTAACCAGTGACCGCAGAATTCGCCCTATAGTGAGTCGTATTACAATTCACTGGCCGTCGTTTTA
CAACGTCGTGACTGGGAAAACCCTGGCGTTACCCAACTTAATCGCCTTGCAGCACATCCCCCTTTCGCC
AGCTGGCGTAATAGCGAAGAGGCCCGCACCGATCGCCCTTCCCAACAGTTGCGCAGCCTGAATGGCGA
ATGGACGCGCCCTGTAGCGGCGCATTAAGCGCGGCGGGTGTGGTGGTTACGCGCAGCGTGACCGCTA
CACTTGCCAGCGCCCTAGCGCCCGCTCCTTTCGCTTTCTTCCCTTCCTTTCTCGCCACGTTCGCCGGCTT
TCCCCGTCAAGCTCTAAATCGGGGGCTCCCTTTAGGGTTCCGATTTAGTGCTTTACGGCACCTCGACCC
CAAAAAACTTGATTAGGGTGATGGTTCACGTAGTGGGCCATCGCCCTGATAGACGGTTTTTCGCCCTTT
GACGTTGGAGTCCACGTTCTTTAATAGTGGACTCTTGTTCCAAACTGGNAACAACACTCAACCCTATCTC
GGTCTATTCTTTTGATTTATAAGGGATTTTGCCGATTTCGGCCTATTGGTTAAAAAATGAGCTGATTTAA
CAAAAATTTAACGCGAATTTNACAAATATTAACGCTT

Q230:12)A1/160G-34:Plasmid DS:GC Rich +++ M13-48 REVERSE (24)/MGIF-0:Primer:N : 204004699

CTTGACCTGATTCGCCAGCTATTTAGGTGACACTATAGAATACTCAAGCTTGCATGCCTGCAGGTCGAC
TCTAGATCGGACAGCAGCCTGACGCTGGTTGCATCGGACGATACTACATGCCAGTTGGACTAACGGCT
CTACCGTGCATCATGGACTAACCAGTGACCGCATCGGACAGCAGCCTGACGCTGGTTGCATCGGACGA
TAATACATGCCAGTTGGACTAACGGCGCTACCGTGCATCATGGACTAACCAGTGACCGCATCGGACAG
CAGCCTGACGCTGGTTGCATCGGACGATACTACATGCCAGTTGGACTAACGGCGCTACCGTGCATCAT
GGACTAACCAGTGACCGCATCGGACAGCAGCCTGACGCTGGTTGCATCGGACGATACTACATGCCAGT
TGGACTAACGGCGCTACCGTGCATCATGGACTAACCAGTGACCGCATCGGACAGCAGCCTGACGCTGG
TTGCATCAGACGATACTACATGCCAGTTGGACTAACGGCGCTACCGTGCATCATGGACTAACCAGTGAC
CGCATCGGACAGCAGCCTGACGCTGGTTGCATCGGACGATACTACATGCCAGTTGGACTAACGGGCGC
TACCGTGCATCATGGACTAACCAGTGACCGCAGAATTCGCCCTATAGTGAGTCGTATTACAATTCACTG
GCCGTCGTTTTACAACGTCGTGACTGGGAAAACCCTGGCGTTACCCAACTTAATCGCCTTGCAGCACAT
CCCCCTTTCGCCAGCTGGCGTAATAGCGAAGAGGCCCGCACCGATCGCCCTTCCCAACAGTTGCGCAG
CCTGAATGGCGAATGGACGCGCCCTGTAGCGGCGCATTAAGCGCGGCGGGTGTGGTGGTTACNCGCA
GCGTGACCGCTACACTTGCCAGCGCCCTAGCGCCCGCTCCTTTCGCTTTCTTCCCTTCCTTTCTCGCCA
CGT

Q230:8)1/160G-30:Plasmid DS:GC Rich +++ M13-48 REVERSE (24)/MGIF-0:Primer:N : 204004699

TNNNTGNTTCNCCAGCTATTTAGGTGACACTATAGAATACTCAAGCTTGCATGCCTGCAGGTCGACTCT
AGATCGGACAGCAGCCTGACGCTGGTTGCATCGGACGATACTACATGCCAGTTGGACTAACGGCGCTA
CCGTGCATCATGGACTAACCAGTGACCGCATCGGACAGCAGCCTGACGCTGGTTGCATCGGACGATAC
TACATGCCAGTTGGACTAACGGCGCTACCGTGCATCATGGACTAACCAGTGACCGCATCGGACAGCAG
CCTGACGCTGGTTGCATCGGACGATACTACATGCCAGTTGGACTAACGGCGCTACCGTGCATCATGGA
CTAACCAGTGACCGCATCGGACAGCAGCCTGACGCTGGTTGCATCGGACGATACTACATGCCAGTTGG
ACTAACGGCGCTACCGTGCATCATGGACTAACCAGTGACCGCAGAATTCGCCCTATAGTGAGTCGTATT
ACAATTCACTGGCCGTCGTTTTACAACGTCGTGACTGGGAAAACCCTGGCGTTACCCAACTTAATCGCC
TTGCAGCACATCCCCCTTTCGCCAGCTGGCGTAATAGCGAAGAGGCCCGCACCGATCGCCCTTCCCAA
CAGTTGCGCAGCCTGAATGGCGAATGGACGCGCCCTGTAGCGGCGCATTAAGCGCGGCGGGTGTGGT
GGTTACGCGCAGCGTGACCGCTACACTTGCCAGCGCCCTAGCGCCCGCTCCTTTCGCTTTCTTCCCTTC
CTTTCTCGCCACGTTCGCCGGCTTTCCCCGTCAAGCTCTAATCGGGGGGCTCCCTTTAGGGTTCCGATT
TAGTGCTTTACGGCACCTCGACCCCAAAAAACTTGATTAGGGTGATGGTTCACGTAGTGGGCCATCGCC
CTGATAGACGGTTTTTCGCCCTTTGACGTTGGAGTCCACGTTCTTTAATAGTGGACTCTTGTTCCAACTG
GAACAACACTCAACCCTATCTCGGTCTATTCTTTTGATTTATAAGGGATTTNGCCGATTTCGGCCTATGG
TTAAAANTGAGCTGATTTACAAAATTTACGCGAATTTAACAAATATANCCNTTAAATTTCTGATGGGTATT
TCTCTTACCATNTTGCGGATTNCNACCCAATGGGGACNTCANANATTGCTTGATGCCCAAATNAGCAGC
CCAACCGCAAACCGTTAAGGCCTGAGGNTGTTGTCCGATCGTANANANTGNACNTTCGGANTCTGNCA
NGTTTCCTTNCCANCGGAAAAGGCNGGACCATTNAGTAGCGAAAGGTTACCNGGCTTNGGAGGNGAC
NTNTTTTAATATTCCNGAACCGAGTTATNAGAAAGTNTCGNCTCTTGNTCTTTCCACGAAATNATGGGG
GNNNGTNNANTATCAATNNTNTTTGGTNTCGANNNCTTATGCCATNGNAATNNNAG

REFERENCES

1. From the classic talk that Richard Feynman gave on December 29th 1959 at the annual meeting of the American Physical Society at the California Institute of Technology (Caltech) was first published in the February 1960 issue of Caltech's *Engineering and Science*.
2. E. Winfree, F. Liu, L. A. Wenzler, and N.C. Seeman, Design and Self-Assembly of Two-Dimensional DNA Crystals, *Nature* 394, 539-544 (**1998**).
3. Daubendiek,S.L., Ryan,K. and Kool,E.T. (1995) Rolling circle RNA synthesis: circular oligonucleotides as efficient substrates for T7 RNA polymerase. *J. Am. Chem. Soc,* **117**, 7818-7819.
4. T.A. Brown Gene Cloning and DNA analysis, Fourth Edition
5. Liu,D., Daubendiek,SL., Zillman,M.A., Ryan,K. and Kool,E.T. (1996) Rolling circle DNA: small circular oligonucleitides as efficient templates for DNA polymerases. *J. Am. Chem. Soc,* **118**, 1587-1594
6 .Heiko Kunhn, Vadim V.Demidov and Maxim D. Frank-kamenetskii. (2002) Rolling-circle amplification under topological constraints. *Nucleic Acid Research,* **30**(2),574-580.
7. Girish Nallur, Chenghua Luo, Linhua Fang, Stephanie Cooley, Varshal Dave, Jeremy Lambert, Kari Kukanaskis, Stephen kinsmore, Roger Lasken and Barry Schweitzer. (2001). Signal amplification by rolling circle amplification on DNA microarrays. *Nucleic Acids Research,* **29** (23)**,** No.23 **e118**
8. Paul M.Lizardi, Xiahoua Huang, Zhengrong Zhu, Patricia Bray-Ward, David C. Thomas and David C.Ward. (1998). Mutation detection and signal-molecule counting using isothermal rolling-circle amplification. *Nature Genetics*, **19**, 225-232
9. Andrew Fire and Si-Qun Xu. (1995). Rolling replication of short DNA circles. *Proc. Natl. Acad. Sci*, **92**, 4641-4645
10. Jason D. Kahn and Donald M. Crothers. (1992). Protein-induced bending and DNA cyclization. *Proc. Natl. Acad. Sc* **89**, 6343-6347.
11. David Shore, Jorg Langowski, and Robert L. Baldwin. (1981). *Proc. Natl. Acad. Sc* **78**, 4833-4837.
12. Ethel Rubin, Squire Runney IV, Shaohui Wang and Eric T.kool. (1995). Convergent DNA synthesis a non-enzymatic dimerization approach to circular oligideoxynucleotides. *Nucleic Acids Research* **23** (17), 3547-53
13. Yanzheng Xu and Eric T. Kool (1997). A novel 5'-iodonucleoside allows efficient nonenzymatic ligation of single-stranded and duples DNAs. *Tetrahedron Letters* **38**, 5565-5598.
14. A 1.7-kilobase single-stranded DNA that folds into a nanoscale octahedron. William. M. Shih et al. *Nature* 427, 618-21 (2004).
15. A sister-strand exchange mechanism for recA-independent deletion of repeated DNA sequences in Escherichia coli.Lovett ST, Drapkin PT, Sutera VA Jr, Gluckman-Peskind TJ. *Genetics.* 1993 Nov;135(3):631-42.
16. DNA-Based Assembly of Gold nanocrystals. Alivisatos, A. P. et al *Angew. Chem. Int. Ed*. **38** 1808-1812 (1999)
17. Synthesis of inorganic materials with complex form. Mann, S. & Ozin, G. A. *Nature* **382**, 313-318 (1996)

18. Organization of 'nanocrystal molecules' using DNA. Alivisatos, A. P. et al. *Nature* **382**, 609-611 (1996)
19. Semiconductor Clusters, Nanocrystals, and Quantum Dots. Alivisatos, A. P. *Science* **271**, 933-937 (1996)
20. A DNA-based method for rationally assembling nanoparticles into macroscopic materials. Chad, A. M. et al *Nature* **382**, 607-609 (1996)
21. Hayat, M.A. (ed.) Colloidal Gold: Principals, Methods, and Applications (Academic, San Diego, 1991)
22. Creighton,J. A. et al J. *Chem. Soc. Faraday II* **75**, 790-798 (1979)
23. Self-Organization of CdSe Nanocrystallites into Three-Dimensional Quantum Dot Superlattices. Murray et al *Science* **270**, 1335-1338 (1995)
24. Motte, L. et al *Adv. Mater*. **8,** 1018-1020 (1996)
25. Semiconductor Nanocrystals Covalently Bound to Metal Surfaces Using Self Assembled Monolayers. Alivisatos, A. P. et al *J. Am. Chem. Soc.* **114,** 5221-5230 (1992)
26. Nanocrystals gold molecules. Whetten, R. L. et al. *Adv. Mater*. **8**, 428-433 (1996)
27. Kimizuka, N. & Kunitake, T. *Adv. Mater*. **8** 89-91 (1996)
28. Novel Gold-Dithiol Nano-Networks with Non-metallic Electronic Properties. Brust, M. et al. *Adv. Mater*. **7** 795-797 (1995)
29. Self-Assembly of a Two-Dimensional Superlattice of Molecularly Linked Metal Clusters. Andres, R. P. et al. *Science* **273**, 1690-1693 (1996)
30**.** Spatially Confined Chemistry: Fabrication of Ge Quantum Dot Arrays. Heath, J. R. et al. *J. Phys. Chem*. **100,** 3144-3149 (1996)
31. G. Schmid, A. Lehnert*, Angew. Chem*. **1989**, *101,* 773-4
32. Tutorial by Bill Ross; initial biotin/streptavidin tetramer by Richard Dixon from the momomer from Brookhaven by P.C. Weber, D.H. Ohlendorf, J.J. Mendolowski, and F.R. Salemme (1992).
33. "Energy transfer: a spectroscopic ruler." Stryer L, Haugland RP. *Proc Natl Acad Sci USA* **58**, 719-726 (1967).
34. Alivisatos, A. P. et al. *Nano lett*, **3,** 33-36 (2003)
(*). Information from promega (Carballeira, *Biotechniques* **9**, 276 (1990).